

九州工業大学学術機関リポジトリ



| | |
|------------|---|
| Title | Application of Enhanced HHT Method for Oscillation Analysis in Power System Based on CampusWAMS |
| Author(s) | 劉, 青 |
| Issue Date | 2015-02 |
| URL | http://hdl.handle.net/10228/5444 |
| Rights | |

Doctoral Dissertation

Application of Enhanced HHT Method for
Oscillation Analysis in Power System
Based on CampusWAMS

キャンパスWAMSによる改良されたヒルベルトホーン変
換を用いた電力系統動揺特性解析

By

劉青

(Student ID: 11589501)

Supervisor: Prof. Yasunori Mitani, PhD.

Department of Electrical and Electronic Engineering

Graduate School of Engineering

Kyushu Institute of Technology

February 2015

Acknowledgements

First and foremost, I would like to express my deepest gratitude to my supervisor, Prof. Dr. Yasunori Mitani, for his constant guidance, valuable advice, and patient support during my entire course of studies at Kyushu Institute of Technology. His profound academic knowledge and illuminating comments about my research were very valuable and helpful, not only to my doctoral study, but also to my future work.

I also would like to express my sincere gratitude to my dissertation committee members: Prof. Dr. Hikita, Prof. Dr. Sakamoto and Assoc. Prof. Dr. Watanabe, Prof. Dr. Toyoda for their precious time and valuable suggestions, comments.

In addition, I would like to thank all lab members, staff members, other students of Kyushu Institute of Technology and all my friends for their continuous encouragement and support that always enabled me to persevere with my study during last four years in Japan.

Finally, I would like to express my love and gratitude to my parents and my family for their endless support, encouragement and enduring love.

劉青

February 2015

Abstract

This dissertation presents a complete oscillation monitoring system based on real-time wide-area measurements from PMUs. This oscillation monitoring system employs the enhanced Hilbert-Huang transform (EHT) to analyze power system oscillation characteristics and estimate the damping of oscillatory modes from ambient data. This new oscillation system can give an indication of the damping of transient oscillations that will follow a disturbance, once it occurs. The application is based on a system identification procedure that is carried out in real-time.

This research studies various low frequency oscillation analysis algorithms. It mainly introduces the concept, character and implementation process of FFT, WLT and EHT method. According to the characteristics of low frequency oscillation signal we can get advantage and disadvantage of these algorithms.

It is important to remember that power system is actually a high-order time-varying nonlinear system. Only under certain circumstances can it be simplified to linear or time-invariant systems. Although ambient condition is reasonably modeled as a linear

system, for system response following some events, nonlinearities play an important role in the measured data. HHT is a new type of nonlinear and non-stationary signal processing method. Compared with other methods, HHT has absolute advantage of analyzing low frequency oscillation signal because the power system responses following system disturbances contain both linear and nonlinear phenomena. Nevertheless, the traditional methods, whether FFT or WLT, etc. the signals are approximately processed as linear signal when analysis non-linear and non-stationary signals. This feature is the main advantage of HHT algorithm, which is also widely used by the reasons. Secondly, HHT method is adaptive, which means that can be adaptive extracted from the signal decomposed by EMD itself. It is based on an adaptive basis, and the frequency is defined through the Hilbert transform. Consequently, the "base" of Fourier transform is the trigonometric functions, the "base" of wavelet transform requires pre-selected. Therefore, HHT has completely adaptability. Third, it is suitable for analysis mutation signal. Due to the Heisenberg uncertainty principle constraint, many traditional algorithms must be satisfied the product of frequency window by time window is constant. This property makes these algorithms cannot achieve high precision both in time domain and frequency domain at the same time. Nevertheless, there is no uncertainty principle limitation on time or frequency resolution from the convolution pairs based on a priori bases. For these reasons, it can be said applying HHT method to dealing with power system oscillation signal is a good choice. However, it is still have some issues need to be resolved carefully.

To ensure accurate monitoring of system dynamics with noise-polluted WAMS measurements, several key signal-processing techniques are implemented to improve HHT method in this research: Data pre-treatment processing, the boundary end effect problem caused by the Empirical mode decomposition(EMD) algorithm and the boundary end effect problem caused by Hilbert transform based on Auto-Regressive and Moving Average Model (ARMA). There are six methods: a). polynomial extension method, b). slope method extension method, c). parallel extension method, d). extreme point symmetric extension method, e). mirror method f). Boundary local characteristic scale extension methods are used to inhibit the boundary end effects, which results in a serious distortion in the EMD sifting process.

Furthermore, an integrated scheme for the monitoring and detection of low-frequency oscillations has been developed based on HHT algorithm for oscillation analysis in CampusWAMS projects. By analyzing the real-time synchro-phasors, the proposed scheme is competent to identify the characteristics of the low-frequency oscillations in real-time.

Third, this dissertation presents an estimation algorithm method based on enhanced HHT for the parameters of a low frequency oscillation signal in power system.

In the end, the developed scheme is tested with simulated signals and measurements from CampusWAMS. An oscillation monitoring system based on real-time wide-area measurements from PMUs is established. It can determine the center range frequency of the concerned mode automatically and accurately, which is

then be used to determine the parameter of the extraction. The extracted mode frequency, damping and mode shape can be detected by this oscillation monitoring system. The results have convincingly demonstrated the validity and practicability of the developed scheme.

Contents

| | |
|--|--------|
| Acknowledgements | i |
| Abstract | iii |
| Contents | vii |
| List of Figures | x |
| List of Tables | xiv |
| Chapter1. Introduction..... | - 1 - |
| 1.1 Research Background and Motivation..... | - 1 - |
| 1.2 Objective of Research..... | - 7 - |
| 1.3 Outline of the Thesis..... | - 8 - |
| Chapter2. Wide-Area Measurement System Using Synchrophasors Technology | - 11 - |
| 2.1 Synchrophasor Technology..... | - 12 - |
| 2.2 Development of WAMS..... | - 15 - |
| 2.3 WAMS in the World..... | - 17 - |
| 2.4 The CampusWAMS | - 26 - |

| | |
|--|--------|
| Chapter3. On-line Oscillation Characteristics Monitoring Algorithm Analysis..... | - 31 - |
| 3.1 Background of Power System Low Frequency Oscillation | - 32 - |
| 3.1.1 Low Frequency Oscillation Mechanism..... | - 32 - |
| 3.1.2 Theoretical of Measurement-based Analysis..... | - 35 - |
| 3.2 Traditional Method of Low Frequency Analysis | - 38 - |
| 3.2.1 The FFT Method | - 39 - |
| 3.2.2 The Wavelet Method | - 44 - |
| 3.3 New Method of Low Frequency Analysis (HHT) | - 47 - |
| 3.3.1 The Empirical Mode Decomposition Method..... | - 48 - |
| 3.3.2 Hilbert Transform to IMF of Low-frequency Oscillation | - 50 - |
| 3.3.3 Hilbert Spectrum Analysis | - 51 - |
| 3.3.4 Low-frequency Oscillation by Hilbert Transform..... | - 52 - |
| 3.4 Summary | - 57 - |
| Chapter4. The Enhanced HHT Method..... | - 59 - |
| 4.1 Issues of Hilbert Huang Transform..... | - 60 - |
| 4.1.1 The Boundary End Effect..... | - 62 - |
| 4.1.2 Pseudo IMF Component..... | - 63 - |
| 4.1.3 Identify the Parameters..... | - 63 - |
| 4.2 Improved Program for HHT Method..... | - 64 - |
| 4.3 Data Pre-treatment Processing..... | - 65 - |
| 4.3.1 DC Removal Processing..... | - 66 - |
| 4.3.2 Digital Band-pass Filter Algorithm Processing..... | - 66 - |

| | |
|--|---------|
| 4.4 Inhibit the Boundary End Effect | - 69 - |
| 4.4.1 The Boundary End Effect Caused by EMD Algorithm..... | - 69 - |
| 4.4.2 Inhibit the Boundary End Effects Caused by EMD | - 70 - |
| 4.4.3 The Boundary End Effect Caused by Hilbert Transform | - 75 - |
| 4.4.4 Inhibit the Boundary End Effect Caused by Hilbert Transform..... | - 78 - |
| 4.5 Parameter Identification..... | - 83 - |
| 4.6 Summary..... | - 84 - |
| Chapter5. The Developed Oscillation Monitoring System..... | - 87 - |
| 5.1 Proposed Algorithm Test..... | - 88 - |
| 5.1.1 Case I | - 88 - |
| 5.1.2 Case II | - 92 - |
| 5.2 The Oscillation Monitoring System Based on Enhanced HHT Method | - 94 - |
| 5.2.1 Simulink Test..... | - 96 - |
| 5.2.2 Tested with Measurements from CampusWAMS | - 98 - |
| 5.3 Summary..... | - 101 - |
| Chapter6. Conclusions..... | - 103 - |
| Reference..... | - 105 - |

List of Figures

| | | |
|---------------|--|--------|
| Figure 2 - 1 | Synchrohpasor Definition | - 14 - |
| Figure 2 - 2 | reference phase angles at remote locations due to GPS synchronization- | 14 - |
| Figure 2 - 3 | Phasor measurement unit block diagram | - 15 - |
| Figure 2 - 4 | A schema of WAMS..... | - 16 - |
| Figure 2 - 5 | Milestones in wide area measurement system | - 17 - |
| Figure 2 - 6 | Central European WAMS devices[29] | - 19 - |
| Figure 2 - 7 | PMUs location for the CampusWAMS in Japan..... | - 26 - |
| Figure 2 - 8 | Data file recording scheme..... | - 29 - |
| Figure 2 - 9 | PMUs location for the CampusWAMS in Thailand..... | - 29 - |
| Figure 2 - 10 | PMUs location for the CampusWAMS in Singapore and Malaysia .- | 30 - |
| Figure 3 - 1 | Concept of measurement-based analysis..... | - 36 - |
| Figure 3 - 2 | phase difference between Kyushu University and Osaka University Stations..... | - 39 - |
| Figure 3 - 3 | The FFT analysis for the phase difference shown in Figure 3 - 2..... | - 42 - |

| | | |
|---------------|---|--------|
| Figure 3 - 4 | Extracted low-frequency oscillation extracted | - 43 - |
| Figure 3 - 5 | 20 minutes phase difference between Kyushu University and..... | - 43 - |
| Figure 3 - 6 | Wavelet components with use of Symlets wavelet..... | - 46 - |
| Figure 3 - 7 | Algorithm of EMD..... | - 49 - |
| Figure 3 - 8 | The EMD analysis in waveform of phase difference | - 53 - |
| Figure 3 - 9 | The HHT analysis in instantaneous frequency of phase difference | - 54 - |
| Figure 3 - 10 | The HHT spectrum in instantaneous frequency of phase difference.- | - 55 - |
| Figure 3 - 11 | Wavelet spectrum | - 56 - |
| Figure 3 - 12 | Phase difference around 240 seconds..... | - 56 - |
| Figure 4 - 1 | Test sin signal | - 61 - |
| Figure 4 - 2 | EMD analysis result | - 61 - |
| Figure 4 - 3 | Time-domain spectrum of HHT (Instantaneous frequency)..... | - 61 - |
| Figure 4 - 4 | Oscillation mode extraction algorithm | - 65 - |
| Figure 4 - 5 | Pre-treatment process | - 68 - |
| Figure 4 - 6 | FFT spectrum of butterworth filtered data | - 68 - |
| Figure 4 - 7 | FFT spectrum of butterworth filtered data in detail | - 68 - |
| Figure 4 - 8 | The extreme extending method | - 71 - |
| Figure 4 - 9 | The Mirror extension method..... | - 72 - |
| Figure 4 - 10 | The Parallel Extension Method | - 73 - |
| Figure 4 - 11 | The boundary local characteristic time scale extension method | - 74 - |
| Figure 4 - 12 | Inhibit the boundary effect problem of the EMD algorithm by mirror extension method..... | - 75 - |

| | | |
|---------------|---|--------|
| Figure 4 - 13 | Sine signal and its Hilbert transform..... | - 76 - |
| Figure 4 - 14 | Instantaneous frequency of sine signal..... | - 76 - |
| Figure 4 - 15 | HT computing process | - 77 - |
| Figure 4 - 16 | Integral periodic sampling of the data sequence | - 77 - |
| Figure 4 - 17 | ARMA process..... | - 80 - |
| Figure 4 - 18 | Algorithm of Inhibit the boundary end effect caused by Hilbert transform autoregressive–moving-average (ARMA) models | - 81 - |
| Figure 4 - 19 | Extend data based on ARMA method | - 82 - |
| Figure 4 - 20 | The signal based on ARMA extension | - 82 - |
| Figure 4 - 21 | Processed instantaneous frequency spectrum | - 82 - |
| Figure 5 - 1 | Pre-treatment EMD result (sampling time 1/100)..... | - 89 - |
| Figure 5 - 2 | Pre-treatment EMD result (sampling time 1/30)..... | - 89 - |
| Figure 5 - 3 | EMD result (sampling time 1/100)..... | - 90 - |
| Figure 5 - 4 | EMD result (sampling time 1/30)..... | - 91 - |
| Figure 5 - 5 | Oscillation signal..... | - 92 - |
| Figure 5 - 6 | EMD result..... | - 93 - |
| Figure 5 - 7 | Algorithm of oscillation monitoring system | - 95 - |
| Figure 5 - 8 | Simulink system..... | - 96 - |
| Figure 5 - 9 | Simulink signal..... | - 97 - |
| Figure 5 - 10 | Hilbert marginal spectrum of simulink signal | - 97 - |
| Figure 5 - 11 | Amplitude of extract oscillation mode | - 97 - |
| Figure 5 - 12 | The extract oscillation mode | - 98 - |

| | | |
|---------------|--|---------|
| Figure 5 - 13 | Extract a short time data of the extracted oscillation mode | - 98 - |
| Figure 5 - 14 | Waveforms of phase difference between Miyazaki University and Nagoya Institute of Technology University Stations..... | - 99 - |
| Figure 5 - 15 | Hilbert marginal spectrum..... | - 99 - |
| Figure 5 - 16 | Amplitude of extract oscillation mode | - 100 - |
| Figure 5 - 17 | Extract the oscillation mode..... | - 100 - |
| Figure 5 - 18 | Extract a short time data of the extracted oscillation mode | - 100 - |

List of Tables

Table 2 - 1 PMUs of the CampusWAMS in Japan..... - 28 -

Table 5 - 1 Parameters identification result - 93 -

Chapter1. Introduction

1.1 Research Background and Motivation

Modern interconnected wide-area power systems around the world are faced with serious challenging issues in global monitoring, stability, and control mainly due to increasing size, changing structure, emerging new uncertainties, environmental issues, and rapid growth in distributed generation [1]. Under this circumstance, any failure in the planning, operation, protection, and control in a part of the power system could evolve into the cause of cascading events that may even lead to a large area power blackout.

In previous decades, due to economic pressure from electricity markets and environmental constraints, power system operators have been forced to operate power transmission systems in highly stressed conditions closer to the system limits than ever before [2]. In this same period, the number, and size, of large-scale power system blackouts has increased. For example, the US-Canada blackout on August 14, 2003 [3] and the Italy blackout on September 28, 2003 [4] September 2003 Sweden-Denmark blackout, July 2004 Greece blackout [5], involved more than 100

million customers. It is rare for large-scale power system blackouts to be directly caused by a single large disturbance. However, a single large disturbance in a stressed system may cause a series, or cascade, of unplanned and unexpected sequential events. These events will incrementally increase the stress on the system and force it into a more vulnerable state of operation. If proper protection and control actions are not taken quickly and properly (e.g. load shedding, reactive power support and controlled islanding), then the system may experience further cascading events and separate into unplanned islands, or even completely collapse [6-8].

Whilst it is impossible to develop a solution that completely eliminates the possibility of a blackout, several measures can be implemented to minimize the probability of a blackout occurring. For many years, Energy Management System (EMS) has been used for the on-line monitoring of system conditions and assessment of system security. Traditional EMS uses measurements with a low-refresh rate (several seconds to one minute), from a Supervisory Control and Data Acquisition (SCADA) system, to estimate the system operating condition and to perform off-line system stability studies [9]. The EMS can provide sufficient information and support for normal steady-state system operation and to plan the system response to slow changes in the operating conditions. However, EMS is not capable of capturing system dynamics, particularly when the system is subjected to large disturbances. In addition, off-line studies cannot be used to fully anticipate all of the conditions faced by operators. These unplanned contingencies have the potential to initiate a cascade of events that will lead to a system blackout.

Furthermore, attempts to avert climate change through the introduction of renewable energy policies will force radical changes in future power systems. The most significant of these is that a large percentage of electrical energy will be

generated using renewable resources (wind, solar and tidal). In 2013, renewable power capacity expanded at its fastest pace to date. Renewable power generation continued to grow strongly, reaching almost 22% of the global mix, compared with 21% in 2012 and 18% in 2007 [10].

This will prove problematic as electricity generation using renewable resources is highly influenced by climatic conditions and the resulting intermittent nature of the renewable resources. This will make the operation of future power systems more variable and unpredictable. In addition, renewable energy generation and transmission requires the support of power electronic technologies such as HVDC and SVC. The use of these technologies will introduce further complexity and uncertainty into power systems [11][12]. The introduction of further variation, complexity and unpredictability to power systems will dramatically increase the likelihood of large scale power system blackouts.

Therefore, to maintain system reliability and make efficient use of sustainable energy, power system monitoring should be a key technology to achieve flexible operation in the system. This will prove a serious problem, as current systems already find themselves increasingly vulnerable to such blackouts in the absence of a real time wide area monitoring system.

The advent and deployment of phasor measurement units (PMUs) provides a powerful tool to solve the mentioned problems using the measurement based methodologies. Compared to conventional measurement from supervisory control and data acquisition (SCADA) system, modern phasor measurement provides the crucial information of bus phase angle which has close relation with power system dynamic and stability. More importantly, the time synchronization information is embedded in phasor measurement so that phasor data from multiple distant locations in a wide-area

power system can be correctly and accurately processed. Thanks to this unique feature, a wide-area measurement and monitoring system (WAMS) based on multiple PMUs can be constructed to enhance the ability of the power system operator for monitoring and control of power system dynamic. Owing to these unique advantages of phasor measurement, the measurement-based approach becomes feasible and applicable to power system.

For the measurement-based approach, a beforehand prepared mathematic model based on the knowledge of overall system information is not necessary and only the measurements of outputs and/or inputs of power system are assumed to be available. Traditionally, all aspects of the analysis of power system dynamic and stability are built on the dependence of the mathematic model of power system components and network [13][14]. Thus the result from each modal analysis is valid for only one operating point. For a real power system, its operating point keeps changing due to changes in load pattern and system topology. Furthermore, power transfers among power companies have become more and more unpredictable in recent years because of market deregulation, making it more difficult to predict actual system behaviours based on modal analysis for limited number of system conditions. The measurement-based approach constructs an online and real-time snapshot-model of power system dynamic using these real system measurements, which can achieve quick, timely and accurate representation of real system dynamic.

In WAMS, the data from the PMUs are tagged with an accurate time stamp from global positioning system (GPS) clock and sent to phasor data concentrators located in control centers through digital communication channels. These measurements from the whole power system are synchronized in time and provide time-synchronized voltage and current phasor, as well as frequency measurements with synchronization

accuracy better than microseconds, which offer great potential for many applications in whole power system.

In recent years, power oscillations are a growing concern among power system operators worldwide. Essentially, the potential for inter-area power oscillations depends on the strength of the tie lines between different areas and the load on the ties [15]. Wide-area monitoring based on PMU measurements provide a large amount of data which can be categorized into two different types: the ambient type data and the system disturbances type data. The first type data is collected when power system is in normal operating condition without major system disturbances. It can be studied through a linearization of system model equations. This problem is usually associated with the appearance of low-damped or un-damped oscillations in the system due to lack of sufficient damping torque. The second type data is the measurements immediately after small or large disturbances to the power system, it belongs to the large-disturbance rotor angle stability, more commonly referred to as transient stability, corresponds to the ability of generators to maintain synchronism when subjected to severe disturbances such as a short circuits or outages of major transmission lines etc.

Without knowledge of generator and line parameters, the measurement-based approach primarily employs statistical signal processing technique and system identification theory to discover the characteristic of low-frequency oscillation mode which usually buries in the bus voltage phase angle or tie line power variations due to random and constant load variations. Currently, there are many analysis algorithms based on the concept of measurement-based approach for power system oscillation, which mainly include: Fourier Transform, Wavelet analysis, Prony and a family of autoregressive (AR) methods, Subspace method, and Hilbert-Huang transform (HHT).

Fast Fourier Transformation (FFT) method is used to monitor and estimation scheme of power system inter-area oscillation based on wide-area phasor measurements from the CampusWAMS [16]. Wavelet (WLT) analysis results are limited by mother wavelet, and wavelet components and wavelet spectra are meaningful only to the selected mother wavelet. Prony method was effective to estimate damping, amplitude, and frequency of various oscillation modes from ringdown type measurement data [17]. In [18], the autoregressive (AR) linear prediction model associated with robust recursive least square algorithm was applied on the combined ambient and ringdown signal to identify power oscillation mode. The subspace method was also proposed to perform low-frequency oscillation mode estimation based on collected response measurement when small probing signal is injected [19]. In order to estimate the eigen-properties of multiple oscillation modes simultaneously, they are also faced with the difficulties such as carefully and correctly selecting suitable model order and solving high order linear polynomials. HHT is an empirically based data-analysis method. Its basis of expansion is adaptive, so that it can produce physically meaningful representations of data from nonlinear and non-stationary processes [20]. Compared with other methods, HHT has absolute advantage of analysing low frequency oscillation signal (nonlinear and non-stationary signal). However, over the past few years, the full theoretical base has not been fully established. Up to this time, most of the progress with the HHT has been in its application, while the underlying mathematical problems have been mostly left untreated. All the results have come from case-by-case comparisons conducted empirically [20].

Hence, it is necessary to solve the key problems of applying HHT method regarding monitoring power system oscillation dynamic behaviour based on wide-area synchronized phasor measurements. These key problems mainly include the boundary

effect problem caused by HHT; parameter estimation based on HHT method and how to extract the useful damping information from PMU.

1.2 Objective of Research

This dissertation describes a new complete oscillation monitoring system that employs CampusWAMS data to estimate the damping of oscillatory modes from ambient data and system disturbance type data based on enhanced HHT method. This new oscillation system can give an indication of the damping of transient oscillations that will follow a disturbance, once it occurs. The application is based on a system identification procedure that is carried out in real-time.

First, this research studies various low frequency oscillation analysis algorithms. It mainly introduces the concept, character and implementation process of FFT, WLT and HHT method. According to the characteristics of low frequency oscillation signal we can get advantage and disadvantage of these algorithms.

Second, an integrated scheme for the monitoring and detection of low-frequency oscillations has been developed based on HHT algorithm for oscillation analysis in CampusWAMS projects.

By analysing the real-time synchro-phasors, the proposed scheme is competent to identify the characteristics of the low-frequency oscillations in real-time. To ensure accurate monitoring of system dynamics with noise-polluted WAMS measurements, several key signal-processing techniques are implemented to improve HHT method:

- Data pre-processing: cut the direct current processing and band-pass filter processing.

- Inhibit the boundary effect problem of the Empirical mode decomposition algorithm, which results in a serious distortion in the Empirical Mode Decomposition (EMD) sifting process. There are some methods: a). polynomial extension method, b). slope method extension method, c). parallel extension method, d). extreme point symmetric extension method, e). mirror method f). Boundary local characteristic scale extension method are used to inhibit endpoints effect caused by EMD
- Inhibit the boundary effect problem caused by Hilbert transform based on Auto-Regressive and Moving Average Model (ARMA).

Third, present an estimation algorithm method based on enhanced HHT for the parameters of a low frequency oscillation signal.

In the end, the developed scheme is tested with simulated signals and measurements from CampusWAMS. An oscillation monitoring system based on real-time wide-area measurements from PMUs is established. This oscillation monitoring system can detect poorly damped oscillatory modes which include: mode frequency, damping and mode shape. The results have convincingly demonstrated the validity and practicability of the developed scheme.

1.3 Outline of the Thesis

This thesis is structured as follows:

Chapter 2 introduces the concept of synchrophasor technology. Then it describes the recent development of PMU-based WAMS projects in major world. The CampusWAMS (campus wide-area measurement system) used throughout this thesis in order to demonstrate the feasibility of the proposed methods is also presented in this chapter.

Chapter 3 presents various low frequency oscillation analysis algorithms. It mainly introduces the concept, character and implementation process of FFT, WLT and HHT method. According to analysis the characteristics of low frequency oscillation signal we can get advantage and disadvantage of these algorithms.

Chapter 4 presents several key signal-processing techniques are implemented to improve HHT method. First, cut the direct current and design the band-pass Butterworth filter in order to collect the useful information from PMU data. Second, inhibit the boundary effect problem of based on extension method (caused by EMD) and Auto-Regressive and Moving Average Model (ARMA) (caused by Hilbert transform). Third, present an estimation algorithm method based on enhanced HHT for the parameters of a low frequency oscillation signal.

Chapter 5 presents an integrated scheme for the monitoring and detection of low-frequency oscillations has been developed based on enhanced HHT algorithm in CampusWAMS projects. It can determine the centre rage frequency of the concerned mode automatically and accurately, which is then be used to determine the parameter of the extraction. The extracted mode frequency, damping and mode shape can be detected by this oscillation monitoring system.

Chapter 6 summarizes the proposed oscillation monitoring system of this thesis. Challenging issues and future research trend are also discussed.

Chapter2. Wide-Area Measurement System Using Synchrophasors Technology

As the electric power grid continues to expand and as transmission lines are pushed to their operating limits, the dynamic operation of the power system has become more of a concern and has become more difficult to get accurately model. In addition, the ability to affect real-time system control is developing into the need to prevent wide scale cascading outages.

For decades, control centres have estimated the “state” of the power system (the positive sequence voltage and angle at each network node) from measurements of the power flows through the power grid. It is very desirable to be able to “measure” the system state directly and/or augment existing estimators with additional information.

Before Synchronized phasor measurement technology, all necessary power measurements in order for operation and control of power system come from supervisory control and data acquisition (SCADA) system. Various power system applications are running based on SCADA data, such as system monitoring, state estimation, fault location, disturbance analysis, etc. For SCADA data, only the

magnitude of voltage and current as well as real power and reactive power are measured. The angle of voltage at all buses or current on all lines have to be estimated based on available SCADA data using state estimation algorithms based on unsynchronized data points collected at a central location every 2-4 seconds, which could contain unpredictable errors. It is well known to power system engineers that the voltage phase angle more accurately, phase angle difference between any two buses plays a crucial role in the analysis, monitoring and control of power system stability. Therefore, the availability of bus voltage angle information due to synchrophasors technology can thoroughly open a new vision to operators for real-time observation and operation of a large power system.

This chapter introduces basic concepts of synchrophasors technology and answers questions, for the non-specialist, such as what is the WAMS? How it works? Why we need CampusWAMS?

2.1 Synchrophasor Technology

The concept of using phasors to describe power system operating quantities dates back to 1893 and Charles Proteus Steinmetz's paper on mathematical techniques for analyzing Alternating Current (AC) networks [21]. A phasor is a complex number that represents both the magnitude and phase angle of the sine waves found in electricity. Although phasors have been clearly understood for over 100 years, the detailed definition of a time-synchronized phasor has only recently been codified in the IEEE 1344 and the soon-to-be voted IEEE C37.118 Synchrophasor for Power Systems standards. Synchrophasors are time-synchronized phasor measurements. Satellite synchronized clocks allow time-stamped measurements that enable data to be aligned on reference time base. In other words, phasor measurements that occur at the same

time are called "synchrophasors", as are the PMU devices that allow their measurement.

An AC waveform can be mathematically represented by the equation:

$$X(t) = X_m \cos(\omega t + \theta) \quad (2.1)$$

In the phasor representation as:

$$X = X_m / \sqrt{2} \angle \theta \quad (2.2)$$

Where: X_m is magnitude of the sinusoidal waveform; $\omega = 2\pi f$, f is the instantaneous frequency; θ is angular starting point for the waveform

For a synchrophasor, the instantaneous phase angle is relative to a cosine function at nominal system frequency synchronized to Universal Time Coordinated (UTC). The time source of high accuracy is available from Global Positioning System (GPS). Adding in the absolute time mark, a synchrophasor is defined as the magnitude and angle of a cosine signal as referenced to an absolute point in time as shown in Figure 2 - 1. Time strobes are shown as UTC Time Reference 1 and UTC Time Reference 2. At the instant that UTC Time Reference 1 occurs, there is an angle shown as "+ θ " and, assuming a steady-state sinusoid, there is a magnitude of the waveform of X_1 . Similarly, at UTC Time Reference 2, an angle, with respect to the cosine wave, of "- θ " is measured along with a magnitude or X_2 . The measured angle is required to be reported in the range of $\pm\pi$. It should be emphasized that the synchrophasor standard focuses on steady-state signals, that is, signals wherein the frequency of the waveform is constant over the period of measurement.

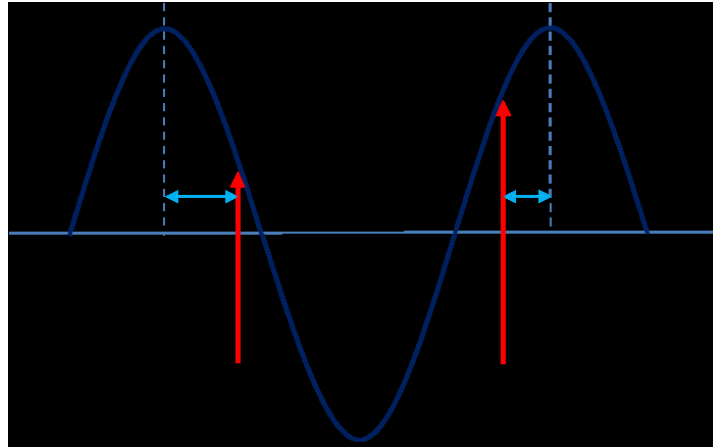


Figure 2 - 1 Synchronopasor Definition

The phase angle differences is very important in an AC power system, because that power flows from a higher voltage phase angle to a lower voltage phase angle, not as in DC circuits, power flows from high voltages to low voltages. The larger the phase angle difference between the source and the sink, the greater the power flow between those points implying larger the static stress being exerted across that interface and closer the proximity to instability.

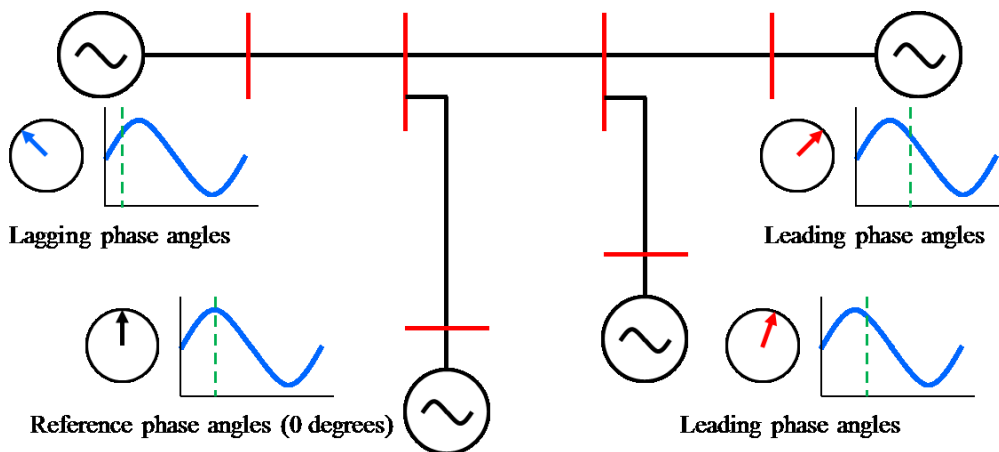


Figure 2 - 2 reference phase angles at remote locations due to GPS synchronization

The phase angle differences between two sets of phasor measurements are independent of the reference. Typically, one of the phasor measurements is chosen as the “reference” and the difference between all the other phase angle measurements (also known as the absolute phase angle) and this common “reference” angle is

computed and referred to as the relative phase angles with respect to the chosen reference (see Figure 2 - 2).

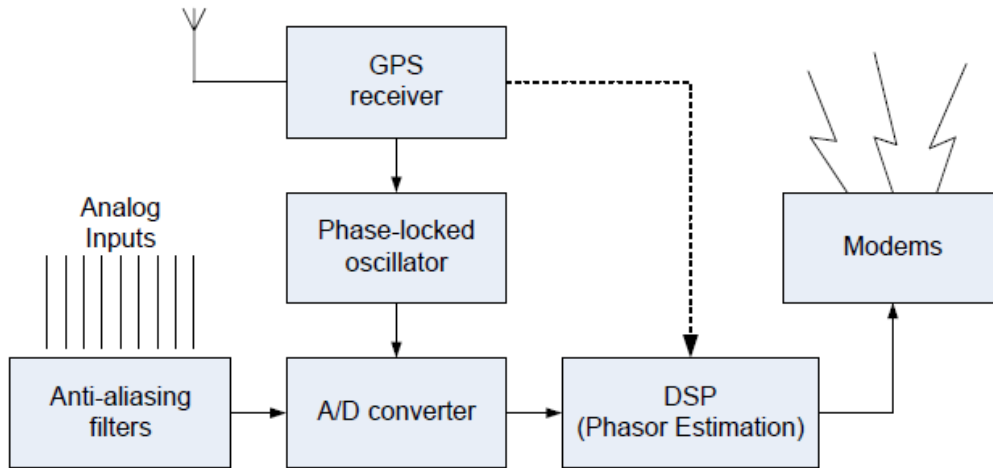


Figure 2 - 3 Phasor measurement unit block diagram

Synchrophasor technologies and systems use monitoring devices PMU that measure the instantaneous voltage, current, and frequency at specific locations in an electric power transmission system (or grid). Figure 2 - 3 illustrates major hardware block of a modern PMU. The synchrophasor data streams of 30 or more a second from PMUs are sent through a communications network to phasor data concentrators (PDCs), which collect, time-align and quality-check the data before sending them on for use in advanced applications.

2.2 Development of WAMS

Most of the synchrophasor projects are developing WAMS to collect synchrophasor measurements from PMUs that are on their power system or across the interconnection if they are a reliability coordinator, as shown in Figure 2 - 4. This figure shows a typical schema for a wide-area phasor measurement system including the communication and application levels. The measured data are collected by phasor

data concentrators (PDCs) via a communication network. The concentrated data could be exchanged between utilities by using the standard data format including the time stamp of the synchronized GPS time. The important function of a PDC is to receive, parse, and sort incoming data frames from the multiple PMUs [1]. While transmission operators are installing the PMUs, the real challenge is to build interconnection-wide networks of PMUs that share information across utilities and regional transmission organizations.

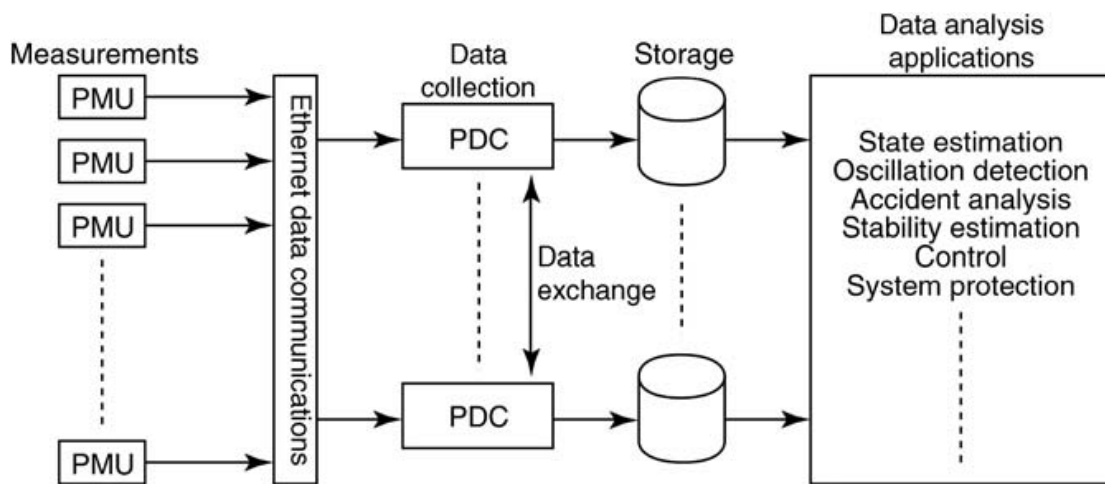


Figure 2 - 4 A schema of WAMS

The first prototypes of the modern PMU built at Virginia Tech were deployed at a few substations of the Bonneville Power Administration (BPA), the American Electric Power Service Corporation, and the New York power Authority[22]. This was resulted from this fact that the Western System Coordinating Council (WSCC) faced a critical lack of dynamic information throughout the 1980s. As a result, a general plan to address this problem was formed in 1990. The first commercial manufacture of PMUs with Virginia Tech collaboration was started by Macrodyne in 1991 [23]. Therefore, the Western Interconnection of the North America power system was the first test-bed for WAMS implementation. In 1995, the US Department of Energy (DOE) and the Electric Power Research Institute (EPRI) launched the WAMS project.

The aim of this project was to reinforce the Western System Dynamic Information Network called WesDINet. Dynamic information provided by WAMS of WesDINet has been very important and useful for understanding the breakups. This dynamic information can also be used for the purpose of avoiding future disturbances. Furthermore, during deregulation and restructuring process, information resources provided by this WAMS were utilized for maintaining the system reliability [24].

IEEE published first standard in 1995 governing the format of data files created and transmitted by the PMU. A revised version of the standard was issued in 2005 [25]. The latest version of IEEE standard was revised in 2011 [26]. Figure 2 - 5 shows the milestones in wide area measurement system.

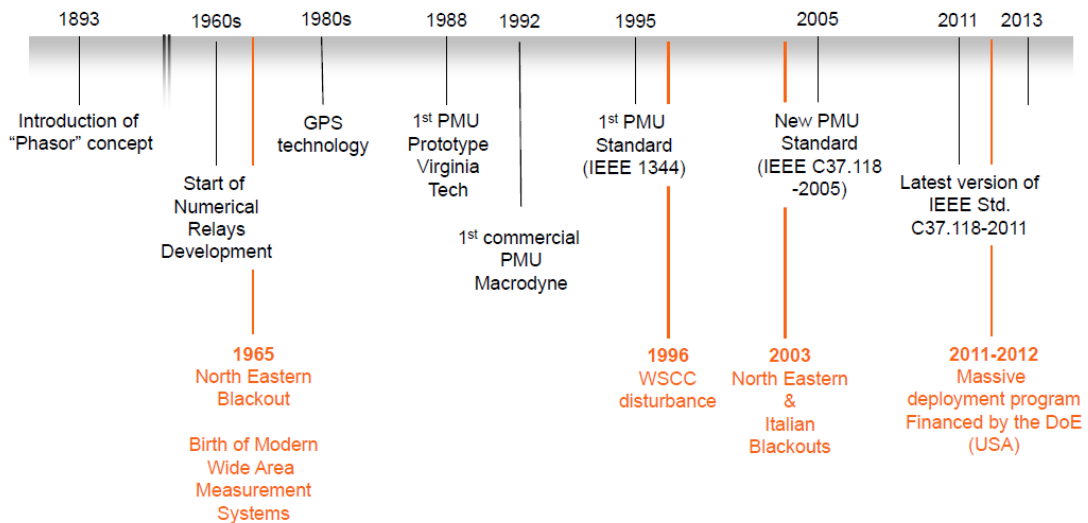


Figure 2 - 5 Milestones in wide area measurement system

2.3 WAMS in the World

In recent years, the interest in phasor measurement technology has reached a peak. In most countries installing the PMUs and getting to know the PMU system behaviour through continuous observations of system events has been the first step. All installations are reaching for a hierarchical WAMS so that the measurements obtained

from various substations on the system can be collected at central locations from which various monitoring, protection, and control applications can be developed. In this section, the current state and recent activities in WAMS development in major world economies are summarized based on the reports in [27-29].

1) North America

In the Western part of the United States, starting in 2002, the research and prototype testing efforts were combined with a real-time dynamic monitoring system (RTDMS) workstation for offline analysis by the California Independent System Operator (CAISO). In parallel, the deployment of real-time PMU data analysis, voltage, and dynamic stability assessment and data visualization applications were further enhanced by deploying the latest technology at BPA and several relevant utilities. For Eastern part of the United States, the establishment of the Eastern Interconnection Phasor Project (EIPP) was also started in 2003 and gained momentum as a result of the Northeast North America blackout of August 2003. Since early 2007, two projects have been combined to become the North American Synchrophasor Initiative (NASPI) that also covers Canada and Mexico. As of 2009, in excess of 200 PMUs are in service across the North America, and approximately 20 systems are being installed and implemented for various power applications.

In addition, the frequency monitoring network (FNET) which obtains GPS-synchronized wide-area measurements in a low-cost, easily deployable manner has been implemented in Virginia Tech. Over 40 Frequency Disturbance Recorders units have been deployed covering the three major interconnections of North America power grid to detect and analyse power system disturbances in near real-time.

2) UCTE (Central European)

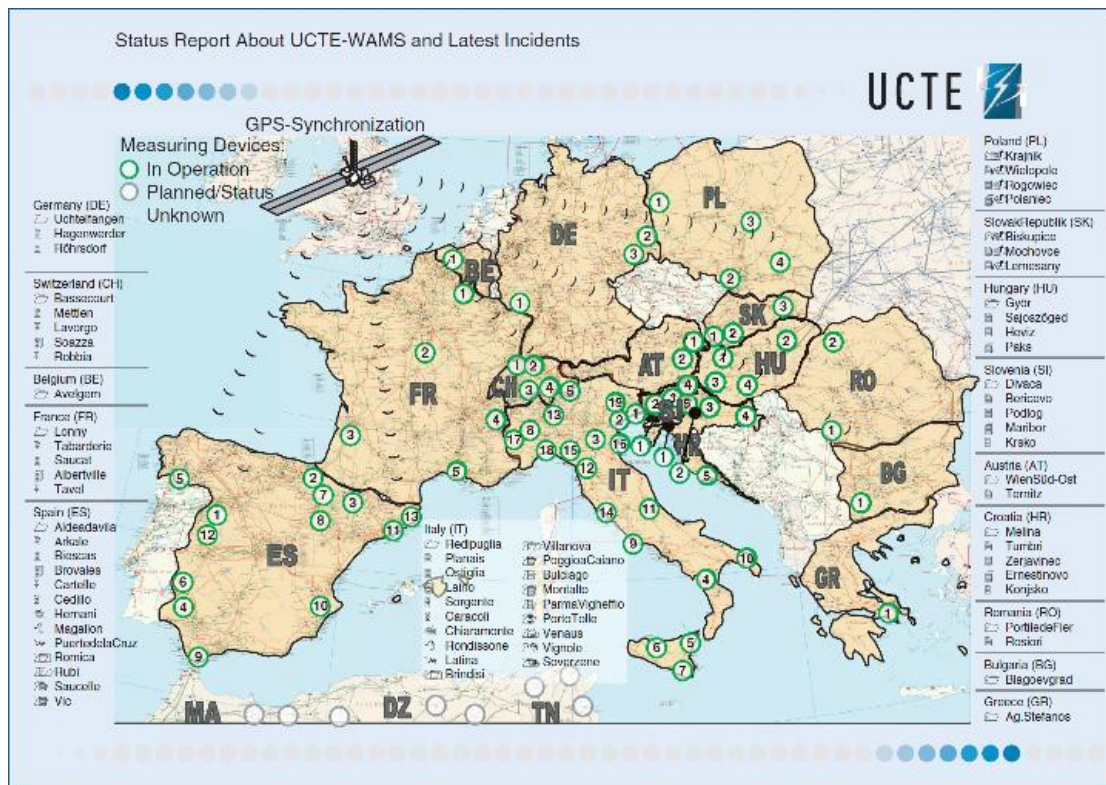


Figure 2 - 6 Central European WAMS devices[28]

Within the highly meshed power system of central Europe a multitude of WAMS are currently in operation (Figure 2 - 6). Inside the UCTE, wide-area phasor measurements are exchanged between the transmission system operators (TSOs) in order to calibrate the system dynamic models or for post-mortem analysis. One major focus currently is the monitoring of the occasional appearance of poorly damped inter-area oscillations. In the centre of the system and the southeast part, activities of exchanging online measurements between several data concentrators have already started and are in the phase of further extensions. The additional basic functions of these online devices include voltage phase angle difference monitoring, line thermal monitoring between two substations, voltage stability monitoring, and online monitoring of system damping.

3) Nordic (Northern European)

The PMU activities in Norway started around the year 2000. The TSO Statnett has built several projects. The PMU data are integrated with the Statnett SCADA system and recently a visualization tool based on LabVIEW was developed to combine PMU data and digital fault recorder data. In the very near future a project on phasor-based damping control of SVC and HVDC devices will be launched.

In Finland, the TSO Fin grid has installed a considerable number of PMUs. They are currently used for disturbance monitoring. A near-term goal is to present damping information in real-time, which may be extended to feedback control of an HVDC link or SVC to improve damping of inter-area oscillation.

Since 2005, streaming PMUs have been installed by the TSO Energinet.dk in Denmark. In order to monitor the ac interconnection with Germany, one of these is actually located in Germany. The main application so far is disturbance analysis, but future applications include monitoring of power plant operation, thermal line monitoring, and stability indicators.

In Sweden the TSO Svenska Kraftnat installs PMUs in their main stations as these are upgraded, which is done with a pace of about two stations a year. The plan is to integrate phasor data with the SCADA system to realize disturbance. Future use includes real-time monitoring of oscillations in the control centre and improved state estimation.

Since Iceland is isolated from the other countries in the Nordel system, the transmission system is relatively weak and electromechanical oscillations are an important issue to the TSO Landsnet. The system is therefore monitored using seven PMUs sending data to the national control centre, where damping of oscillatory

modes is presented in real time. The monitoring system has also been used for tuning of power system stabilizers with good results.

4) Russia

Synchronous interconnection of the 14 national power systems of Eastern Europe, Central Asia, and Siberia from the western borders of the Ukraine to Baikal and from Tajikistan to Kola Peninsula has been achieved. Interconnection consists of the unified power system (UPS) of Russia and Kazakhstan; the interconnected power system (IPS) of other 12 nations. It is the most geographically extended power system in the world, spanning eight time zones. Dynamic behaviour investigation of such an extended power system needs information on electromechanical transient parameters with high resolution and synchronized by GPS time tags. Such information is provided by IPS/UPS WAMSs. Development of this system started in 2005. Currently 26 PMU s are located in the major power plants and substations from the east to the west and from the south to the north of this immense interconnected power grid.

Phasor measurements in the IPS/UPS are currently used primarily for system performance monitoring and analysis. One of the important phasor measurements applications is the reference dynamic model validation. Another application considered is low-frequency oscillation monitoring, including assessment of amplitudes and decrements of oscillations with a frequency range of 0.02-0.2 Hz.

5) China

China owns one of the largest power networks in the world. Currently, the national power system is organized into two huge power grids, i.e. China State Grid and China Southern Grid, as well as several separated provincial power grids (e.g., Xinjiang, Tibet). Two grids are interconnected by HVDC links. Inside each grid, there are also

HVDC links connecting sub-grids. To securely and efficiently operate such a complex system is a real challenging problem. To meet the new challenges and at the same time to utilize the most up-to-date information and communication technologies in the power industry, numerous efforts have been made to develop PMU/WAMS applications in China since the middle 1990s.

The installation of PMUs in the China power grid began in 1995. By the end of 2002, Chinese manufacturers began to provide their own commercial PMUs, which have been commissioned in the China power grid since 2003. By the end of March 2007, about 400 PMUs had been commissioned. These are installed at the substations and power plants of 500 kV and 330 kV voltage levels. Furthermore, it is reported in [14] that by the June of 2009, over 1000 PMUs have been commissioned in China power grid and all the 500 kV and above substations and 100-MW and above power plants have PMUs. With more than one manufacturer of PMUs, a Chinese standard on PMUs and WAMS was drafted by the State Grid Company and manufacturers in 2003 and issued in 2005. The standard defines the transmission protocol of historical data, provides technical specification for manufacturers and allows interchange of data between a wide variety of users of both real-time and offline phasor measurements.

The functions of China WAMS include visualization of dynamic processes and available transmission capacity, wide-area data recording and playback, and online low-frequency oscillation analysis, etc. Due to the long transmission distances and weak interconnections, inter-area low-frequency oscillations are a severe problem in China. As the only tool capable of capturing the oscillation data, the WAMS plays an important role in low-frequency oscillation identification and control in China. The closed-loop low-frequency identification and damping control system has passed the field test. Other PMU applications, such as state estimator, security assessment,

adaptive protection, and emergency control are also currently undergoing development.

6) Korea

Korea's primary goal for synchronized phasor data use has been to monitor the system dynamics and to build a database for validating the simulation models. In Korea National Control Centre they monitor the system conditions at the sampling rate of 10 times per second. For archiving purposes the phasor data is kept for two minutes in normal condition. When a major disturbance occurs, data for eighteen minutes after the disturbance, plus two minutes before, are stored permanently for later analysis. For monitoring purposes the instantaneous phasor measurement are stored for one second in normal conditions and for 15 seconds in fault conditions for later analysis such as validating operations of the protection system and electromagnetic transient models. On line TSA and VSA tools are also under development.

7) India

In India, large generation addition is taking place, and continuous expansion of the grid through increasing grid connectivity is leading to the geographical spread of the grid. Power flow is taking place in multiple directions coupled daily/seasonal basis. Under this situation, it becomes important to know the dynamic state of the grid and this issue calls for development of an intelligent grid on the basis of WAMS. Toward achieving this objective, the POWERGRID, the central transmission utility, initiated the work for development of an intelligent grid comprising WAMS, remedial action scheme (RAS) and system integrated protection scheme (SIPS), etc., for dynamic state estimation and control purposes. For this, the following staged approach is

adopted: In the first stage, a few PMU s (four to five in each region) are to be installed at critical buses in all the regional grids. Output of these PMUs can be used to validate the offline simulation models, especially exciter and governor characteristics of large generators. Based on the output of these PMUs, a common state estimator is to be developed by combining regional state estimators. Based on the success of stage 1, more PMU s are to be installed at various buses. All the PMU data are to be stored in different PDCs. Further, data from a number of PDCs will be collected at a central location. After installing PMUs, many phenomena hitherto unknown, such as poorly damped oscillations, can be detected. In the final step, RAS and SIPS for regulation and control purpose are to be developed.

8) Australia

The major power system in Australia encompasses the states of Queensland, New South Wales, Victoria, South Australia and Tasmania, with voltage levels ranging from 500kV down to 110kV. This interconnected system represents a power system that stretches for 5000 km with a maximum demand of about 30 GW. The long, thin nature of this system, which hugs the coast of eastern and southern Australia, has long presented unique problems in terms of oscillatory stability, both in design and operation. . With new phasor measurement technology, it is possible to monitor system damping and ensure that the system is operated within its technical envelope. The TSO, NEMMCO, employs both short term and long term model-estimators to achieve this. NEMMCO, together with PowerLink, the transmission network service provider in Queensland, have installed a Psymetrix Power Dynamics Management (PDM) system with a number of measurement nodes in various locations around the power system. The Psymetrix PDM employs advanced signal processing techniques

to continually assess system damping by monitoring the oscillations in steady state power transfers.

9) Brazil

The Brazilian National Interconnect Power System (SIN) is characterized with a dominant hydroelectric power generation and long-distance power transfers from generation parks to load centres. Studies for phasor measurement applications in Brazil were started in the early 1990s. Since late 2000, the Brazilian independent system operator ONS has launched two WAMS-related projects which aim to implement a large-scale synchronized phasor measurement system (SPMS) for both offline and real-time applications. One project is "Deployment of a Phasor Recording System". The main goal of this project is to specify and deploy a SPMS to record SIN system dynamics during long duration wide-area disturbances, envisioning the most probable future real-time applications. Another project is "Application of Phasor Measurement Data for Real-Time System Operation Decision Making". The main goal of this project is to extend the initial SPMS for control center real-time applications, such as phasor visualization, modal frequency alarming, and state estimator improvement for supporting system dispatcher real-time decisions.

During 2007, ONS investigated the effective use of phasor measurement technology to improve real-time system operation. The following four were chosen for a proof-of-concept pilot implementation: a tool to monitor system oscillations in SIN and alarm dispatchers for oscillations with poor damping; a tool to monitor the stresses of the electric power transmission system based on the angle differences; a tool to assist the dispatchers to resynchronize islands using angle differences information; A tool to assist the dispatchers to close loops in parts of the SIN using angle differences information.

10) Other Countries

It has been reported that the following countries have installed and integrated phasor measurement units for research or to develop working prototypes for wide area monitoring and control: Switzerland, 4 units; Croatia, 2 units; Greece, 2 units; Mexico, more than 4 units and South Africa, 2 units.

2.4 The CampusWAMS

In this thesis, the CampusWAMS, which is the written abbreviation of Campus Wide-Area Measurement System, is used to specially represent the phasor measurement system that was initially proposed and started to construct since 2002 by one research group under the leadership of Prof. Mitani of Kyushu Institute of Technology [30]. Since the multiple phasor measurements from the CampusWAMS will be used in the following chapters of the thesis, some necessary information of the CampusWAMS, such as its cover range and technical specification, is given in this subsection.

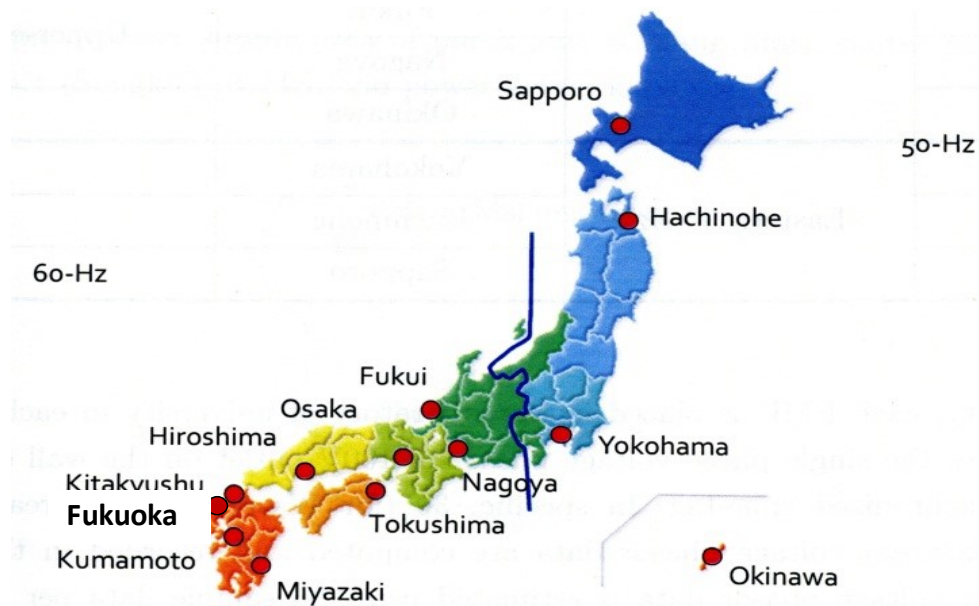


Figure 2 - 7 PMUs location for the CampusWAMS in Japan

Until now, the CampusWAMS has been developed to cover the typical power supply areas of the entire Japan nation-wide power grid. In specific, the CampusWAMS presently encompasses 13 PMUs: 10 of them are installed in the supply area of Western Japan 60-Hz system and another 3 in the supply area of Eastern Japan 50-Hz system. The locations of these 13 PMUs are marked with red-filled circle associated with respective city name in Figure 2 - 7. All PMU are the same model NCT2000 Type-A manufactured by Toshiba [31].

In Japan, there are ten independent power companies which individually operate their own power network as well as the tie-lines that link them to the adjacent companies. Because each power company is independent operating entity, there is no way to collect synchronized phasor measurements of transmission high voltage level from all power companies at present. For the CampusWAMS, however, at least one PMU is installed in the supply network of each power company; therefore, the CampusWAMS is in fact a unique wide-area monitoring system which spreads over the overall power supply area of ten companies and continuously provides synchronized phasor measurements of practical systems.

For reference and later use, 13 PMUs in the CampusWAMS of Japan are numbered and grouped as Table 2 - 1. Three groups are defined for eight PMUs in the Western Japan power system. The lower-end group includes University of Miyazaki, Kumamoto University, Kyushu University and Kyushu Institute of Technology. The upper-end group includes University of Fukui and Nagoya Institute of Technology. The centre group includes Hiroshima University, University of Tokushima and Osaka University.

Table 2 - 1 PMUs of the CampusWAMS in Japan

| No. | Area | Location | Group |
|-----|---------------|------------|-----------|
| 1 | Western 60 Hz | Miyazaki | Lower end |
| 2 | | Kumamoto | |
| 3 | | Kitakyushu | |
| 4 | | Fukuoka | |
| 5 | | Hiroshima | Center |
| 6 | | Tokushima | |
| 7 | | Osaka | |
| 8 | | Fukui | Upper end |
| 9 | | Nagoya | |
| 10 | | Okinawa | |
| 11 | Eastern 50 Hz | Yokohama | |
| 12 | | Hachinohe | |
| 13 | | Sapporo | |

In reality, each PMU is placed in the laboratory of university in each city. Every PMU measures the single phase voltage phasor of 100V outlet on the wall of laboratory with GPS-synchronized time-tag. In specific, 30 (for Western 60-Hz area) or 25 (for Eastern 50-Hz area) voltage phasor data are computed and recorded in the PMU per second and each voltage phasor data is estimated using 96 sample data per voltage sine-wave cycle. Afterwards, for every 20 minutes, the voltage phasor data saved in each PMU are automatically transmitted and collected into multiple data servers and saved as one single data file for future offline analysis. That is to say, each data file contains the 1,200s measurements of single phase voltage waveform. There

are 36,000 phasor data in case of Western 60-Hz area and 30,000 phasor data in case of Eastern 50-Hz area. The developed analysis applications run in other computers and read data from these servers to process.

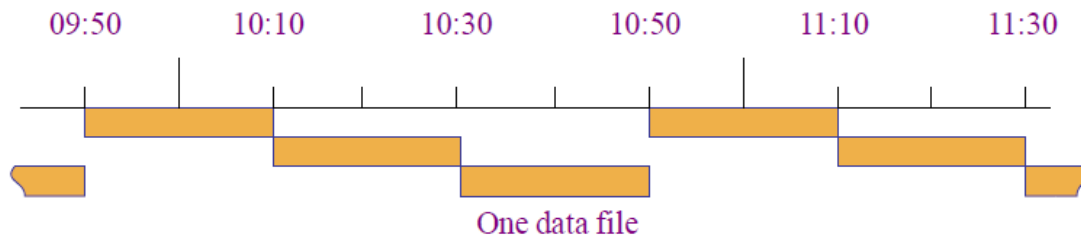


Figure 2 - 8 Data file recording scheme

Thus, a wide-area measuring and monitoring system is constructed. Moreover, the start time-point of above-mentioned 20 minutes setting can be specified as required. Currently, as illustrated in Figure 2 - 8, three data files are generated for the time sections from 50-min to 10-min, 10-min to 30-min and 30-min to 50-min respectively in the period of one hour.



Figure 2 - 9 PMUs location for the CampusWAMS in Thailand

From 2004, the project of CampusWAMS was extended to install PMU in the power grid of several countries in Southeast Asia such as Thailand, Singapore and Malaysia. The CampusWAMS of Thailand power system, as shown in Figure 2 - 9, consists of three PMUs which are placed at three universities respectively. Three PMUs cover the typical power supply area of north part (Chiang Mai), center part (Bangkok), and south part (Songkla) of Thailand power network. Figure 2 - 10 demonstrate PMUs location for the CampusWAMS in Singapore and Malaysia.



Figure 2 - 10 PMUs location for the CampusWAMS in Singapore and Malaysia

Similarly, these PMUs measure the single phase voltage phasor of 220V wall outlet in the laboratory with GPS-synchronized time-tag. Because the nominal frequency of Thailand power system, Singapore and Malaysia power system are 50Hz, 25 phasor data are computed and recorded in the PMU per second. The phasor measurements of every 20 minutes are transmitted and saved into data servers as one single data file.

Chapter3. On-line Oscillation Characteristics Monitoring Algorithm Analysis

Power system oscillation signal is typically nonlinear and non-stationary signals. In recent years, how to detect and analyze low frequency oscillation phenomenon exists in the power system has become a focus of research topics. For this reason, experts and scholars around the world have done a lot of research in regard to the oscillating signal in the field the power system time-frequency analysis, and made a number of processing methods on the oscillation signal such as Hilbert-Huang transform (HHT) [32], fast Fourier transform (FFT) Method [30], Wavelet Transform (WLT) Method [33], Prony's Method, Matrix Pencil Method, Hankel Total Least Squares (HTLS) Method etc. [34].

This chapter describes low frequency oscillation mechanism and employs the HHT method, the WLT method and the FFT method to analyze the inter-area (global) oscillation characteristics. The data are collected from a network of distributed PMUs through a national project called Campus WAMS, which is introduced in chapter 2, and then the recorded phase difference data are analyzed using WLT, FFT and HHT

methods, respectively. A comprehensive comparison is performed, and it is demonstrated that HHT offers more flexibility in terms of detailed profile and enough description, which can be beneficial for power system small signal stability analysts following estimation of system low-frequency oscillation. The results could be useful for on-line tuning of power system stabilizers.

3.1 Background of Power System Low Frequency Oscillation

3.1.1 Low Frequency Oscillation Mechanism

Low frequency oscillations (LFO) are generator rotor angle oscillations having a frequency between 0.1 -2.0 Hz [35]. It can be classified as local and inter-area mode [35][36]:

Local modes are associated with the swinging of units at a generating station with respect to the rest of the power system. Oscillations occurred only to the small part of the power system. Typically, the frequency range is 1Hz -2 Hz.

Inter-area modes are associated with swinging of many machines in one part of the system against machines in other parts. It generally occurs in weak interconnected power systems through long tie lines. Typically frequency range is 0.1Hz-1 Hz. This oscillation has greater harmful because that once it happened, it will spread to the whole system through junctor.

In general, the mechanism of low frequency oscillation damping mechanism is divided into Negative Damping Mechanism, Resonance (forced oscillation) Mechanism, Harmonic Oscillation Mechanism, and Nonlinear Mechanism, which include Chaotic Theory and Branch Theory.

A. Negative Damping Mechanism

Due to the increase of enlargement factor of the excitation system, the real part of numerical value of characteristic root which corresponds with the rotor mechanical oscillations is changed by the positive, which produces the negative damping effect and counterbalances positive damping, making total damping of the system negative or very small. Once the disturbance appears, the system shafting will turn up increasing oscillation, initiating low frequency vibration of the system.

B. Resonance (forced oscillation) Mechanism

Inputting or disturbing signal of the system have some kinds of characteristic relationship with natural frequency of system, it may cause resonance when it represents the low frequency oscillation is in low frequency area.

C. Harmonic Oscillation Mechanism

The power system is influenced by periodic disturbance outside, and when the disturbance frequency and natural frequency of system has some kinds of special relationships, it will have sympathetic vibration. When it is in the low frequency zone, it represents the low frequency vibration.

D. Chaotic Phenomenon

The chaos is a very complex phenomenon that cause by various parametric interactions in the nonlinear system. In common usage, "chaos" means "a state of disorder" [37]. It is one kind of long dynamic behavior that is very sensitive to initial conditions. It often presents continuous rule-less oscillation the following operational factor of system in the power system.

E. Branch Theory

The term Hopf bifurcation (also sometimes called Poincar'e-Andronov-Hopf bifurcation) refers to the local birth or death of a periodic solution (self-excited oscillation) from equilibrium as a parameter crosses a critical value. Bifurcations are the qualitative changes in the system behavior under variations of system parameters [38][39]. If the key parameters of a power system such as mechanical input power, electrical load, and transmission-line length are varied, it is possible for the stable equilibrium point of the system to lose stability for some parameter values. At such a loss of stability the system undergoes a local bifurcation, which can give rise to new equilibria or limit cycles [40]. The analysis of local bifurcations is performed by studying the dynamics near equilibria. Of the local bifurcations, Hopf bifurcations are readily evident in power systems as important mechanisms of oscillatory behavior.

As mentioned above, negative damping mechanism is widely recognized mature theory in both engineering field and academia field for analysis the cause of the low-frequency oscillations. Although the forced oscillation mechanism have also been used in many engineering projects, it is mainly used in the design and manufacturing stages. And it is rarely applied to analyze and study the low-frequency oscillations in

research field. Currently, the Branch Theory, correlation analysis is limited by system size and the order of the equation due to the complexity of the calculation. Since the late appearance of chaos theory and its high complexity, this nonlinear mechanism is still in its initial theoretical discussion stage. It always targeted at small systems for the study. All in all, it is commonly believed that low-frequency oscillations occur due to negative damping system.

3.1.2 Theoretical of Measurement-based Analysis

After the introduction of wide-area time-synchronized phasor measurements, measurement-based analysis becomes possible. Owing to the high-speed, high accuracy and time-synchronization sample technology of modern PMU, the variables that tightly relate to the dynamic of small-signal stability, such as bus voltage angle, bus frequency or tie-line active power, are readily available. Even the measurements of these dynamic variables come from distant, wide-spread multiple locations of a large power system, it is safe to compare or process them together due to time-synchronization among all measurement locations. Based on these real-time phasor measurements, new methods can be developed to perform online or near real-time small-signal stability analysis.

3.1.2.1 Concept of Measurement-based Method

The measurement-based method is more like the concept of system identification—to identify an approximate model or estimate an quantity that can describe the system

dynamic or its characteristics, given that the output (and/or the input) of a system is measurable.

In this concept, the system to be analyzed is assumed to behave like a 'black-box', i.e. no detail information about the inside of the system is known; only the output and/or input of the system are measured. The object is to find a model—parametric or nonparametric model—that can reproduce the same output with measured data when the same input is applied. Under most situations which are actually more common for a practical power system, only the output of the system is available and the input to the system is either unidentifiable or unmeasurable. Figure 3 - 1 explains the underlying theory that to analyze the power system oscillations using the phasor measurements.

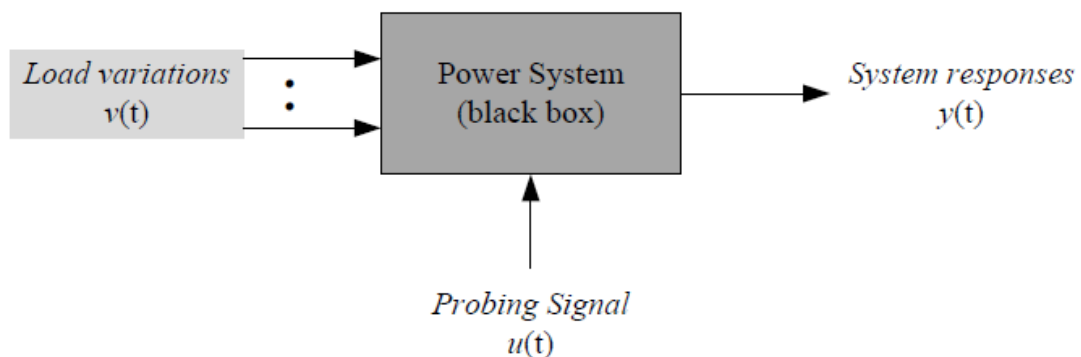


Figure 3 - 1 Concept of measurement-based analysis

3.1.2.2 Characteristic of Measurement-based Method

As seen from the concept of measurement-based method, there mainly have two characteristic:

- Phasor measurement-based methods have no dependence on a complex system mathematical model which can only be formed by knowing all information about the system in advance.
- It is assumed that only the measurement of system output variables (and/or input variables) is available.

Suppose we don't know too much about the detail of the power system to be studied so that it is basically regarded as a black-box. But one thing we do know is that the power system is constantly subjected to the small-disturbances, i.e. some load variations. The feature of load variations in a practical power system is that they are neither predictable nor measurable, which indicates the randomness of the small load variations. Consequently, these random small load variations can be considered as noise inputs (i.e. excitations) to the power system and then the power system will respond to these excitations. Unlike unmeasurable noise inputs, the power system responses to random load variations can be easily measured from various power variables such as bus voltage or line current. Therefore, the key point of underlying theory of measurement-based method is: the output signal must contain the effects of both the input signal and the system dynamics. In other words, from the output signal measurements, the characteristic of the dynamics or modes which the system contains can be observed and discovered. Moreover, since the input noise is unknown in this case, the developed method is only based on the measurements of the output signals.

Another way to excite the studied power system is to use probing signal. A well-designed probing signal is usually imposed into the system through some control

devices such as AVR, dc converter and the system responses corresponding to this special signal are measured. Similarly, the output signal must contain the effects of both the probing signal and the system dynamic characteristic. In this case, the developed method can be based on the measurements of both signals because the input probing signal is known.

Either way, the final output measurements contain measurement noise produced by instruments, communication channels, recording systems, and similar devices. It is hard to separate the real responses to input signals from these measurement noises which are basically unpredictable and unmeasurable. Therefore, the developed methods must consider pre-processing the final output measurements before they are used for power system oscillation analysis.

3.2 Traditional Method of Low Frequency Analysis

From phasor measurement of the Campus WAMS, the following signals can be computed: voltage phase difference between two locations and frequency deviation at each location. In general, either phase difference signal or frequency deviation signal can be used to monitor/estimate the characteristic of the inter-area oscillation mode. Here, the phase difference signals are used for this purpose. Figure 3 - 2 shows waveforms of phase difference measured between Kyushu University and Osaka University in 6:50-7:10 of July 16, 2011. It presents a normal situation without a big fluctuation in power system oscillation. It is noteworthy that the FFT cannot be

applied to the non-stationary and non-linear data and the WLT cannot be applied to the non-linear data.

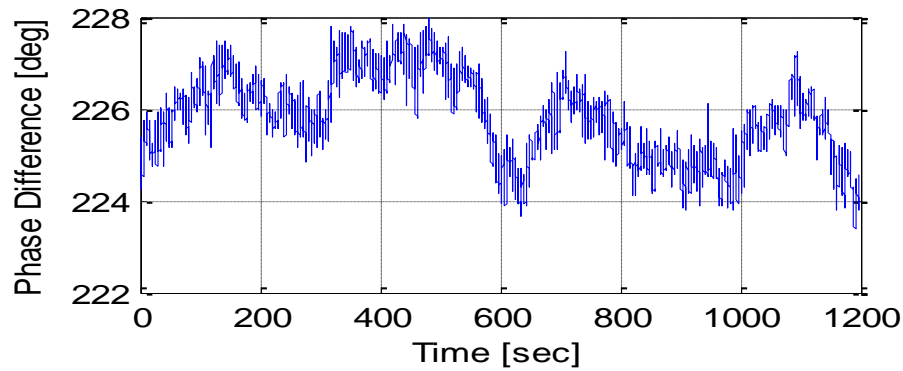


Figure 3 - 2 Phase difference between Kyushu University and Osaka University Stations

3.2.1 The FFT Method

The Fourier transformer has been already used for estimating parameters of various oscillation modes, simultaneously [41]. However, the power system oscillation should change in frequency from location to location, and time to time, even within one oscillation cycle. This intra-frequency oscillation is the hallmark of nonlinear systems. In the past, when the analysis was based on the linear Fourier analysis, this intra-wave frequency variation could not be depicted, except by resorting the harmonics. Thus, any nonlinear distorted waveform can be referred as a “harmonic distortion.” Harmonics distortions are a mathematical artifact resulting from imposing a linear structure on a nonlinear system. They may have mathematical meaning, but physically meaningless.

The Fourier series are made up of sines and cosines; the Fourier transform is a generalization of the Fourier series, and is performed by exponentials and complex numbers. The Fourier analysis has wide applications in mathematics and engineering such as heat transfer, wave propagation, circuit analysis, electronic circuit analysis, and vibrations. Interesting to note is the Fourier kernel, $e^{2\pi i\omega t}$, which is a solution to an n th order linear differential equation which, in turn, is used to model various physical; it is one reason why Fourier analysis has such wide applications.

On the interval $[-\pi, \pi]$, and arbitrary function $f(t)$ which is periodic and single-valued could be represented by the trigonometric series:

$$f(t) = a_0 + \sum_{n=1}^{\infty} a_n \cos nt + \sum_{n=1}^{\infty} b_n \sin nt \quad (3.1)$$

For a periodic interval T ,

$$f(t) = a_0 + \sum_{n=1}^{\infty} a_n \cos n\omega t + \sum_{n=1}^{\infty} b_n \sin n\omega t \quad (3.2)$$

where $\omega = 2\pi/T$, $a_n = 2/T \int_t^{t+T} f(t) \cos n\omega t dt$, $b_n = 2/T \int_t^{t+T} f(t) \sin n\omega t dt$,

T = period of $f(t)$.

For a signal or function $f(t)$, the Fourier transform is defined as:

$$F(\omega) = \int_{-\infty}^{+\infty} f(t)e^{-i\omega t} dt \quad (3.3)$$

and the inverse Fourier transform to recover the original signal or function is defined as:

$$f(t) = \frac{1}{2\pi} \int_{-\infty}^{+\infty} F(\omega)e^{-i\omega t} d\omega \quad (3.4)$$

These two Fourier transform equations are called a Fourier transform pair. The original function is in the time domain t , which is transformed into the frequency domain ω . The resulting transformed signal gives an indication of the frequency

components that contribute to the original signal when a spectral plot of amplitude versus frequency components is constructed. The function $f(t)$ can be continuous or discrete; however, the preceding definition for the Fourier transform intrinsically assumes to be continuous. The discrete Fourier transform (DFT) of a discrete signal, $f(t)$, designated as F_n , is defined as:

$$F_n = \frac{1}{N} \sum_{j=1}^N f_j e^{-2\pi i n j / N} \quad (3.5)$$

and the inverse discrete Fourier transform as:

$$f_j = \sum_{n=0}^{N-1} F_n e^{2\pi i n j / N} \quad (3.6)$$

where n and j are indices.

The DFT is a digital tool used to analyze the frequency components of discrete signals, while the continuous Fourier transform is an analogue tool used to analyze the frequency components of continuous signals. A fast Fourier transform (FFT) is an algorithm that efficiently implements the DFT on a computer. Usually, power spectral density (PSD) plots are preferred to Fourier transform plots; PSD, in this research, is equivalent to the square of the amplitude of the Fourier transform, which has a continuous dependence on absolute frequency (or in this case, wavenumber (cycles/m)). If P denotes PSD, then

$$P = k|A|^2 \quad (3.7)$$

where A is the amplitude of Fourier transform and k the appropriate scaling constant.

A property of the PSD is given as follows:

$$\int_0^{\infty} P(f) df = \sigma^2 \quad (3.8)$$

where σ^2 is the variance of the original signal.

In other words, the total variance of the signal is recovered upon integrating the plotted spectral values over the frequency range.

In this study, the FFT filter uses a kind of data filtering technique in the pure frequency domain. At first, the FFT of original data is computed; then, the FFT components beyond the designated frequency band are set to zero; and finally the Inverse FFT is applied to the remaining data. Thus, the extracted data only contains components within interested frequency range.

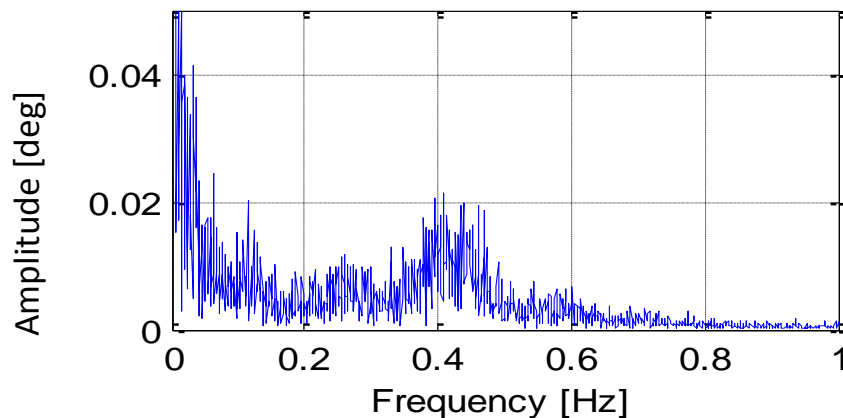


Figure 3 - 3 The FFT analysis for the phase difference shown in Figure 3 - 2

Here, we would like to examine the above extraction method of a power system oscillation. The obtained phase differences shown in Figure 3 - 2 are analyzed by the FFT in order to examine the frequency characteristics. These results are set out in Figure 3 - 3. As seen the existence of this dominant inter-area oscillation mode is observed at a frequency around 0.4 Hz. This result is almost matched with the given one for Japan West Power System in [42]. In the next step, a frequency band of 0.4 ± 0.05 Hz is considered and the other data have been removed.

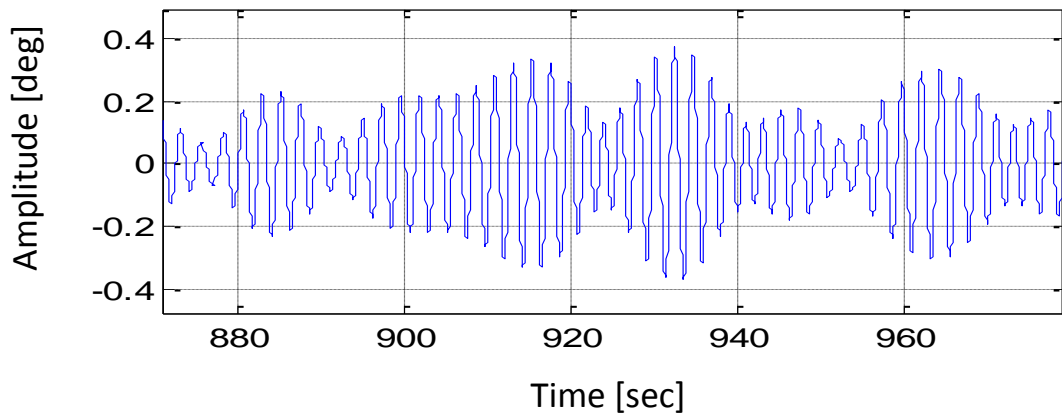


Figure 3 - 4 Extracted low-frequency oscillation extracted

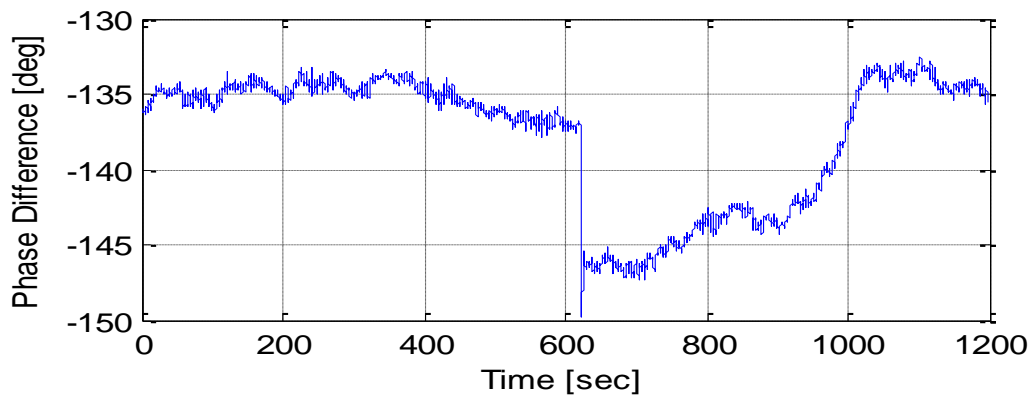


Figure 3 - 5 20 minutes phase difference between Kyushu University and Osaka University in Oct.04, 2011

Figure 3 - 4 demonstrates the power system low-frequency oscillation extracted from phase differences shown in Figure 3 - 3 at a frequency around 0.4 Hz using Inverse FFT method. In this figure, the amplitude of obtained signal oscillation data corresponding to dominant inter-area oscillation mode of Kyushu University and Osaka University in western Japan 60 Hz power system is not important and it is only useful for analyze stationary and linear data. For example, consider Figure 3 - 5, which shows phase difference measured between Kyushu University and Osaka

University from 13:30 to 13:50 in Oct. 04, 2011. The large step change after 600s is due to outage of a nuclear power generation unit (Genkai nuclear power unit 4) in Kyushu Electric Power Company. The FFT method is not effective for application in such cases.

3.2.2 The Wavelet Method

Wavelet analysis with high resolution is also known as a temporal frequency analysis method, which also shows the discrete transform is made in time domain and spectra analysis is made in time frequency domain. Although the wavelet transform was introduced to solve the problem by presentation of frequency and energy content in the time domain, it still suffers from the convolution of a priori basis functions with the original signal. The wavelet base (or mother wavelet) selection is an important problem for wavelet analysis applied in engineering, because using different mother wavelets to analyze same problem will produce different results. Therefore, wavelet analysis results are limited by mother wavelet, and wavelet components and wavelet spectra are meaningful only to the selected mother wavelet. Although these problems exist in wavelet analysis, it is still an effective method to analyze non-stationary data [43].

The WLT method is introduced to circumvent the Heisenberg uncertainty using adjustable-width basis functions called wavelets that could stretch or compress depending on whether the wavelet is on a low-frequency section or a high-frequency section of the signal being analyzed. A wavelet has a finite duration and zero mean.

The result is a localized analysis that gives both good frequency and temporal resolutions, just as classical Fourier analyses. The WLT method has the following general definition:

$$W(d, \tau; X, \psi) = \frac{1}{\sqrt{|d|}} \int_{-\infty}^{+\infty} X(t) \psi^* \left(\frac{t-\tau}{d} \right) dt \quad (3.9)$$

where W is the wavelet coefficient, d is the dilation or scale factor (for frequency scale), τ is the translation of the origin (for temporal location), and $\psi^*((t - \tau)/d)$ is the basic wavelet function (mother wavelet). The example forms of the mother wavelet include the Symlet, Haar, Mexican Hat, Coiflet, Daubechies, and Morlet wavelets. Basically, wavelet analysis can be summarized in the following steps:

Step 1. Choose mother wavelet type.

Step 2. Compare with the beginning section of the signal at time, t_0 ; compute W_0 .

Step 3. Slide wavelet to next section of signal at time, t_0+1 ; compute W_1 .

Step 4. Compute all W_i for all times.

Step 5. Use wavelets of various scales of interest (stretched or compressed) and repeat steps 1-4.

Step 6. Plot graph of scales vs. time with magnitude of W_i being colour intensity at each time-scale coordinate.

A desirable feature of the WLT method is the uniform resolution for all scales; however, this feature can be disadvantageous when there is a poor resolution since it will affect all the scales. Additional disadvantages include spectral leakage and it being non-adaptive (only the chosen basic wavelet is used in the whole analysis).

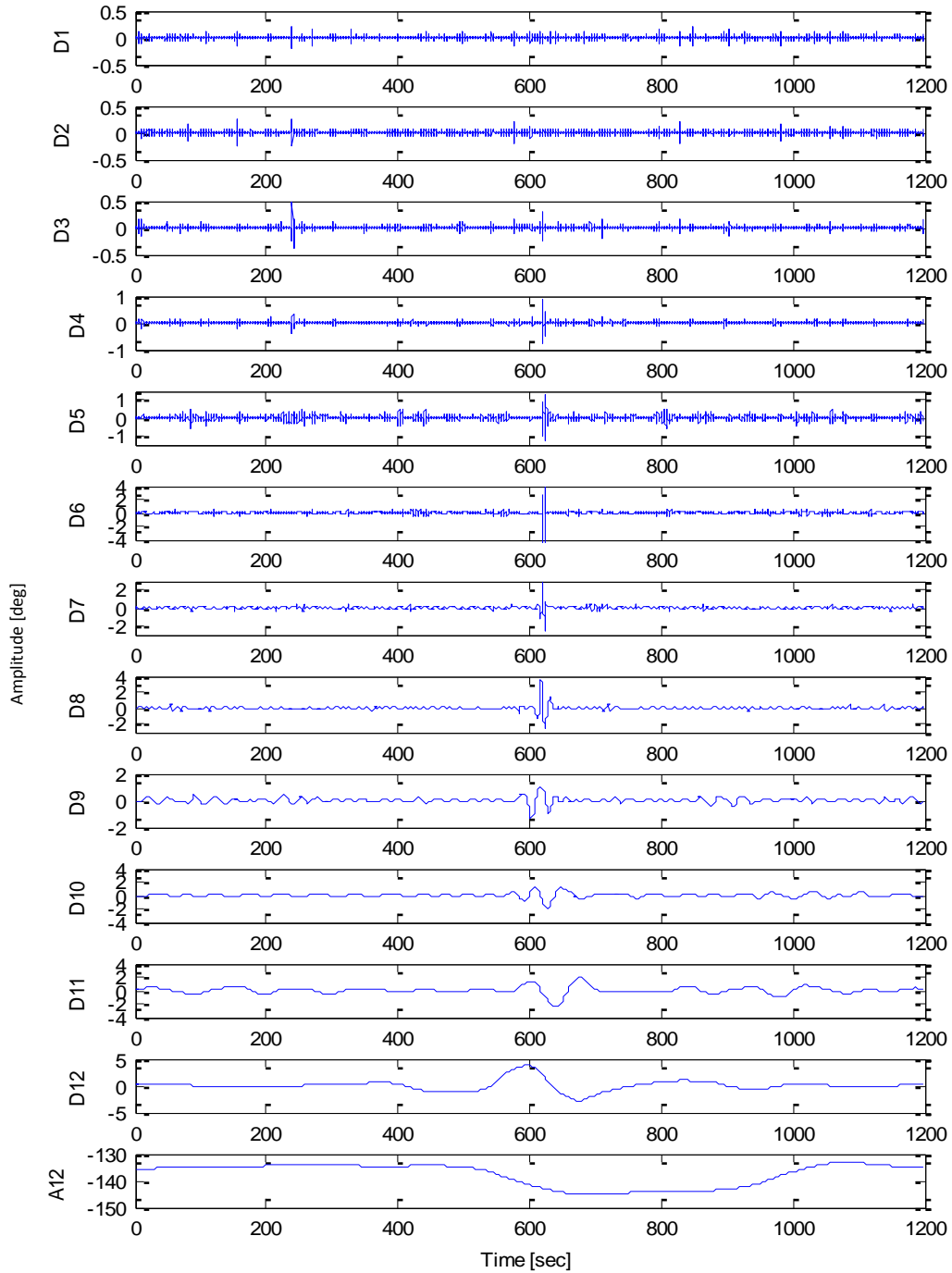


Figure 3 - 6 Wavelet components with use of Symlets wavelet

The Symlet wavelet function is almost used in wavelet analysis. Here, it is also used as a base function to do wavelet analysis. The application of WLT method leads to the decomposition of phase difference plot. Figure 3 - 6 shows decomposed phase difference signal between Kyushu University and Osaka University. Some on/off

switching behaviors are observed from 0 to 1200 seconds in D1, D2 and D3. These waveforms were isolated from the original data to eliminate any effect of the switching behaviors. This result shows that the influences generated by load fluctuations are eliminated. This technique could be very useful for the extraction of noises. A significant fluctuation around the 620 seconds can be seen in D4 to D12. The Low frequency oscillations due to generator rotor angle oscillations have a frequency between 0.1-2.0 Hz and can be classified based on the oscillation source [35]. However, using the wavelet it is not known which signal is between 0.1-2.0 Hz. Therefore, one may apply the FFT to every wavelet to convert the original data to the signals containing main power system low-frequency oscillations. In this case, D1 to D3 signals are over 2Hz and D8 to D12 signals are under 0.1 Hz, and they do not probably include the power system low frequency oscillations.

3.3 New Method of Low Frequency Analysis (HHT)

Hilbert-Huang Transform (HHT) is a fully adaptive time-frequency analysis methods, suitable for both non-linear and non-stationary signal analysis as well as for linear and stationary signal analysis [44]. The HHT applies empirical model decomposition (EMD) to decompose the low frequency oscillation signals and calculate the instantaneous parameters including frequency of every model component. Then, it calculates the damping ratio of every model component based on above parameters and the derived formulas. This method can be applied to analyze strong

non-linear oscillation models in power systems and design damping controllers in future.

3.3.1 The Empirical Mode Decomposition Method

The empirical mode decomposition (EMD) was performed to extract intrinsic mode function (IMF) from low-frequency oscillation signal. The EMD can prominent the local character of original signal. Each of these oscillatory modes is represented by an IMF with the following definition:

- In the whole dataset, the number of extreme and the number of zero-crossings must either equal or differ at most by one.
- At any point, the mean value of the envelope defined by the local maxima and the envelope defined by the local minima is zero.

With the above definition for the IMF, one can then decompose any function as follows: (a) take the low-frequency signal $s(t)$, identify all the local extremes, and then (b) connect all the local maxima by a cubic spline line as shown in the upper envelope. Repeat the procedure for the local minima to produce the lower envelope. The upper and lower envelopes should cover all the data between them. Their mean is designated as $m(t)$, and the difference between the data is $c(t)$. (c). If $c(t)$ satisfies the definition of an IMF, it can be considered as one of the component of IMF. If $c(t)$ did not satisfy the definition of an IMF, it should repeat the procedure until it satisfies the definition.

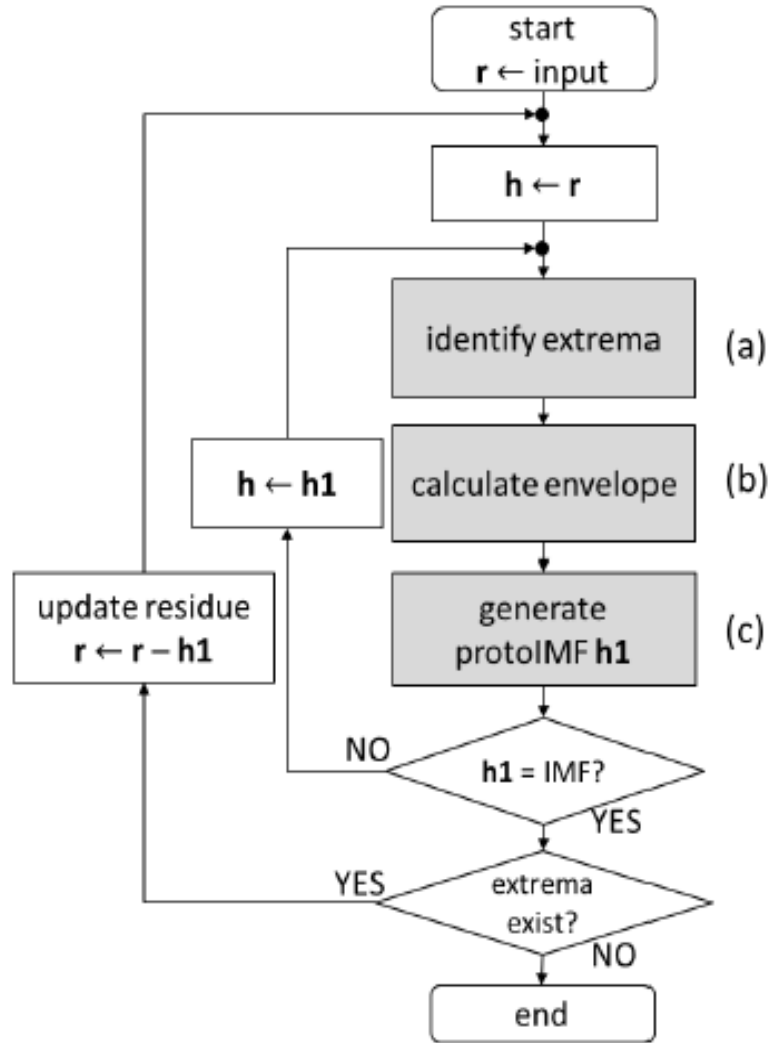


Figure 3 - 7 Algorithm of EMD

Subtract the decomposed component from the original signal, and then repeat the sifting processes to the residue component, finally the original signal was decomposed to the sum of several oscillation IMF and a final residue [44]:

$$s(t) = \sum_{i=1}^n c_i(t) + r \quad (3.10)$$

in which $c_i(t)$ is the component of IMF; r is the residue component.

The whole process of above is EMD decompose of low-frequency signal, which can be concluded as Figure 3 - 7.

3.3.2 Hilbert Transform to IMF of Low-frequency Oscillation

For any continuous time signal $X(t)$, applying the Hilbert transform to each IMF component, the transform can be expressed as the following form:

$$Y(t) = \frac{1}{\pi} \int_{-\infty}^{\infty} \frac{X(t)}{t-T} dt \quad (3.11)$$

Multiple conjugate pairs compared of $X(t)$ and $Y(t)$, than achieved the analysis signal:

$$Z(t) = X(t) + jY(t) = a(t)e^{j\theta(t)} \quad (3.12)$$

in which $a(t)$ is the instantaneous amplitude, $\theta(t)$ is the phase, and in here,

$$a(t) = \sqrt{X^2(t) + Y^2(t)} \quad (3.13)$$

$$\theta(t) = \tan^{-1} \frac{Y(t)}{X(t)} \quad (3.14)$$

The instantaneous frequency is as following function:

$$f(t) = \frac{1}{2\pi} \frac{d\theta(t)}{dt} \quad (3.15)$$

$$\omega(t) = \frac{d\theta(t)}{dt} \quad (3.16)$$

For each IMF low-frequency signal, it can achieve analysis function through Hilbert transform:

$$Z_i(t) = c_i(t) + j\tilde{c}_i(t) = a_i(t)e^{j\theta_i(t)} \quad (3.17)$$

Then instantaneous amplitude and instantaneous frequency of each IMF can be achieved [44].

3.3.3 Hilbert Spectrum Analysis

Eq. (17) enables us to represent the amplitude and the instantaneous frequency in a three-dimensional plot, in which the amplitude is the height in the time-frequency plane. This time-frequency distribution is designated as the Hilbert-Huang spectrum $H(\omega, t)$:

$$H(\omega, t) = \text{Re} \sum_{i=1}^n a_i(t) e^{-j \int \omega_i(t) dt} \quad (3.18)$$

With the Hilbert-Huang spectrum defined, the marginal spectrum, $h(\omega)$, can be defined as

$$h(\omega) = \int_0^T H(\omega, t) dt \quad (3.19)$$

where T is the total data length.

The Hilbert spectrum offers a measure of amplitude contribution from each frequency and time, while the marginal spectrum offers a measure of the total amplitude (or energy) contribution from each frequency value. The marginal spectrum represents the cumulated amplitude over the entire data span in a probabilistic sense. As pointed out by Huang et al. [45]. The frequency in $h(\omega)$ has a totally different meaning from the Fourier spectral analysis. In the Fourier representation, the existence of energy at a frequency, ω , means a component of a sine or a cosine wave persisting through the time span of the data. Here, the existence of energy at the frequency ω means only that, in the whole time span of the data, there is a higher likelihood for such a wave to have appeared locally. In fact, the Hilbert spectrum is a weighted non-normalized joint amplitude frequency-time distribution. The weight assigned to each time frequency cell is the local amplitude. Consequently, the

frequency in the marginal spectrum indicates only the likelihood that an oscillation with such a frequency exists. The exact occurrence time of that oscillation is given in the full Hilbert spectrum.

Therefore, the local marginal spectrum of each IMF component is given as

$$h_i(\omega) = \int_0^T H_i(\omega, t) dt \quad (3.20)$$

The local marginal $h_i(\omega)$ spectrum offers a measure of the total amplitude contribution from the frequency ω that we are especially interested in.

3.3.4 Low-frequency Oscillation by Hilbert Transform

Figure 3 - 8 shows some extracted waveforms from phase difference between Kyushu Univ. and Osaka Univ. using empirical model decomposition (EMD) function. The application of the EMD transformation leads to the decomposition of a signal. The EMD is based on the local time characteristics of the signal; therefore, the decomposed several intrinsic mode function (IMF) components show the true reflection of the original signal existing different dimensions of oscillations/trends. In Figure 3 - 8 some on/off switching behaviors can also be observed from 0 to 1200 seconds in Imf1, Imf2, Imf3 and Imf4, as well as a significant fluctuation around the 620 seconds from Imf4 to Imf13. From comparison of Figure 3 - 6 and Figure 3 - 8 for the example at hand, it can be seen that the amplitude change in the WLT technique is from low to high; however, for the HHT method it is from high to low.

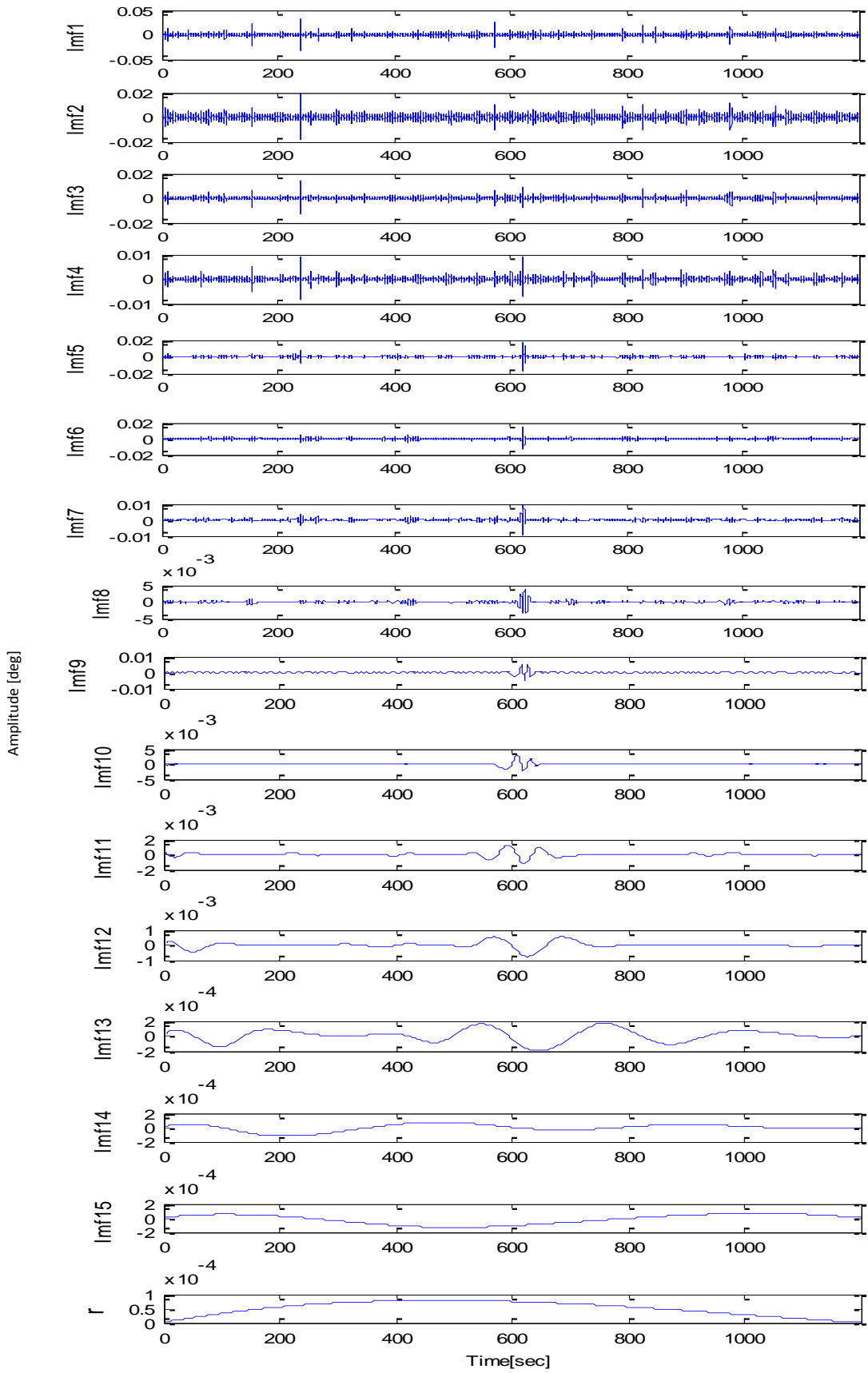


Figure 3 - 8 The EMD analysis in waveform of phase difference

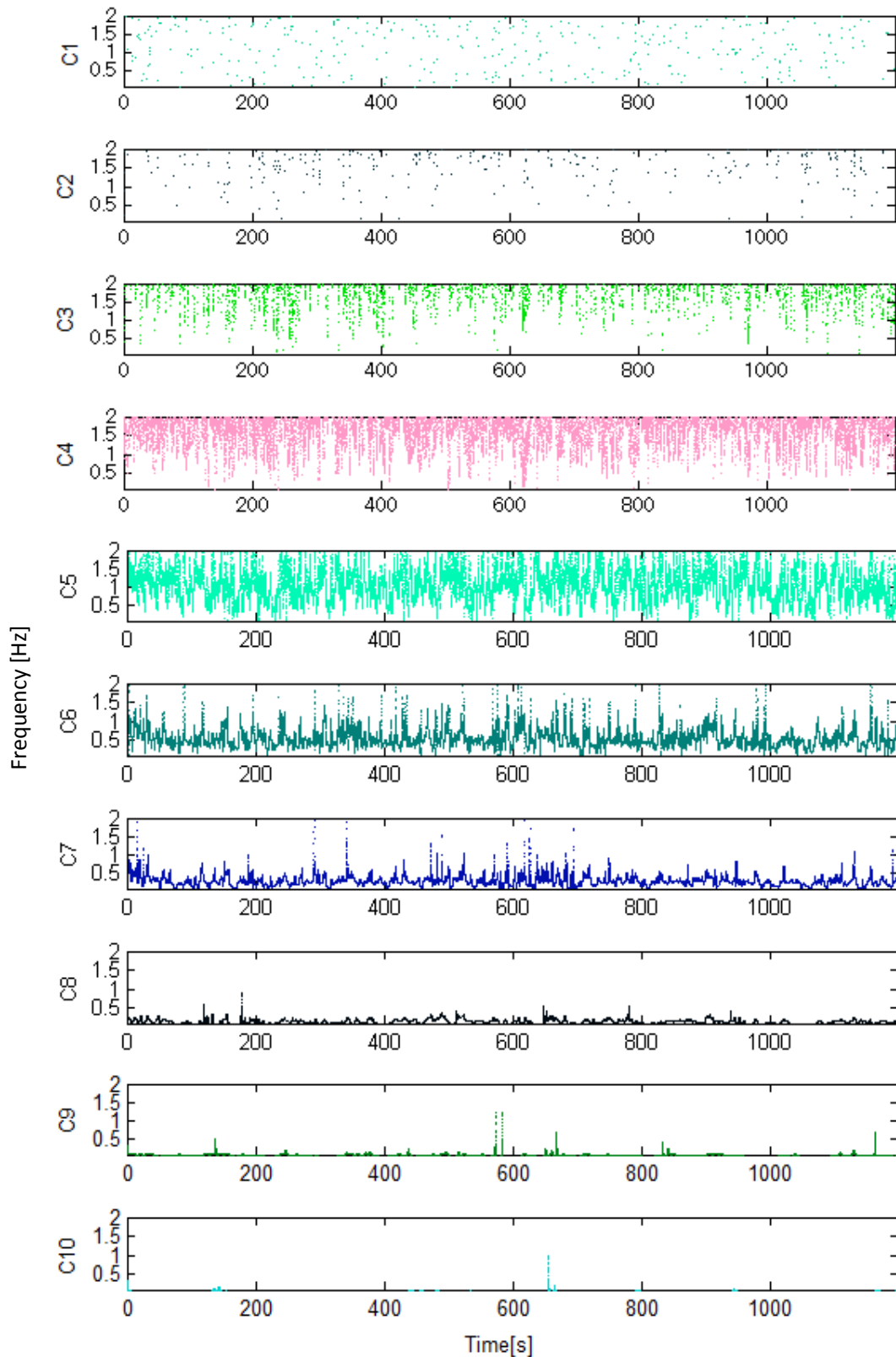


Figure 3 - 9 The HHT analysis in instantaneous frequency of phase difference

After applying Hilbert transform to the IMF waveform, the instantaneous frequency component waveforms within interested frequency range (0.1~2Hz) are

obtained as shown in Figure 3 - 9. The frequency order of c_1, c_2, \dots, c_{10} is from high to low. This means that one of the local frequencies of the c_1 could be higher than same local frequency of c_2 which also reflects the strong localized nature of the EMD algorithm. The characteristics of the EMD frequency from highest to lowest also mean that it can be used to de-noise. For example, c_1 to c_4 and c_8 to c_{15} can be removed from the original signal as shown in Figure 3 - 9.

Next, we turn to know an account of oscillations in power system. Figure 3 - 10 shows the HHT spectrum instantaneous frequency of c_5, c_6 and c_7 , since the center frequencies of these three components are almost between 0.1-2.0 Hz. Finally, the waveforms of phase differences shown in Figure 3 - 11 are analyzed by wavelet in order to compare the frequency characteristics with the HHT method.

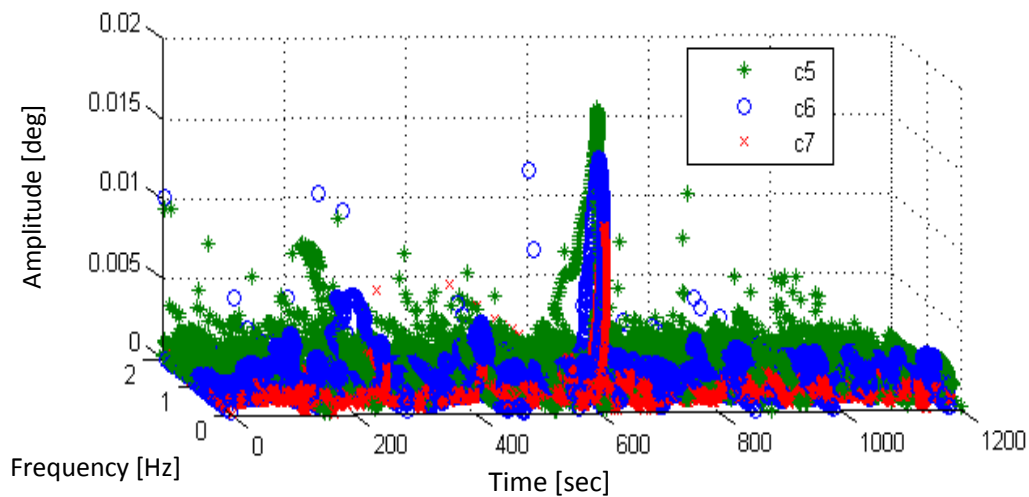


Figure 3 - 10 The HHT spectrum in instantaneous frequency of phase difference

It can be seen that the HHT preserves both good temporal and frequency resolutions. The instantaneous energy content and frequency variations can be easily observed over the time axis for c_5, c_6 and c_7 . There are energy changes at 240

seconds (c5 and c6) and 620 seconds (c5, c6 and c7). A characteristic feature of the WLT is that the energy is spread over different wave-number scales with smooth energy contours. It is not possible to separate out individual wave-number components to determine their contribution to the overall energy of the profile.

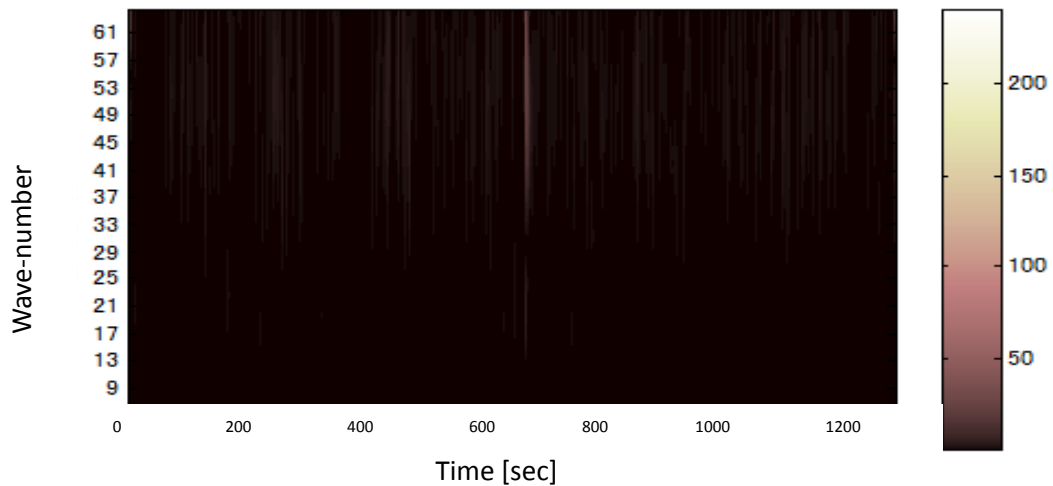


Figure 3 - 11 Wavelet spectrum

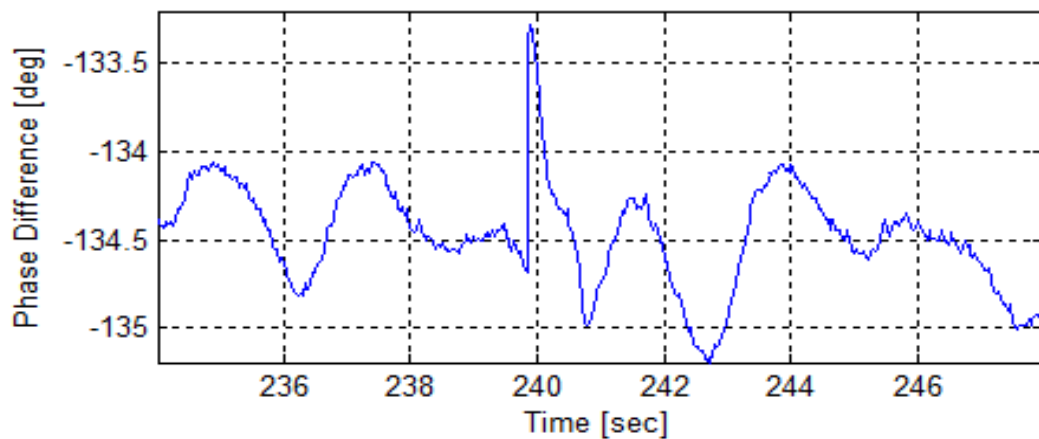


Figure 3 - 12 Phase difference around 240 seconds

However, the wavenumber band could be attributable to the spreading of energy across frequencies. It is also relatively easy to identify the locations of high-energy events along the time. Obviously, the spectral resolution is not as good as in the HHT spectrum. And then, we can turn back to find that the detailed original signal has a

disturbance around 240 seconds as shown in Figure 3 - 12. Therefore, the energy increases can be observed by the HHT rather than the WLT method.

3.4 Summary

This chapter describes low frequency oscillation damping mechanism and introduces underlying theory of measurement-based analysis. In the end, presents three techniques for detection of the global oscillation mode using small signal analysis based on PMU measurements for Japanese 60Hz power system.

The FFT, WLT and HHT data filtering techniques are employed to extract oscillation data. It is demonstrated that the HHT method is more effective in obtaining the required data from phase difference for the purpose of global oscillation mode detection in power system oscillation analysis. As seen from the real measurements, these study outcomes can be summarized as follows:

- 1) The FFT, WLT and HHT methods can be used to analyze the non-stationary signals. Each method can grasp the main small signal oscillation characteristics and achieves the desired effect of de-noising. In this paper, the FFT band is 0.4 ± 0.05 Hz and the HHT band is from 0.1-2.0Hz. Hence, the FFT is more centralized than the HHT, while it may loss some precise information.
- 2) It is demonstrated that the HHT techniques are able to resolve frequency components with better resolution. This is one of the important properties of this method that could be applied to the non-linear and non-stationary signals.

3) The Hilbert spectrum can clearly present the energy distribution with time and frequency. Most energy of Hilbert spectrum is more concentrated in the definite range of time and frequency. It can reflect the true low-frequency oscillation characteristic of power system. Because extracted the waveforms (IMF) from original data, which are based on residue of the last filtering are alterable in the HHT, the EMD is adaptive; it means the IMF can have a variable time-domain amplitude and frequency. The results are useful to monitor the low-frequency oscillation received from phasor difference using the PMU.

Chapter4. The Enhanced HHT Method

After the introduction and comparison of HHT method in chapter 3, it is easy to understand that the HHT method is more effective in obtaining the required data from phase difference for the purpose of global oscillation mode detection in power system oscillation analysis. HHT method has remarkable features. First of all, it can be used to handle nonlinear and non-stationary signals. The traditional methods, whether FFT or WLT, etc. the signals are approximately processed as linear signal when analysis non-linear and non-stationary signals. This feature is the main advantage of HHT algorithm, which is also widely used by the reasons. Secondly, HHT method is adaptive, which means that can be adaptive extracted from the signal decomposed by EMD itself. It is based on an adaptive basis, and the frequency is defined through the Hilbert transform. Consequently, there is no need for the spurious harmonics to represent nonlinear waveform deformations as in any methods with an a priori basis. The "base" of Fourier transform is the trigonometric functions, the "base" of wavelet transform requires pre-selected. Therefore, HHT has completely adaptability. Third, it

is suitable for analysis mutation signal. Due to the Heisenberg uncertainty principle constraint, many traditional algorithms must be satisfied the product of frequency window by time window is constant. This property makes these algorithms cannot achieve high precision both in time domain and frequency domain at the same time. Nevertheless, there is no uncertainty principle limitation on time or frequency resolution from the convolution pairs based on a priori bases.

However, it is still have some issues need to be well resolved in dealing with power system oscillation signal. This chapter will first introduce two key problems for applying HHT method to power system oscillation characteristic analysis, then propose new improvement program to address these issues. At last, present a method to identification parameters of power system.

4.1 Issues of Hilbert Huang Transform

Here, it takes an example in order to show issues of HHT. This is the simplest sin signal, as show in Figure 4 - 1.

$$x = 2\sin(2\pi * 20t) \tag{4.1}$$

Figure 4 - 2 and Figure 4 - 3 shows that EMD result and time-domain spectrum of sin signal by using HHT method. It gets three IMF components and residue signal as shown in Figure 4 - 2. As can be seen from the signal function, it should only get one IMF component. Occurs of the other two IMF in Figure 4 - 2 is because of problems that caused by EMD analysis process itself.

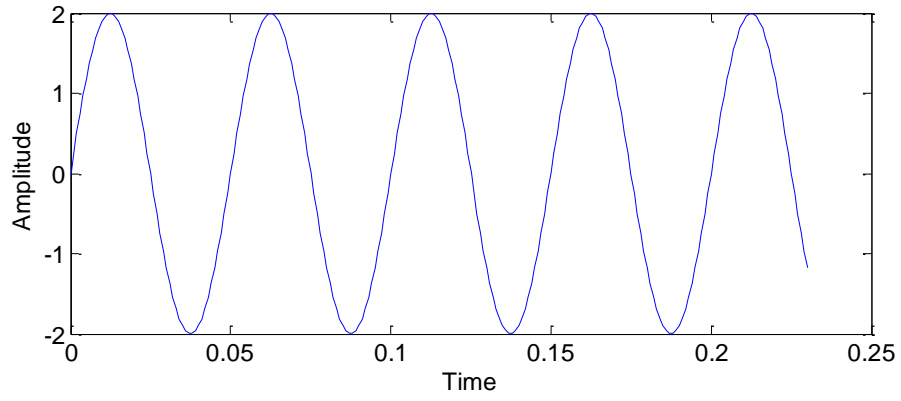


Figure 4 - 1 Test sin signal

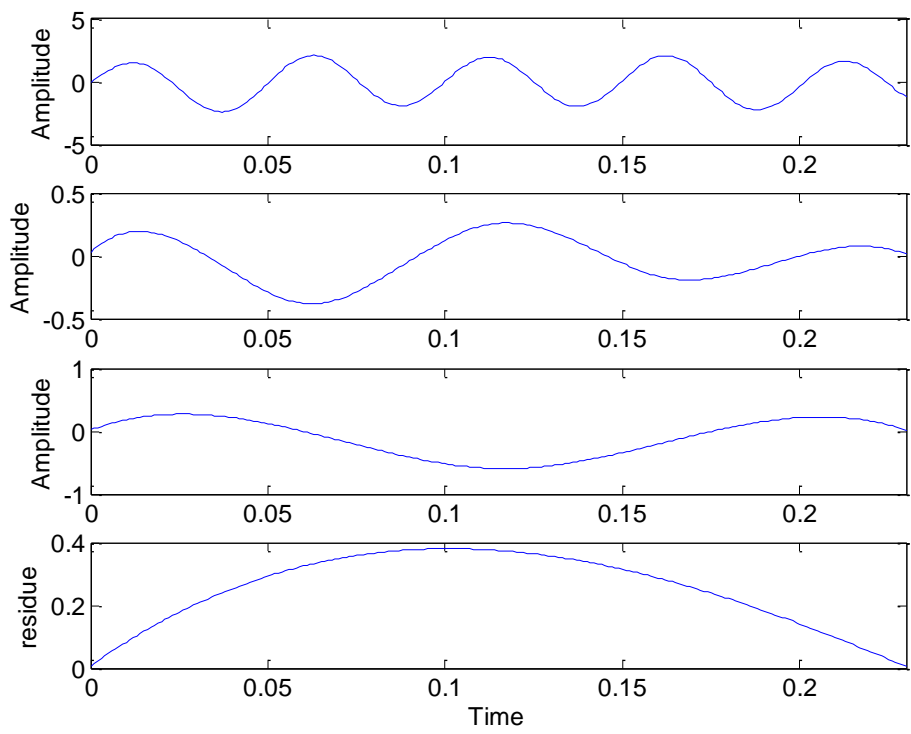


Figure 4 - 2 EMD analysis result

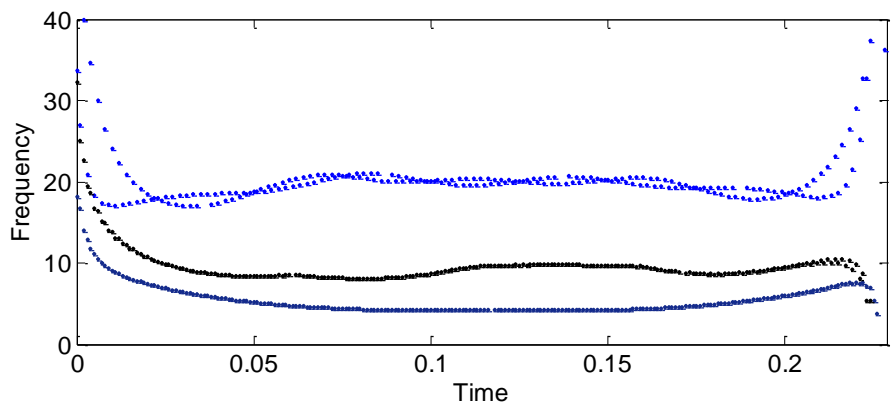


Figure 4 - 3 Time-domain spectrum of HHT (Instantaneous frequency)

Figure 4 - 3 shows that three frequency components change with time. The first frequency component is around 20Hz except the endpoint, which is similar to the frequency of test sin signal. However, it is clear that there are obvious distortion appeared in the both ends of Figure 4 - 3. The reason of appearance of the other two instantaneous frequency components will be discussed next.

From the simple sin signal test, HHT algorithms typically can be included three key issues: 1) boundary end effect; 2) pseudo IMF component caused by EMD decomposition, especially for low-frequency signal; 3) How to identify the parameters in power system oscillation analysis. Then, a brief introduction for reasons of these problems and the impact on signal processing is described.

4.1.1 The Boundary End Effect

Boundary end effect generated in the process of EMD is one of the important factors that affect the quality of EMD.

In general, it often appears distortion ("Gibbs" phenomenon) at signal boundaries when processing signals concentrated in a limited period of time, which called the boundary end effect. The Gibbs phenomenon exists for many integral representations [46-50] and for many series representations as well. The presence of this phenomenon is undesirable, since it is related to the behavior of the series approximating a discontinuous function f at a jump location t , implying non-uniform approximation at t ; so it is important to examine ways to reduce or even avoid it. In [51] and [52], Gibbs phenomenon has been shown to exist for Fourier interpolation. Since most

multi-resolution analyses induce sampling expansions [53], Gibbs phenomenon for wavelet sampling expansions has been examined in [54-56].

In EMD algorithm, every time the "sieve" of a new IMF components have a certain relationship with the old IMF component. Therefore, the distortion at the endpoint will spread to the interior. As a result, the new IMF components have obviously distortion, especially in IMF lower frequency components. Seriously, this will lead to EMD decomposition results are not significant and it can also bring the endpoint distortion in Hilbert transform process which will affect the accuracy of the HSA (Hilbert spectrum analysis).

Therefore, to solve the boundary end effect issue for HHT has a very important theoretical and practical significance.

4.1.2 Pseudo IMF Component

There are a lot of reasons for generating pseudo-IMF components, such as: boundary end effect, termination criterion for IMF component and an unreasonable sampling frequency select. If we can solve the boundary end effect issue, pseudo-IMF component can be eliminated to some extent.

4.1.3 Identify the Parameters

It is well known that the EMD method is based on the local characteristic time scale signal. Any signal can be decomposed into the sum of IMF components adaptively in order to make instantaneous frequency has a real physical meaning.

Afterwards, each IMF component of the instantaneous amplitude and instantaneous frequency can be calculated by the Hilbert transform. In this dissertation, it employs the least squares method combine the HSA to complete power system low frequency oscillation parameter identification algorithm. Usually, 10% - 90% of the source IMF component is used in the identification algorithm. In regard to poor quality of IMF component, parameter identification data used to compress to 20% -80% of the source IMF components in order to avoid boundary end effects and unstable influence on the two ends caused by the Hilbert transform.

4.2 Improved Program for HHT Method

As mentioned in chapter 3.3, HHT algorithm is divided into EMD process and HSA process. The signal need to be preprocessed before applying HHT algorithm - remove direct current (DC) processing and a band-pass filtering processing, band frequency range is from 0.1Hz to 2Hz, as shown in Figure 4 - 4.

The oscillation signal in power system will be respectively decomposed into the low-frequency oscillation analysis and sub-synchronous oscillation analysis. In order that IMF components decomposed by EMD process have actual physical meaning, the decomposition process includes: spline interpolation algorithms (cubic spline interpolation function); endpoint extension algorithms (alternatively direct continuation and extension mirror extension algorithms, etc.); Termination constraint selection and monotonic constraints (stop EMD screening process if extreme point is less than 3 and considered residual function is monotonous).

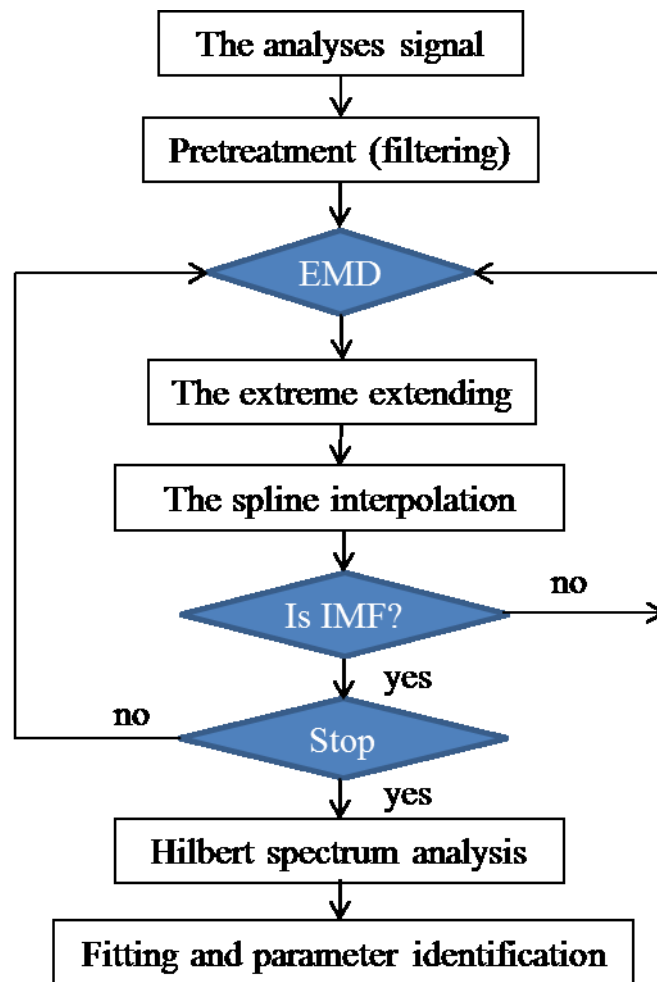


Figure 4 - 4 Oscillation mode extraction algorithm

4.3 Data Pre-treatment Processing

The signal pre-treatment process includes DC removal and band-pass filtering. First, removed the DC part of the signal; second, in order to improve the efficiency of analysis, band-pass filtering algorithm decomposes the useful frequency parts of the oscillating signal processing. Here, the “useful” means that the frequency band is between 0.1Hz to 2Hz, which are describe in chapter 3.1. Next, we will introduce the DC removal process and band-pass filtering.

4.3.1 DC Removal Processing

The simplest way to deal with removing the DC is:

Original Signal $x_i(t)$ (Among them $i=1,2,\dots,N$), \bar{x} is average of $x_i(t)$,

$$\bar{x} = \sum_{i=0}^{N-1} x_i(t)/N \quad (4.2)$$

Then the processed signal $x_i(t)$ can be written as:

$$x(t) = x_i(t) - \bar{x} \quad (4.3)$$

4.3.2 Digital Band-pass Filter Algorithm Processing

In this dissertation, we use the Butterworth filter as the digital low-pass filter. Comparing the FIR (finite impulse response) filter, the advantages of IIR (Infinite impulse response) filter are: amplitude - frequency characteristics is higher efficiency, good accuracy and low computational amount. It can be used to analysis power system oscillation because the nonlinear-phase.

The Butterworth filter is a type of signal processing filter designed to have as flat a frequency response as possible in the pass band. It is also referred to as a maximally flat magnitude filter.

It has a magnitude response that is maximally flat in the pass band and monotonic overall. This smoothness comes at the price of decreased roll off steepness. Elliptic and Chebyshev filters generally provide steeper roll off for a given filter order.

Butterworth filter uses a five-step algorithm:

- It finds the low pass analog prototype poles, zeros, and gain using the function

Butterworth filter prototype.

- It converts the poles, zeros, and gain into state-space form.
- If required, it uses a state-space transformation to convert the low pass filter into a band pass, high pass, or band stop filter with the desired frequency constraints.
- For digital filter design, it uses bilinear transformation method to convert the analog filter into a digital filter through a bilinear transformation with frequency pre-warping. Careful frequency adjustment enables the analog filters and the digital filters to have the same frequency response magnitude at ω_n or at ω_1 and ω_2 .
- It converts the state-space filter back to its transfer function or zero-pole-gain form, as required.

Such as following construct oscillation signal:

$$\delta = 0.5 \sin(2\pi * 0.1t) + 2 \sin(2\pi * 0.4t) + 1.5 \sin(2\pi * 2t) + 0.5 \sin(2\pi * 5t) + 0.2 \sin(2\pi * 15t) + 15 \quad (4.4)$$

As can be seen from the equation, it contains five frequency components: 0.1Hz, 0.4Hz, 2Hz, 5Hz, and 15Hz. After applying the DC processing and the designed butterworth filter, Figure 4 - 5 shows test data in blue color and filtered data in red color. The FFT method is used to verify the performance of filter as show in Figure 4 - 6 and Figure 4 - 7 in detail. We can find that the high frequency (5Hz and 15Hz) signals are removed cleanly.

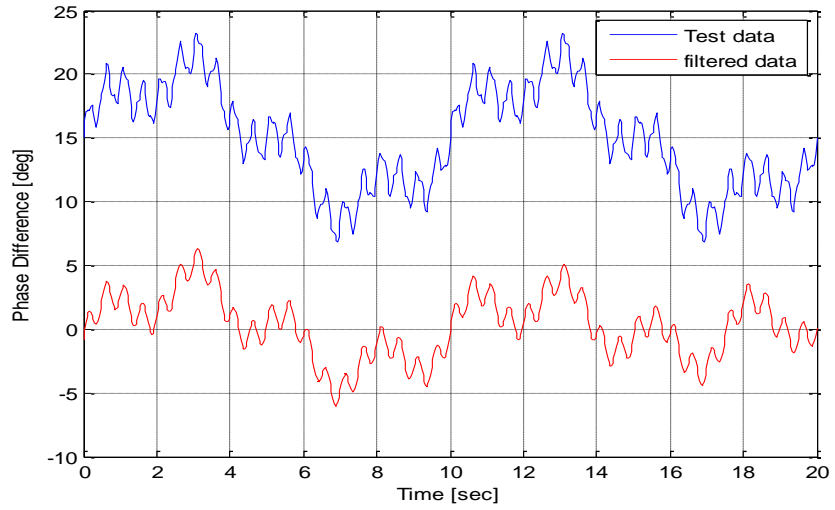


Figure 4 - 5 Pre-treatment process

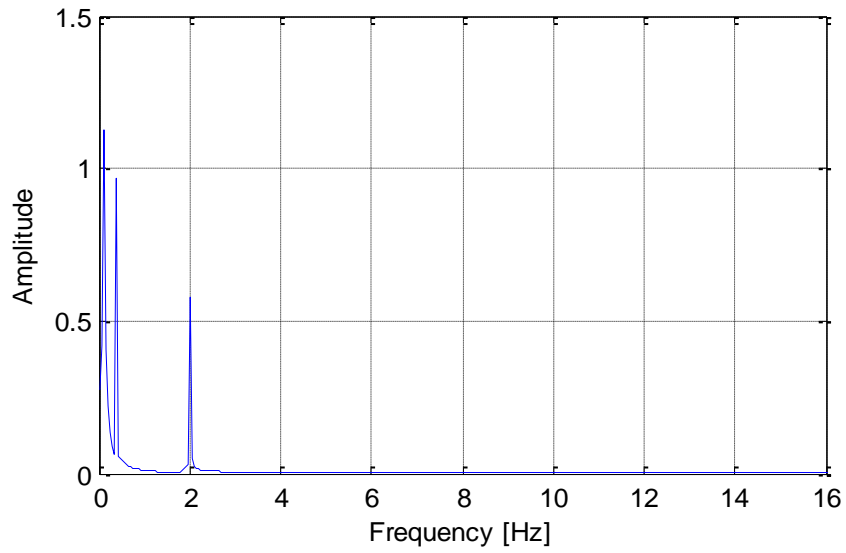


Figure 4 - 6 FFT spectrum of butterworth filtered data

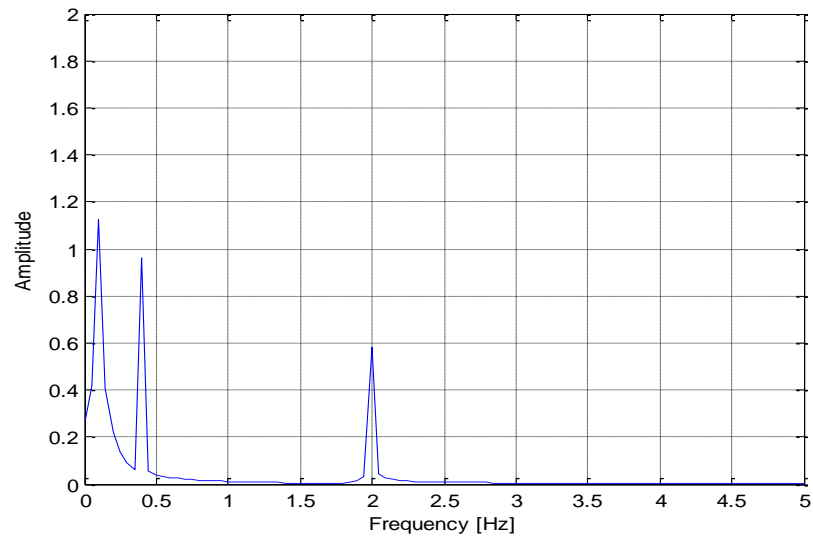


Figure 4 - 7 FFT spectrum of butterworth filtered data in detail

4.4 Inhibit the Boundary End Effect

It produces boundary effect of HHT algorithm for two reasons: one is that, in the EMD process, a cubic spline interpolation to strike a mean envelope. There is an error at the mean envelope endpoint; the other is it performs Hilbert transform to non-integer Periodic sampling signal in HAS, which generate distortion at the endpoint. The following sections describe the reasons for these two boundary effect and Inhibit methods.

4.4.1 The Boundary End Effect Caused by EMD Algorithm

An IMF is a function that must satisfy two conditions according to the algorithm originally developed: Before introducing the iterated shift process, it is necessary to give the definition of intrinsic mode function. It is a function that must satisfy two conditions:

- (a) The difference between the number of local extremes and the number of zero-crossings must be zero or one;
- (b) The running mean value of the envelope defined by the local maxima and the envelope defined by the local minima is zero.

The condition (a) is to assure the signal has narrow band character, and the condition (b) is to assure the instantaneous frequency will not have the unwanted fluctuations induced by asymmetric wave.

And when we use Cubic Spline interpolation, the spline will need to conform to the following stipulations [57]:

1. The piecewise function $S(x)$ is a third degree polynomial;
2. The piecewise function $S(x)$ will interpolate all data points $S(x_i) = y_i$ for $i = 1, 2, \dots, n-1$;
3. $S(x), S'(x), S''(x)$ will be continuous on the interval $[x_1, x_n]$.

For such a signal, the interior extremes are easily identified. However, at both ends of data, first or second order derivatives are required for spline fitting. However, as the data curve does not provide any information on envelop at the ends, the derivatives cannot be given unless the data is extend at two ends.

To solve this problem, Huang used characteristic waves to get the maximum extreme and the minimum extreme [58]. The original signal only has the extreme in the data series, so the extending points outside are not reliable. Different characteristic waves will cause different results, and it is difficult to choose the proper waves for every iterations.

4.4.2 Inhibit the Boundary End Effects Caused by EMD

Although the cubic spline interpolation method brings the boundary effect, we cannot use other spline method to replace it. Because the accuracy of the other spline interpolation function are worse than the cubic spline interpolation method, and only weakening the boundary effect to a certain extent.

Usually, it will increase the extreme points or extending the data sequence at both ends to inhibit the boundary effect in engineering. However, this kind approach cannot be completely accurate extrapolating data sequences because of the strong

randomness of real signals. So, it is need to take some extension rules to obtain a more accurate mean envelope.

In order to solve the boundary effect problem in EMD, We compare several extension methods to inhibit the boundary effect. Take the following mathematical expressions as analyzed signal formula:

$$x = 2 \sin(2\pi * 0.4t) + 0.5 \sin(2\pi * 2t) + 0.2 \sin(2\pi * 15t) + 4 \quad (4.5)$$

4.4.2.1 The Extreme Extension Method

For the extreme extending method, the first step is to find the first maxima point and minima point of the ends part. Then, extreme points in the end are used to extent twice, as show in Figure 4 - 8. In another side of the data, do the same extension.

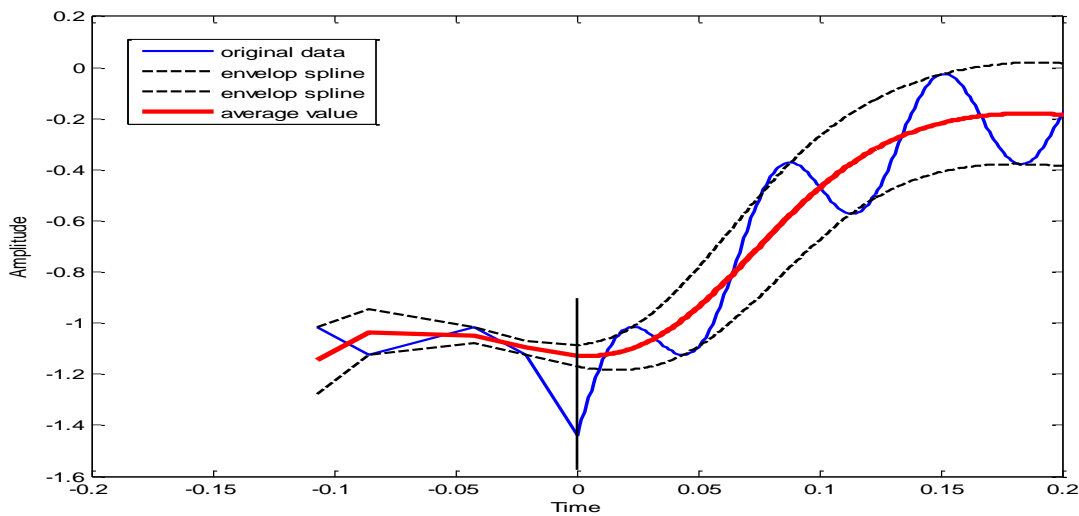


Figure 4 - 8 The extreme extending method

4.4.2.2 The Mirror Extension Method

Mirror extension method place two mirrors at the left and right end points which have the symmetry extreme point. Extending original signal by mirror to obtain a

periodic signal sequence which twice than the original signal. Then connecting this signal to original signal can obtain a periodic signal. Taking the maximum and minimum values of extended signal and seeking upper and lower envelope by cubic spline interpolation function, then seeking average of the envelope.

The result of EMD decomposed which applying a Mirror extension method as shown in Figure 4 - 9. It is evident that the boundary effect has been well inhibited.

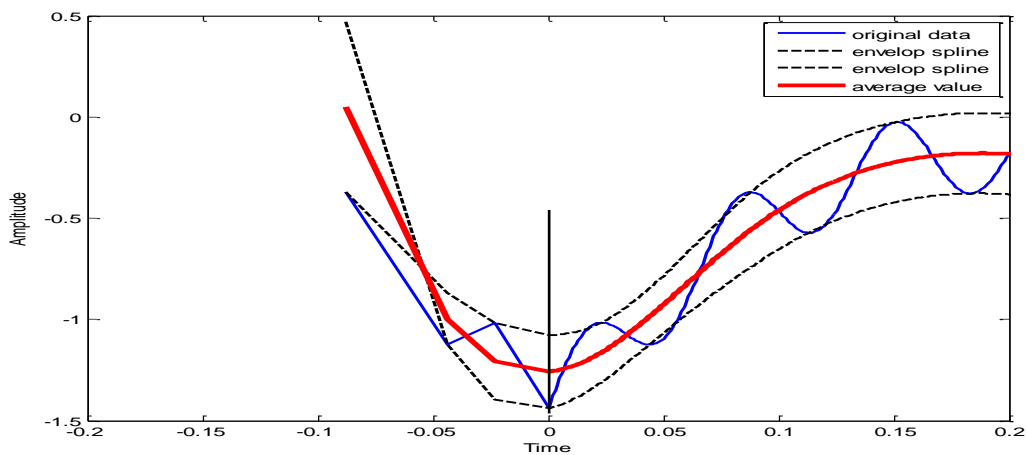


Figure 4 - 9 The Mirror extension method

4.4.2.3 The Direct Extension Method

The first step of direct extension method is to get all the extreme points of the data sequence, and then add the two endpoints of the data sequence as interpolated sequence which will use cubic spline interpolation function to get the envelope. There has an obvious distortion at the endpoint of the intrinsic mode functions (IMF) component had been decomposed.

4.4.2.4 The Parallel Extension Method

Due to equalization of the slope at two adjacent extreme points near the end of signal (a maximum value and a minimum value), see Figure 4 - 10. It is artificial define two extreme points at the ends. It is easily to find that low decomposition accuracy is not high.

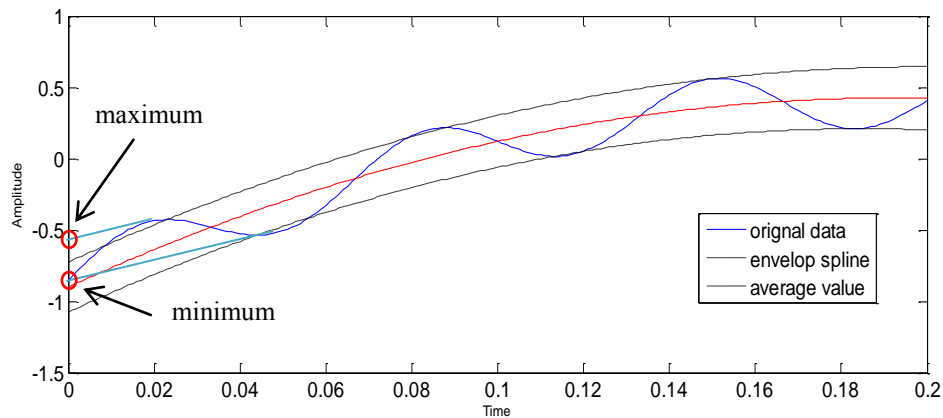


Figure 4 - 10 The Parallel Extension Method

4.4.2.5 Polynomial Fitting Extension Method

For the extreme point sequence of the signal, it take the three extreme points (including maxima value and minima value) at endpoint polynomial approximate fitting value as new extreme points, which is calculated to determine the position of the boundary of the extreme points. This extension method takes a long time than others.

4.4.2.6 The Boundary Local Characteristic Time Scale Extension

Method

The boundary local characteristic time scale extension method is to combine the time interval trends and time interval local extreme point at endpoints, add a pair of maxima and minima at both ends of signal.

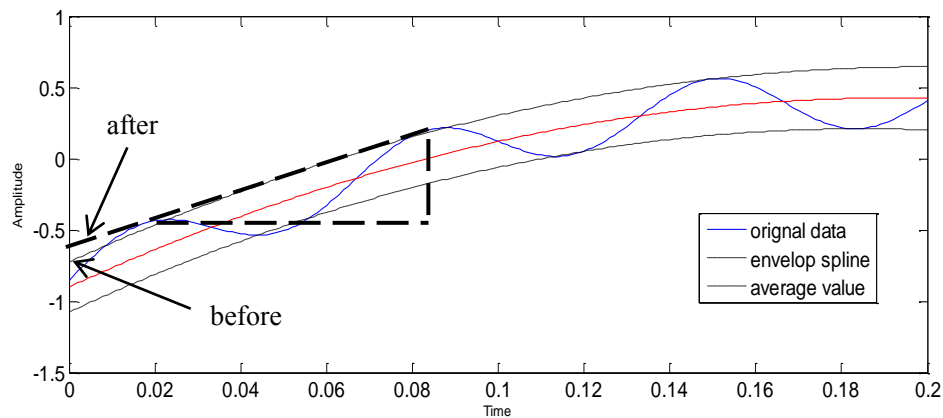


Figure 4 - 11 The boundary local characteristic time scale extension method

In this section, six inhibit methods are given implementation for solving boundary end effect, and constitutes a data extension options library. In the following analysis of this dissertation, it choose the mirror extension method as the inhibit boundary end effect methods. Comparing with Figure 4 - 3, Figure 4 - 12 shows the boundary effect problem of the EMD algorithm is very well inhibited by mirror extension method. At the same time, pseudo-IMF components are also eliminated in this example.

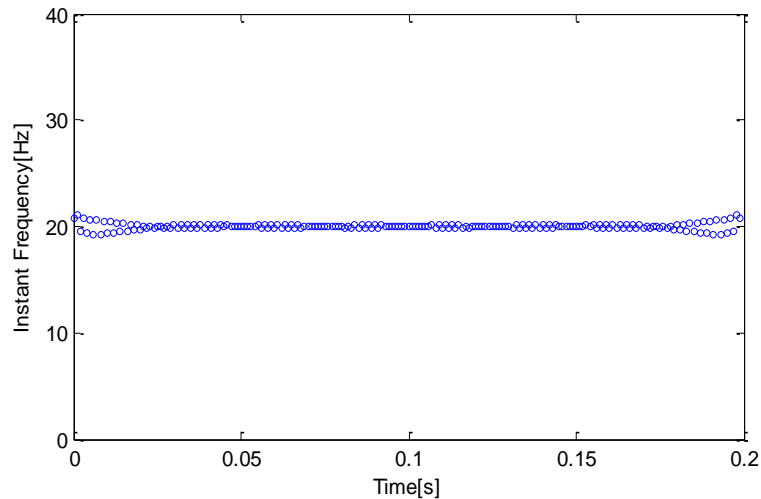


Figure 4 - 12 Inhibit the boundary effect problem of the EMD algorithm by mirror extension method

4.4.3 The Boundary End Effect Caused by Hilbert Transform

The error of instantaneous frequency and amplitude calculated in Hilbert transform will cause some impact on the final results of the analysis, thus affecting the final results of the parameter identification.

Next, the Hilbert transform of a sinusoidal signal and its frequency spectrum calculated to observe boundary effect bring by Hilbert transform. We take the sinusoidal signal Equation (4.1) for example.

Applying Hilbert transform to the signal, the signal waveform and its Hilbert transformed wave are shown in Figure 4 - 13. We can know the ideal sinusoidal signal of Hilbert transform results has $\pi/2$ phase difference between sinusoidal signal and Hilbert transform results. It can be seen from Figure 4 - 13 that the transformed signal has distortion appeared at the both endpoints.

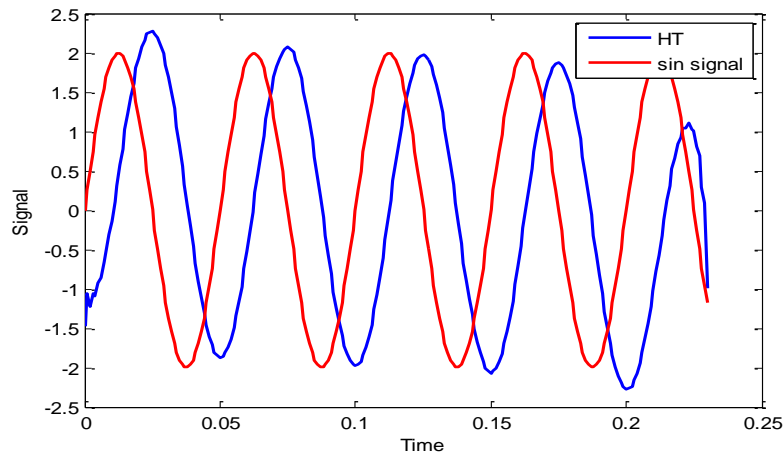


Figure 4 - 13 Sine signal and its Hilbert transform

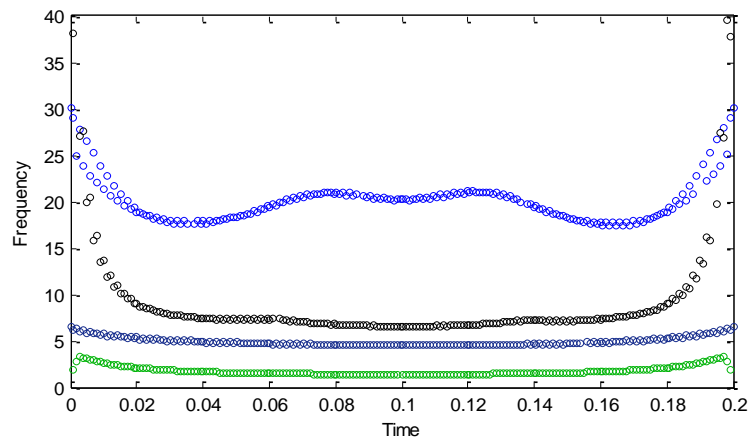


Figure 4 - 14 Instantaneous frequency of sine signal

It is very evident when the error generated by Hilbert transform reflected in the instantaneous frequency spectrum. The instantaneous frequency spectrum of the sin signal is shown in Figure 4 - 14, and we can easily find a very seriously distortion occurs at the endpoints.

To inhibit this endpoint distortion, it must understand the reasons of this distortion at first. As shown in Figure 4 - 15, Hilbert transformation process is to get bilateral spectrum of real signal by applying Fourier transform first. And then, filter to remove

one side of the spectrum, make the amplitude doubled. Finally applying Inverse Fourier transforms to the doubled unilateral spectrum and gets the final result.

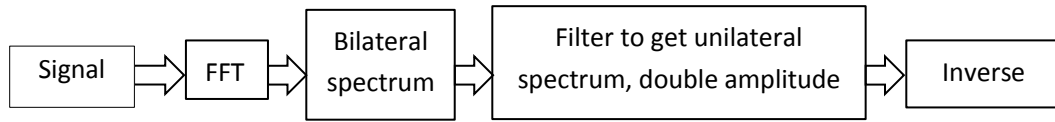


Figure 4 - 15 HT computing process

The core part throughout the process is the Fourier transform. We know the Fourier transform is assumed that all signals are periodic signals, which analysis one period of the signal as periodic signal, so if the signal is not the periodic data series, it is bound to bring some error.

Figure 4 - 16 shows the results of the Hilbert transform to integral periodic sampling of the sin signal. And comparing the non-integral periodic sampling of the data sequence in Figure 4 - 13, it can be seen through Hilbert transform, a non-positive periodic sampling at the endpoint appeared distorted, but there is no distort in the integral periodic sampling sequence.

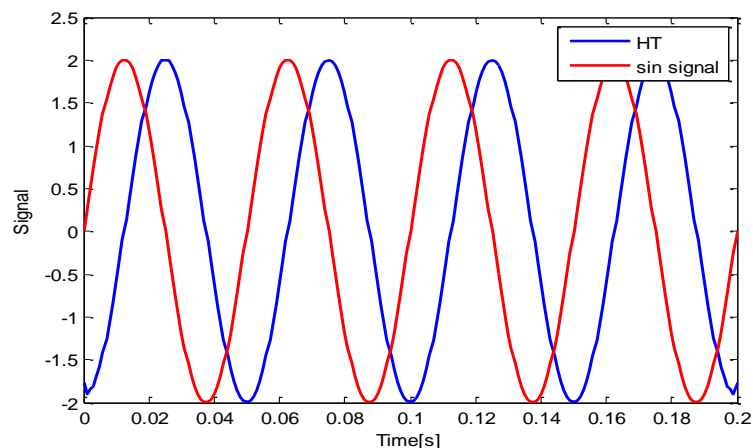


Figure 4 - 16 Integral periodic sampling of the data sequence

Although we know that the endpoint distortion can be inhibited by sampling integral periodic for the signal, it is very difficult to integral periodic sampling of data in the actual complex project. Therefore, it needs to use other methods to inhibit the boundary effect brought by Hilbert transform.

4.4.4 Inhibit the Boundary End Effect Caused by Hilbert Transform

It is because the boundary effect produced by Hilbert transform mainly in the ends of the data, the Hilbert transform results is approximate seen to be obtained by shift $\pm \pi / 2$ phase to the original signal. So we can extend the ends of the original data according to certain rules, and then apply the Hilbert transform to the extension data. Finally remove the Hilbert transform result at extension data, the rest data is the Hilbert transform results of original data.

The most important part of this method is the choice of methods for data extension. In this research the ARMA model is selected to establish extension data.

4.4.4.1 The ARMA Method

For some observed time series, a very high-order AR or MA model is needed to model the underlying process well. In this case, a combined autoregressive moving average (ARMA) model can sometimes be a more parsimonious choice.

An ARMA model expresses the conditional mean of y_t as a function of both past observations, y_{t-1}, \dots, y_{t-p} , and past innovations, $\varepsilon_{t-1}, \dots, \varepsilon_{t-q}$. The number of past

observations that y_t depends on, p , is the AR degree. The number of past innovations that y_t depends on, q , is the MA degree. In general, these models are denoted by ARMA (p, q).

The form of the ARMA (p, q) model is

$$y_t = c + \phi_1 y_{t-1} + \dots + \phi_p y_{t-p} + \varepsilon_t + \theta_1 \varepsilon_{t-1} + \dots + \theta_q \varepsilon_{t-q}, \quad (4.6)$$

where ε_t is an uncorrelated innovation process with mean zero.

In lag operator polynomial notation, $L_i y_t = y_{t-i}$. Define the degree p AR lag operator polynomial $\phi(L) = (1 - \phi_1 L - \dots - \phi_p L^p)$. Define the degree q MA lag operator polynomial $\theta(L) = (1 + \theta_1 L + \dots + \theta_q L^q)$. It can write the ARMA (p, q) model as

$$\phi(L)y_t = c + \theta(L)\varepsilon_t. \quad (4.7)$$

The signs of the coefficients in the AR lag operator polynomial, $\phi(L)$, are opposite to the right side of Equation 5-10.

4.4.4.2 ARMA Process to Inhibit the Boundary End Effect Caused by Hilbert Transform

Due to ARMA model can replace the AR model which need lower order approach with fewer parameters, one of the identification methods of the ARMA model, firstly, is modeled as an enough large order of AR processes. Then fitting the ARMA model for the estimated impulse response obtained from it.

To fit the ARMA model for the estimated impulse response, the Prony method based on coefficient comparison and the Steiglitz-Mcbride method (determine the

optimal coefficient by iterative calculation with the result of Prony method is used as initial value) has been provided.

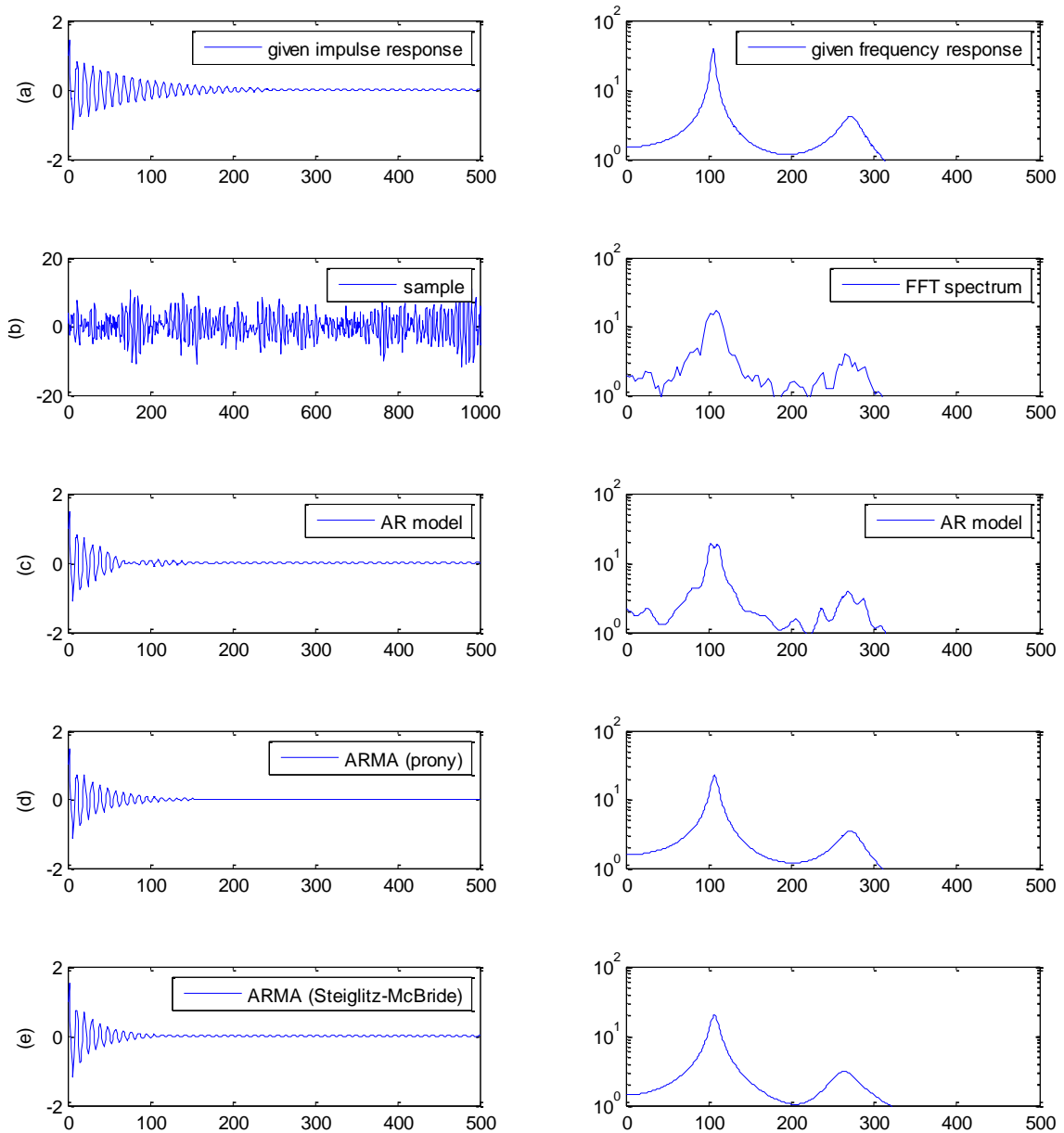


Figure 4 - 17 ARMA process

In the following example, see Figure 4 - 17, for the appropriately gave ARMA process(a), the sample time series (b) is generated, identify the ARMA model from it in reverse, then to judge if they match to the given model or not. Firstly, for the given

sample time series (b), fitting large order (30 order) AR model by Yule-Walker method (c), then for the generated impulse response, fitting the ARMA model by Prony method (d) and Steiglitz-Mcbride method (e).

The basic consideration to extend the ends of the original data according to ARMA method is as shown in Figure 4 - 18. First, establish the ARMA model to make data extension then doing the Hilbert transform, and finally intercept the Hilbert transform results as the result on of the original result signal.

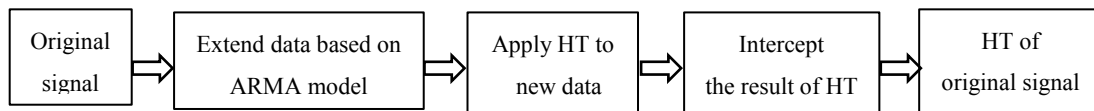


Figure 4 - 18 Algorithm of Inhibit the boundary end effect caused by Hilbert transform autoregressive-moving-average (ARMA) models

Take the Equation (1) for example, Figure 4 - 19 shows the extend data based on the ARMA (prony) method; Figure 4 - 20 shows the signal based on ARMA extension. By applying this method, the distortion at both ends of instantaneous frequency spectrum of non-periodic sampling signals are very well inhibited as shown in Figure 4 - 21.

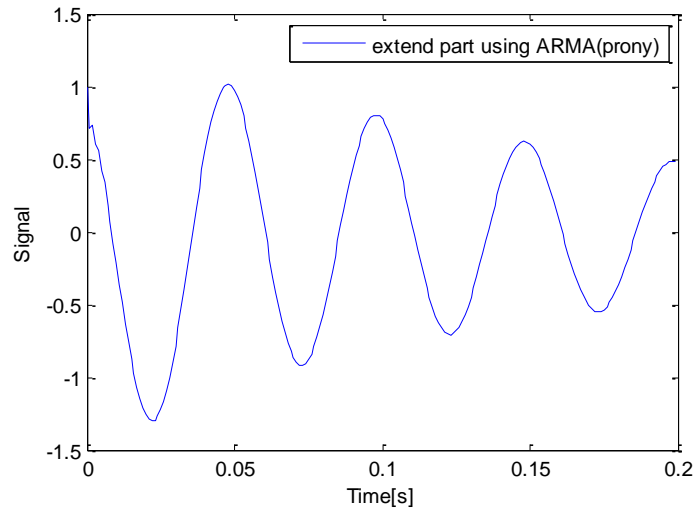


Figure 4 - 19 Extend data based on ARMA method

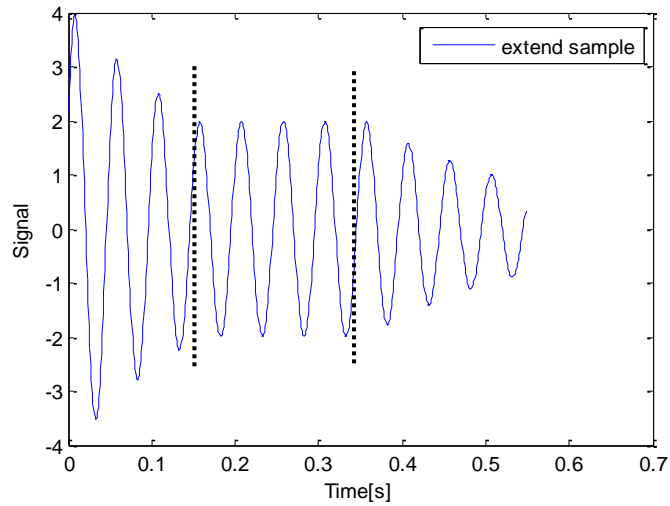


Figure 4 - 20 The signal based on ARMA extension

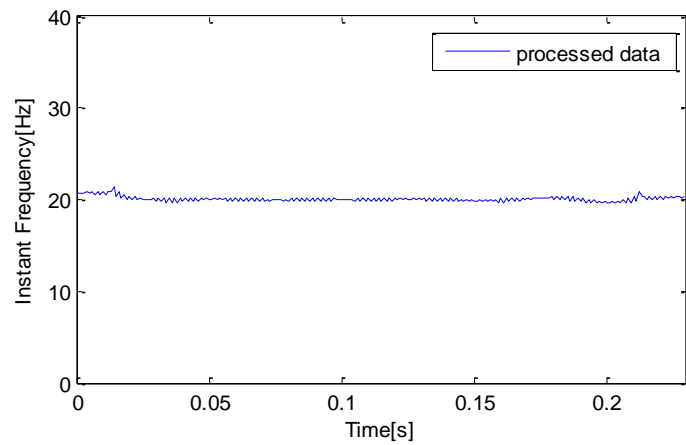


Figure 4 - 21 Processed instantaneous frequency spectrum

4.5 Parameter Identification

In power system, oscillation mode component can be written as:

$$P(t) = Ae^{-\lambda t} \cos(\omega t + \psi) = Ae^{-\lambda t} \cos(2\pi f t + \psi) \quad (4.8)$$

In control theory, the time response function of oscillation mode component can be written as:

$$P(t) = Ae^{-\xi\omega_0 t} \cos(\omega_0\sqrt{1-\xi^2}t + \psi) = Ae^{-\xi\omega_0 t} \cos(\omega_d t + \psi) \quad (4.9)$$

A is initial amplitude, ψ is initial phase, λ is damping coefficient, ω and f are oscillation angular frequency and oscillation frequency, ω_0 is un-damped angular frequency, ω_d is damped angular frequency, ξ is damping ratio

Compare the Equation (4.8) and Equation (4.9), can get:

$$\begin{cases} a(t) = Ae^{-\lambda t} = Ae^{-\xi\omega_0 t} \\ \theta(t) = 2\pi f t + \psi = \omega_d t + \psi \end{cases} \quad (4.10)$$

For the identification of frequency oscillation signal, is to accurately extract the amplitude of the oscillation component of the oscillation frequency and the damping coefficient, and then calculate the damping ratio, which depends on the oscillation frequency and damping factor.

Frequency oscillation signal is seen the decomposed IMF components as an oscillation mode component. Therefore, parameter identification is calculated on the IMF component actually.

In order to obtain more accurate identification results, it should be considered from two aspects: on the one hand to improve the accuracy of damping coefficient and oscillation frequency by using the least squares method, precision damping coefficient

can improve the accuracy of the damping ratio; on the other hand reduce the IMF component data to be calculated.

It needs to make some changes in the analytical signal form, as show in Equation (4.11). Damping coefficient λ identification apply the least squares through the logarithmic curve of instantaneous amplitude function of a single IMF component.

$$\begin{cases} \ln a(t) = -\lambda t + \ln A = -\xi \omega_0 t + \ln A \\ \omega(t) = \frac{d\theta}{dt} = 2\pi f = \omega_d = \omega_0 \sqrt{1 - \xi^2} \end{cases} \quad (4.11)$$

Because that the data for parameter identification is obtained in IMF component, the boundary end effect caused by EMD is just suppressed. It has not been eliminated. At the same time, the endpoint distortion come from Hilbert transform is also not completely eliminated. Therefore, IMF can improve identification accuracy by removing small amounts of data at both ends. In this dissertation, 10% - 90% of the source IMF component is used in the identification algorithm.

4.6 Summary

As the issues of HHT method are introduced and the causes of these issues are deeply analyzed, this chapter proposed the enhanced HHT method. There are two issues mainly solved in this chapter. Firstly, the boundary effect problem of the EMD algorithm is very well inhibited by six extension methods which constitute a data extension options library. They are a). polynomial extension method, b). slope method extension method, c). parallel extension method, d). extreme point symmetric

extension method, e). mirror method and f). Boundary local characteristic scale extension method. Secondly, inhibit the boundary effect problem caused by Hilbert transform successfully based on Auto-Regressive and Moving Average Model (ARMA). At last, present an estimation algorithm method to get the mode parameters of signal based on enhanced HHT successfully.

Chapter5. The Developed Oscillation Monitoring System

In this chapter, the improved algorithm is tested by some construct signal in order to prove the effectiveness of the developed scheme in section 5.1. As introduced in last chapter section 4.2 and 4.3, the improving program for HHT method is needed pre-treatment process to the analysis signal at first, then applying the improved HHT method to extract the low frequency oscillation mode from a large amount of data observed by PMU. However, this kind of processing mode will bring seriously distortion of low frequency component caused by the low sampling time. In order to overcome this defect, another new processing mode is raised. Moreover, we summarize our efforts to develop the final automatic power system oscillation monitoring system which monitors post-disturbance PMU measurements in real-time to detect the danger of growing or poorly damped oscillations in the early stages of the event based on the developed scheme, followed by actual testing cases from real power system measurements which will be present in section 5.2.

5.1 Proposed Algorithm Test

5.1.1 Case I

We take the construct oscillation signal Equation (5.1) for example. It can be used to prove the effectiveness of proposed algorithm process, because that the frequency components of this signal contains power system inter-area oscillation (0.1Hz-1Hz), local oscillation (1Hz -2 Hz) and noise oscillation (over 2Hz).

$$\delta = 0.5 \sin(2\pi * 0.1t) + 2 \sin(2\pi * 0.4t) + 1.5 \sin(2\pi * 2t) + 0.5 \sin(2\pi * 5t) + 0.2 \sin(2\pi * 15t) + 15 \quad (5.1)$$

Next, this research discusses the effect of the sampling time applied by improved EMD algorithm. The results are shown in Figure 5 - 1 which sampling time is 1/100s; in Figure 5 - 2 which sampling time is 1/30s. Both of them include three oscillation modes and one residue. The frequencies of IMF components are from high to low – 2Hz, 0.4Hz, and around 0.1Hz. And then, comparing two results with different sampling time Figure 5 - 1 and Figure 5 - 2, it is easily to find that serious distortion happened in low frequency component which sampling time is 1/30s(Figure 5 - 2), especially in the lowest frequency 0.1Hz. The reason of this distortion is because Gibbs phenomenon happened in butterworth filter processing, which is introduced in section 4.1.1.

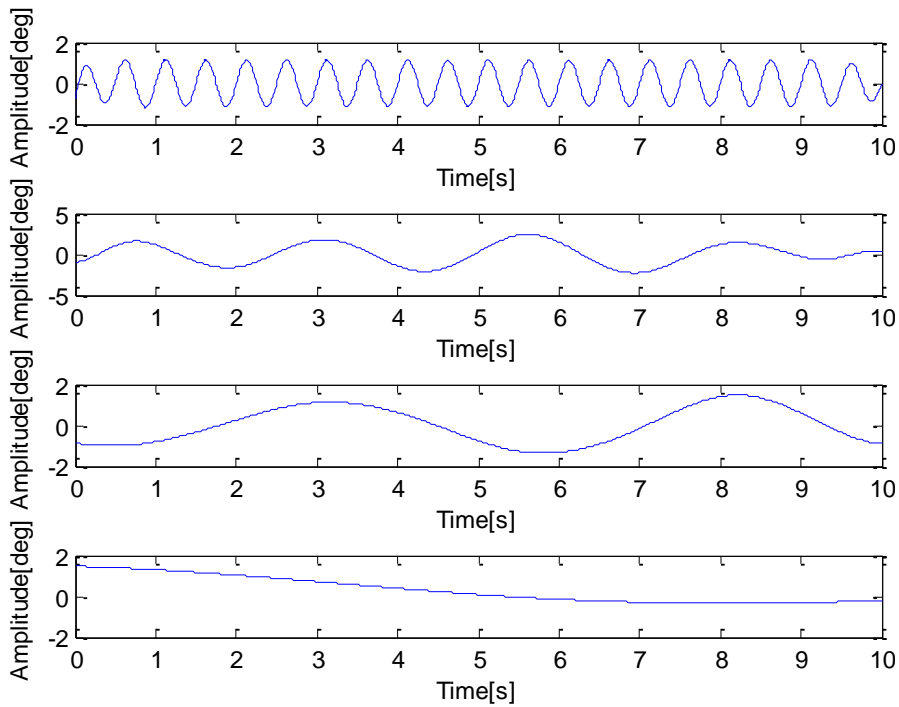


Figure 5 - 1 Pre-treatment EMD result (sampling time 1/100)

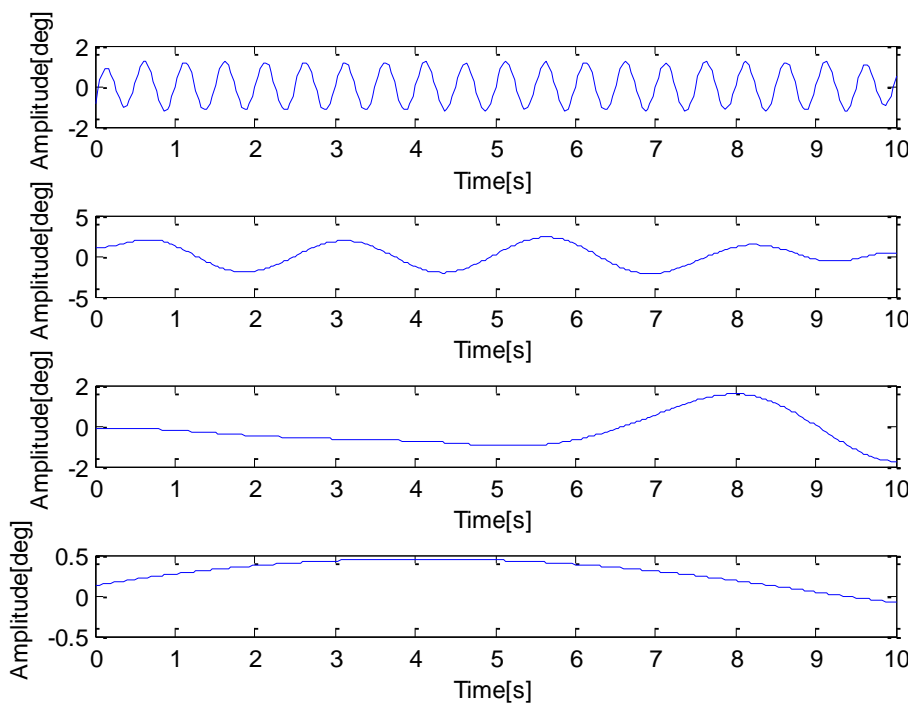


Figure 5 - 2 Pre-treatment EMD result (sampling time 1/30)

It is well known that low frequency oscillation in power system is much more threatening than high frequency oscillation. In order to inhibit the distortion caused by butterworth filter processing, we try to analysis signal without pre-treatment. Figure 5

- 3 which sampling time is 1/100s and Figure 5 - 4 which sampling time is 1/30s show that the EMD result without per-treatment respectively.

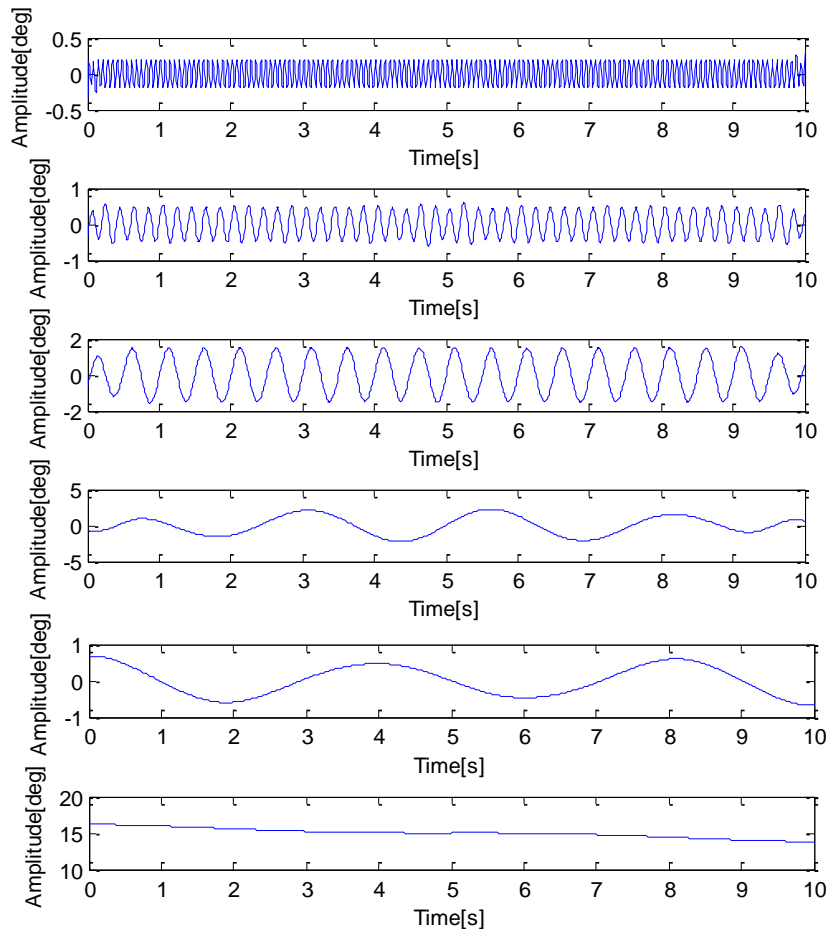


Figure 5 - 3 EMD result (sampling time 1/100)

Figure 5 - 3 includes five oscillation modes and one residue in sampling time 1/100s. The frequencies of IMF components are from high to low – 15Hz, 5Hz, 2Hz, 0.4Hz, and around 0.1Hz. The residue DC component is 15. Figure 5 - 4 includes four oscillation modes and one residue in sampling time 1/30s. The frequencies of IMF components are from high to low – 5Hz, 2Hz, 0.4Hz, and around 0.1Hz. The residue DC component is 15. We can find that, no matter how much the sampling time is,

there are not serious distortion happened in low frequency component. However, high frequency component cannot be observed in the low sampling time situation.

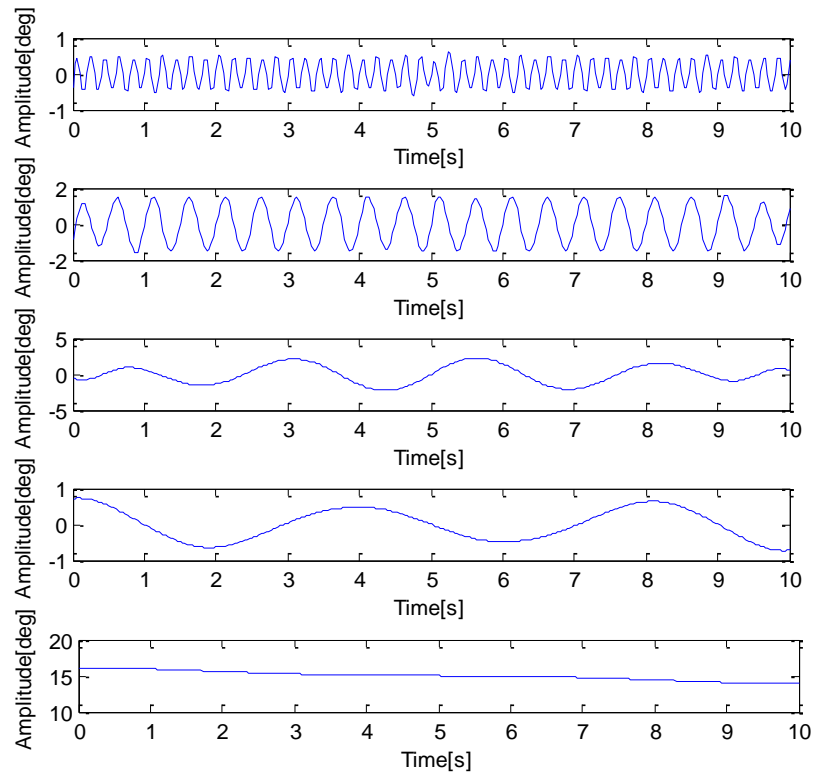


Figure 5 - 4 EMD result (sampling time 1/30)

Next, a comparison of same sampling time situation is discussed. From Figure 5 - 1 and Figure 5 - 3, it can be seen that the pre-treatment process can help to cut down noise performance and high frequency components very well. In the low sampling time situation, pre-treatment process is worked but without high accuracy in dealing with low frequency components after comparing Figure 5 - 2 and Figure 5 - 4. In conclusion, these two comparisons indicate that it have not any effects on the analysis results by applying per-treatment in the high sampling time situation, while in the low sampling time situation high frequency component cannot be observed but without low frequency distortion happened. If we want to observe low frequency components

in high sampling time truly, pre-treatment process is needed. On the contrary, the pre-treatment process should not be applied if we want to observe low frequency components well and truly in low sampling time situation.

5.1.2 Case II

In this case, take another construct oscillation signal including damping for example.

$$x = 3e^{-0.15t} \sin(2\pi * 2t) + 6e^{-0.2t} \sin(2\pi t) + e^{-0.1t} \sin(2\pi * 0.4t) + 15 \quad (5.2)$$

This oscillation signal shown in Figure 5 - 5 contents three decay competent which damping coefficient is -0.15, -0.2, and -0.1; the frequency is 2Hz, 1Hz, and 0.4Hz; and one DC component 15. Then we can get the IMFs (Figure 5 - 6) by applying the improved EMD algorithm.

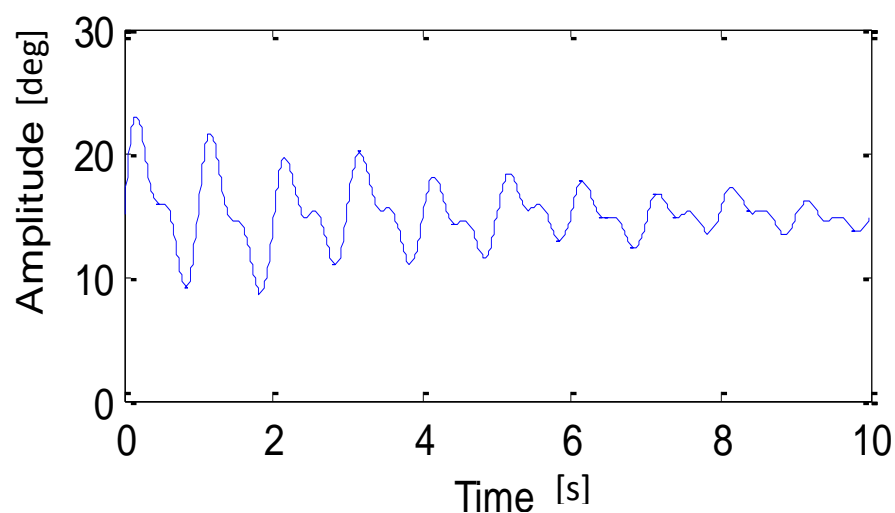


Figure 5 - 5 Oscillation signal

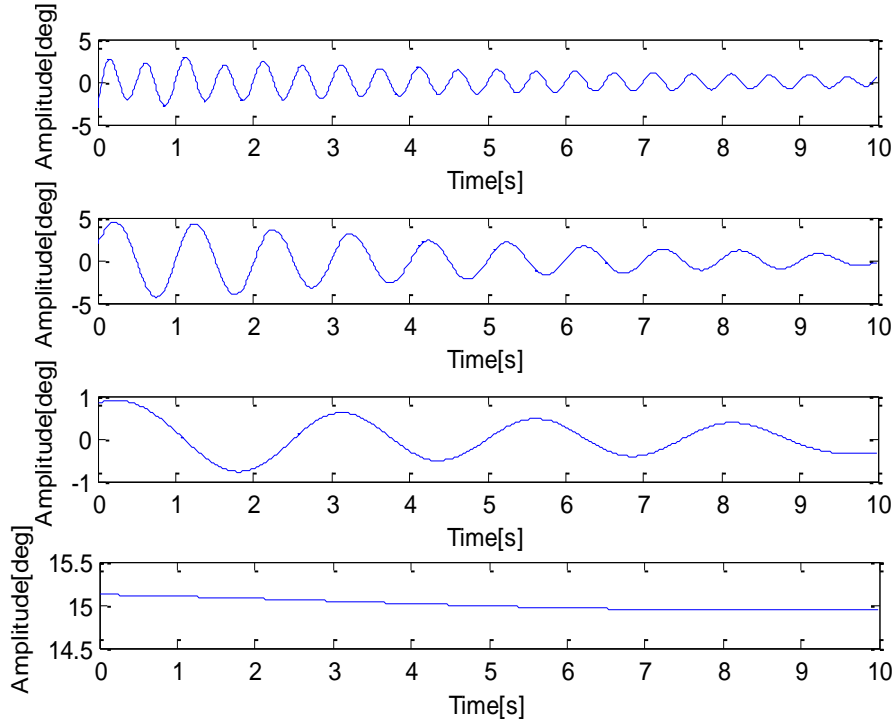


Figure 5 - 6 EMD result

Table 5 - 1 Parameters identification result

| Mode | Frequency | | Damping Coefficient | | Damping Ratio | |
|------|-----------|--------|---------------------|---------|---------------|--------|
| | 1/100 | 1/30 | 1/100 | 1/30 | 1/100 | 1/30 |
| 1 | 2.0800 | 2.0766 | -0.1490 | -0.1516 | 0.0118 | 0.0120 |
| 2 | 0.9936 | 0.9951 | -0.1948 | -0.1978 | 0.0310 | 0.0315 |
| 3 | 0.3917 | 0.3903 | -0.1032 | -0.1000 | 0.0419 | 0.0407 |

Table 5 - 1 shows the parameters of identified to every IMF components. From Table 5 - 1, we can see that the improved HHT method can estimate the frequencies, damping coefficient and damping ratio of three modes quite accurately. And there are not great influences on estimation results by sampling time.

From the results, it can be conclude that the improved HHT algorithms effectively decompose the low-frequency oscillation signal mode, and no matter the sampling time is high or not, it can obtain the correct oscillation parameters from the

decomposed modal signal. This is an effective method for low frequency oscillation signal analysis as long as it can be correctly extracted.

5.2 The Oscillation Monitoring System Based on Enhanced HHT Method

Power system responses following system disturbances contain both linear and nonlinear phenomena. Moreover, presence of noise and switching events in the measurements can upset the accuracy of results. In this section, due to the sampling time of our real-time data come from PMU is 1/30s which introduced in chapter 2, and considering the results discussed in last section: pre-treatment filtering lead to precision reduce to a certain extent in low sampling time situation, a new complete oscillation monitoring system is established. A simplified flowchart of the algorithm is shown in Figure 5 - 7.

The program periodically reads data from the Phasor Data Concentrator (PDC) and preprocess them to deal with issues such as missing channels, bad data etc. After data preprocessing, the original data can be seen as the analyses signal. Any analysis signal will be decompose into IMFs by applying the improved EMD algorithm directly. We try to consider the HHT method as the “filter”, and then decide which IMF should be extract as the oscillation mode. The rule to judge IMFs is an oscillation mode or not is according to HMS (Hilbert marginal spectrum), which offers a measure of the total amplitude (or energy) contribution from each frequency value.

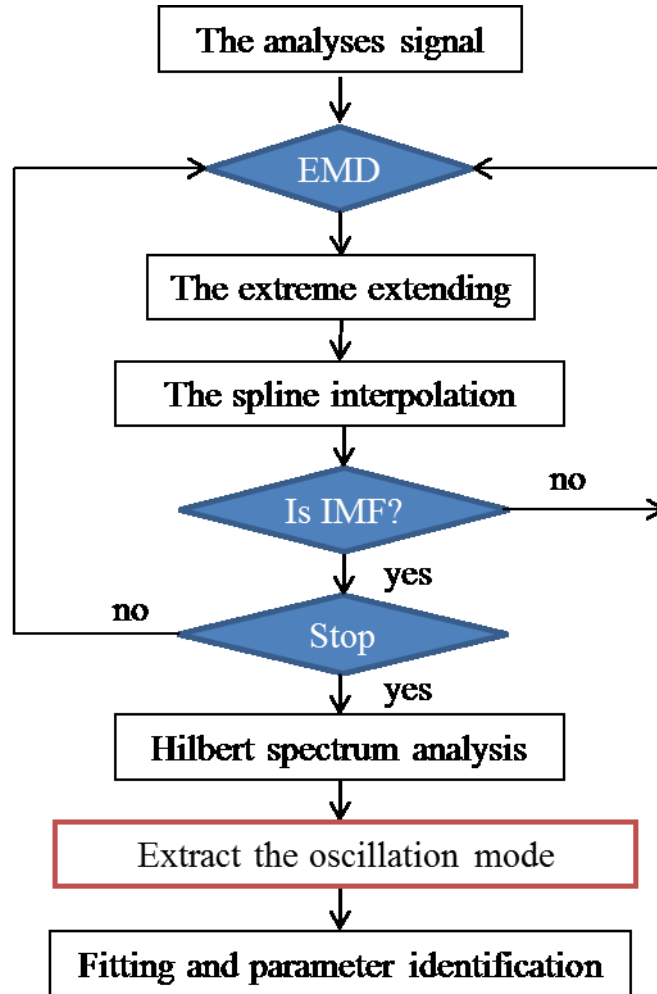


Figure 5 - 7 Algorithm of oscillation monitoring system

As pointed out by Huang et al. [44], the marginal spectrum represents the cumulated amplitude over the entire data span in a probabilistic sense. The frequency in the marginal spectrum indicates only the likelihood that an oscillation with such a frequency exists. The local marginal spectrum offers a measure of the total amplitude contribution from the frequency that we are especially interested in. For this reason, we set the range of center frequency in which the concerned oscillation mode can be readily determined. The last step is to fit and identify the parameters of power system oscillation mode.

5.2.1 Simulink Test

As shown in Figure 5 - 8, it is the simplest system which angular frequency is 2 rad/s, damping coefficient is -0.08, damping ratio is 0.04. The simulink signal is given in Figure 5 - 9. HMS is shown in Figure 5 - 10. Extract the oscillation mode which center frequency range is in 0.1Hz to 0.4Hz. And then, obtain the maximum amplitude value of the extract oscillation mode which is shown in Figure 5 - 11. Figure 5 - 12 describe the extract oscillation mode. Figure 5 - 13 shows that extract a short time data of the extracted oscillation mode from the maximum point, which can be used to estimate parameters of power system oscillation. As a result, the estimated parameters values of power system frequency oscillation are: angular frequency is 1.95 rad/s, damping coefficient is -0.0736, damping ratio is 0.0485.

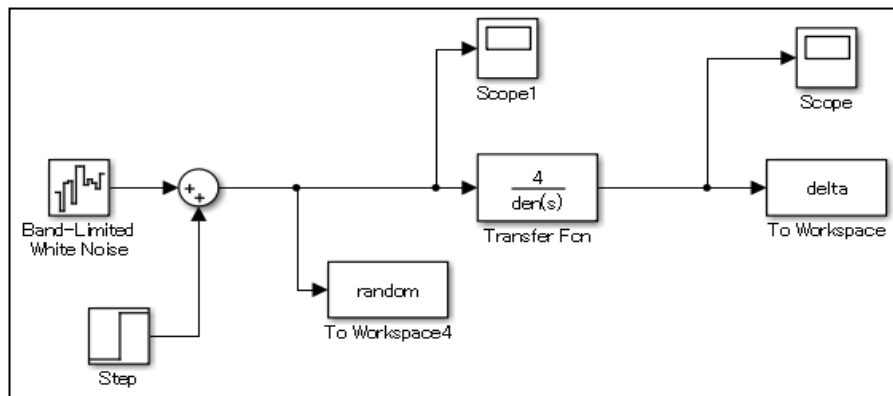


Figure 5 - 8 Simulink system

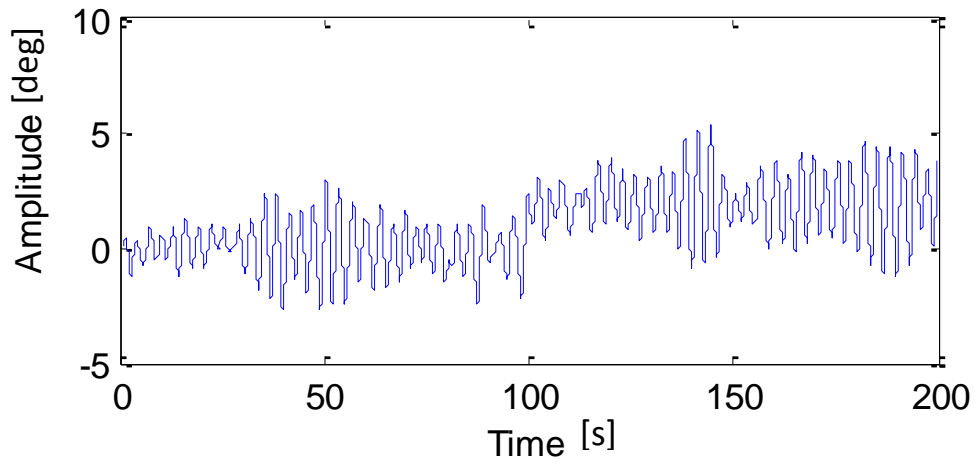


Figure 5 - 9 Simulink signal

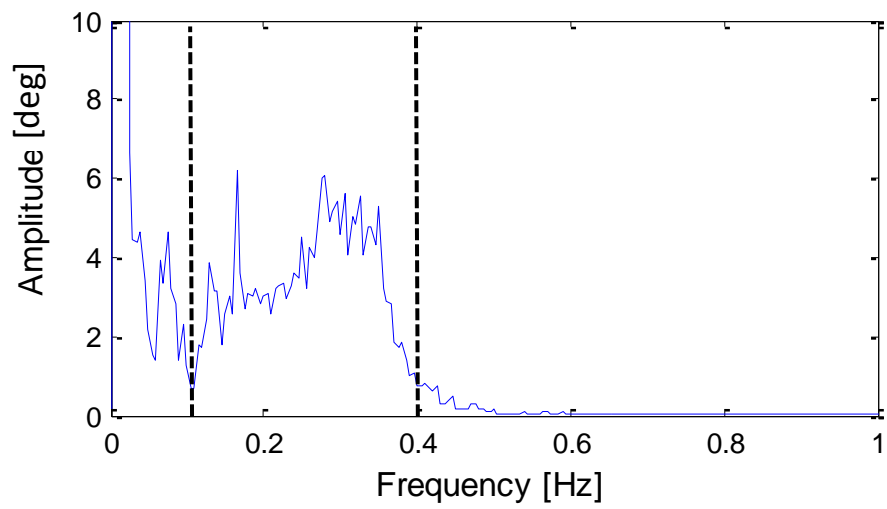


Figure 5 - 10 Hilbert marginal spectrum of simulink signal

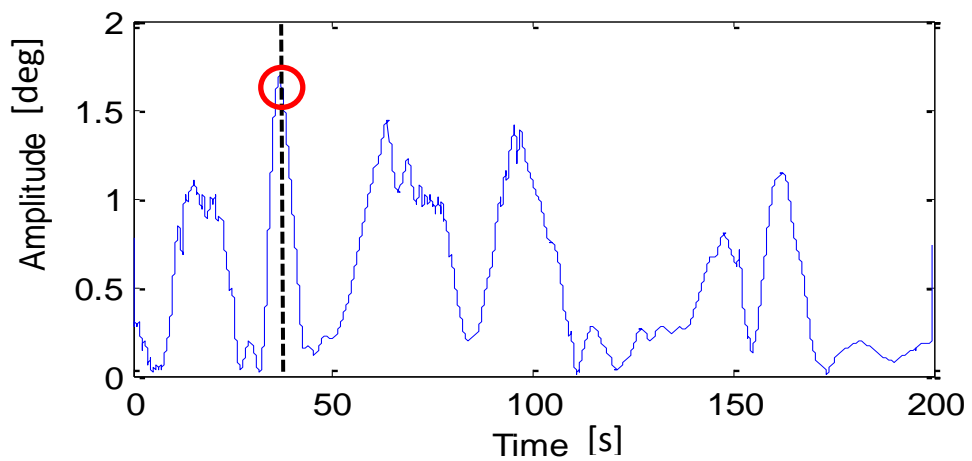


Figure 5 - 11 Amplitude of extract oscillation mode

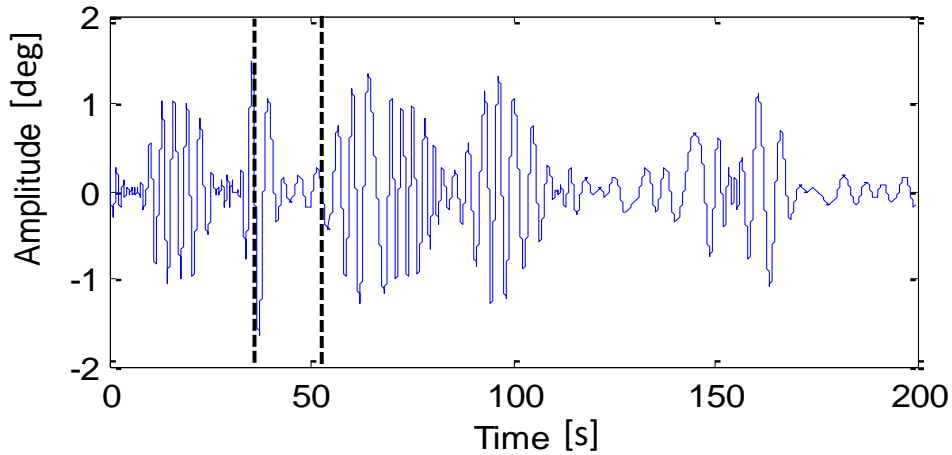


Figure 5 - 12 The extract oscillation mode

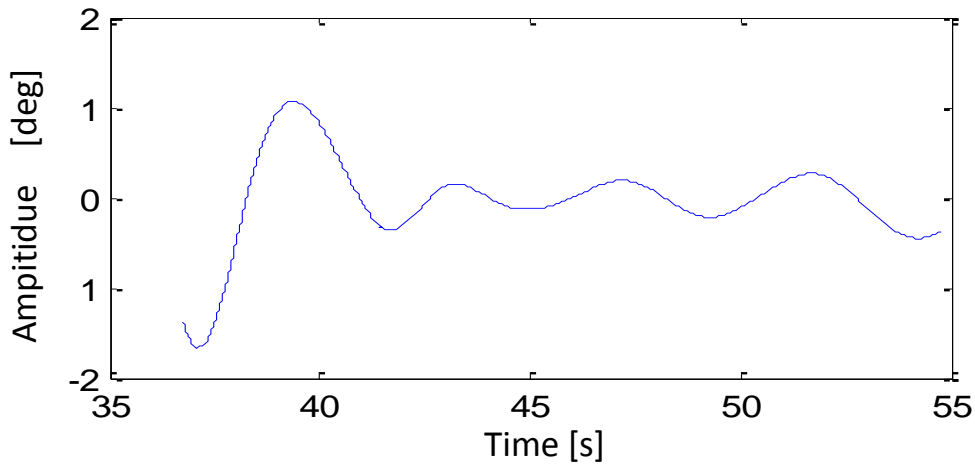


Figure 5 - 13 Extract a short time data of the extracted oscillation mode

5.2.2 Tested with Measurements from CampusWAMS

Figure 5 - 14 shows the waveforms of phase difference between Miyazaki University and Tokushima University Stations. HMS is shown in Figure 5 - 15. Extract the oscillation mode which center frequency range is in 0.3Hz to 0.5Hz. And then, obtain the maximum amplitude value of the extract oscillation mode which is shown in Figure 5 - 16. Figure 5 - 17 describe the extract oscillation mode. Figure 5 - 18 shows that extract a short time data of the extracted oscillation mode from the maximum point, which can be used to estimate parameters of power system

oscillation. As a result, the estimated parameters values of power system frequency oscillation are: angular frequency is 3.4344 rad/s, damping coefficient is -0.06891, damping ratio is 0.0820.

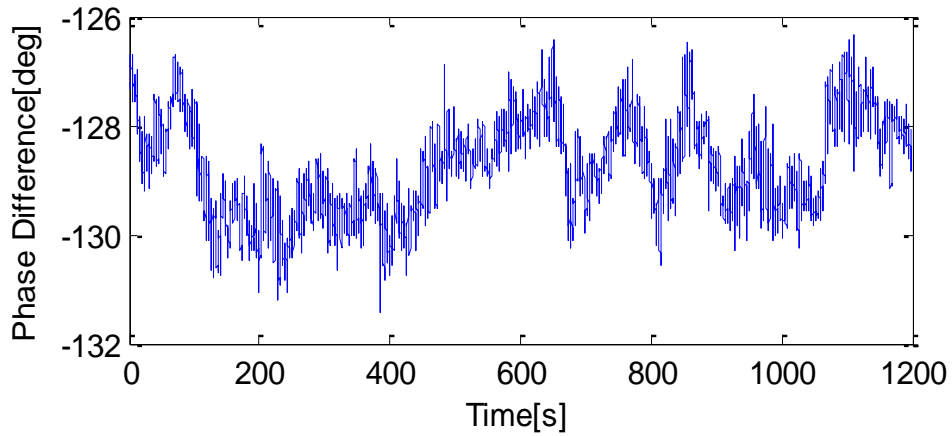


Figure 5 - 14 Waveforms of phase difference between Miyazaki University and Nagoya Institute of Technology University Stations

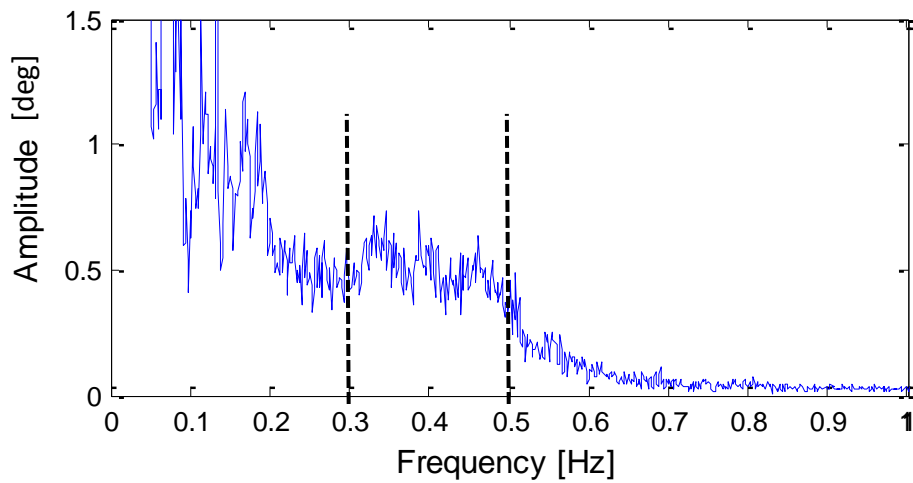


Figure 5 - 15 Hilbert marginal spectrum

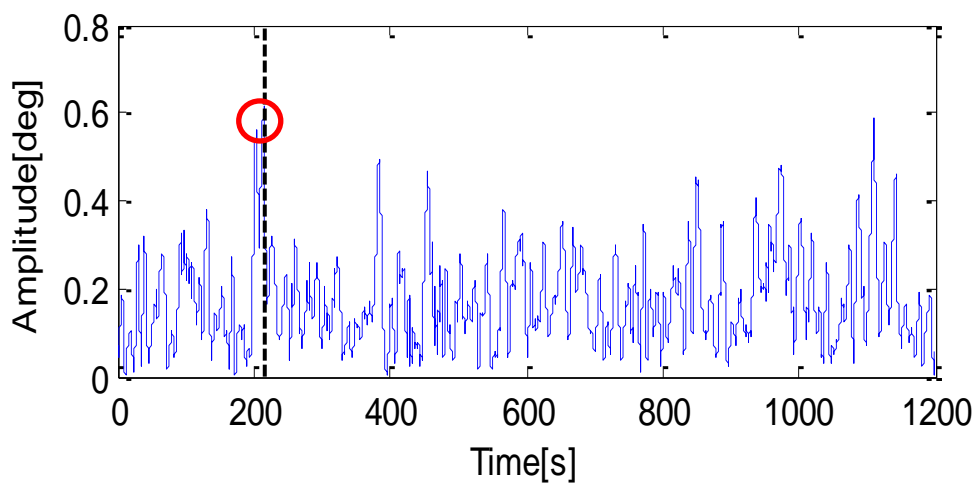


Figure 5 - 16 Amplitude of extract oscillation mode

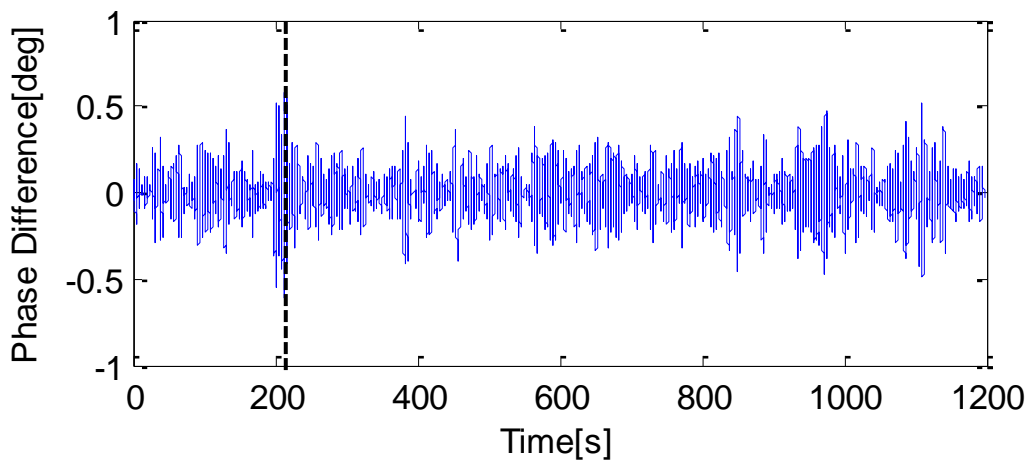


Figure 5 - 17 Extract the oscillation mode

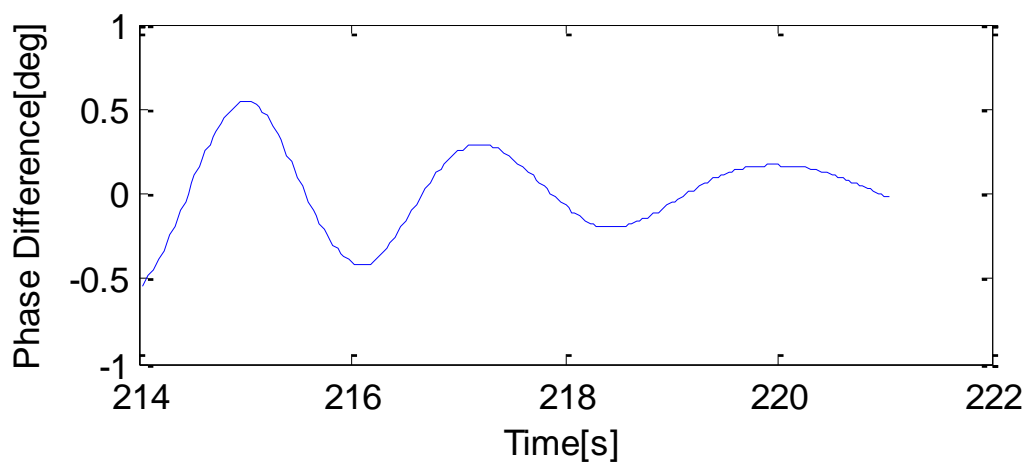


Figure 5 - 18 Extract a short time data of the extracted oscillation mode

5.3 Summary

The oscillation monitoring system based on the enhanced HHT method is proposed in this chapter. It can determine the center range frequency of the concerned mode automatically and accurately, which is then be used to determine the parameter of the extraction. It is shown that the proposed method is easier to implement and computationally more efficient, and thus should be useful for on-line monitoring applications in power systems.

Chapter6. Conclusions

This dissertation presents a complete oscillation monitoring system based on real-time wide-area measurements from PMUs. This oscillation monitoring system employs the enhanced Hilbert-Huang transform (HHT) to analyze power system oscillation characteristics and estimate the damping of oscillatory modes from ambient data. This new oscillation system can give an indication of the damping of transient oscillations that will follow a disturbance, once it occurs. The application is based on a system identification procedure that is carried out in real-time.

The main contributions from this research can be summarized as follows:

- ✓ Study various low frequency oscillation analysis algorithms. It mainly introduces the concept, character and implementation process of FFT, WLT and HHT method. According to the characteristics of low frequency oscillation signal we can get advantage and disadvantage of these algorithms.
- ✓ Data pre-treatment processing is needed to ensure the accurate monitoring of system dynamics with noise-polluted WAMS measurements.

- ✓ Successfully inhibit the boundary effect problem based on extension method (caused by EMD) and Auto-Regressive and Moving Average Model (ARMA) (caused by Hilbert transform).
- ✓ Present an estimation algorithm method to get the mode parameters of oscillation mode in power system based on enhanced HHT.
- ✓ It can determine the center range frequency of the concerned mode automatically and accurately, which is then be used to determine the parameters of the extraction. The extracted mode frequency, damping and mode shape can be detected by this oscillation monitoring system.

Proposed oscillation monitoring in this dissertation is easier to implement and computationally more efficient, the results have convincingly demonstrated the validity and practicability of the developed scheme. And thus should be useful for on-line monitoring applications in power systems.

This research is aimed at small signal stability of power systems. Damping ratios, damping coefficient, frequencies and mode shapes obtained from the oscillation monitoring system are important information for damping controller design. There are many research works in controller design based on wide-area measurements, but there are still many challenging issues in the real world. Controller design based on wide-area measurements will remain a hot topic in the near future.

The proposed methods and corresponding results presented in this thesis have been published in [32][59-64]

Reference

- [1] Bevrani H., Watanabe M., Mitani Y., Power system monitoring and control, Wiley-IEEE Press, New York, USA, 2014
- [2] D. Novosel, "CIEE Phasor Measurement Application Study", project report, for California Energy Commission, KEMA Inc., 2008
- [3] "Final Report on the August 14, 2003 Blackout in the United States and Canada: Causes and Recommendations", US-Canada Power System Outage Task Force, April 2004
- [4] "Final Report of the Investigation Committee on the 28 September 2003 Blackout in Italy," TUCE, April 2004
- [5] Ekraft, "Power failure in Eastern Denmark and Southern Sweden on 23.09.03-Final report on the course of events", Nov. 2004, available at http://www.geocities.jp/ps_dictionary/blackout/Final_report_uk-web.pdf
- [6] "System protection schemes in power networks" , CIGRE working group file, Task Force 38.0219
- [7] "Defense plan against extreme contingencies" , CIGRE working group file, Task Force C2.02.24, April 2007
- [8] V. Terzija, G. Valerde, D. Cai, P. Regulski, V. Madani, J. Fitch, S. Skok, Miroslav M. Begovic and A. Phadke, "Wide-Area Monitoring, Protection and Control of Future Electric Power Networks", IEEE Proceedings, vol. 99, No.1, pp. 80-93, January. 2011
- [9] Y. Hu, V. Madani, R. M. Moraes, and D. Novosel, "Requirements of Large-Scale Wide Area Monitoring, Protection and Control Systems", 10th Annual Conference, Fault and Disturbance Analysis, Georgia Tech, April 2007.

- [10] “Medium-term renewable energy market report 2014”, International Energy Agency, 2014
- [11] N. Tleis, “Technical challenges in delivering Vision 2020”, Presentation, National Grid, April, 2009
- [12] C. Hor, J. Finn, G. Thumm, S. Mortimer, “Introducing series compensation in the UK transmission network”, The 9th IET International Conference on AC and DC Power Transmission, March, 2010
- [13] Antonio Gomez-Exposito, Antonio J. Conejo, Claudio Canizares, "Electric Energy Systems: Analysis and Operation", CRC Press, 1st Edition, July 2008
- [14] Prabha S. Kundur, "Power System Stability and Control", McGraw-Hill, Jan. 1994
- [15] M. Larson, P. Korba, W. Sattinger, P. Owen, "Monitoring and control of power system oscillations using FACTS/HVDC and wide-area phasor measurements", CIGRE 2012 Session, B5-119
- [16] Y. Mitani, O. Saeki, M. Hojo, and H. Ukai, “Online Monitoring System for Japan Western 60 Hz Power System Based on Multiple Synchronized Phasor Measurements”, The Papers of Joint Technical Meeting on Power Engineering and Power System Engineering, IEE Japan, PE-02-60, PSE-02-70 (2002-9) (in Japanese)
- [17] J. F. Hauer, C. J. Demeure and L. L. Scharf, “Initial results in Prony analysis of power system response signals”, IEEE Trans. Power Syst., vol. 5, no. 1, pp.80-89, Feb. 1990
- [18] N. Zhou, J. W. Pierre, D. J. Trudnowski and R.T.Guttromson, “Robust RLS methods for online estimation of power system electromechanical modes”, IEEE Trans. Power Syst., vol. 22, no. 3, pp. 1240-1249, Aug. 2007
- [19] N. Zhou, J.W. Pierre, and J.F.Hauer, “Initial results in power system identification from injected probing signals using a subspace method”, IEEE Trans. Power Syst., vol. 21, no. 3, pp.1296-1302, Aug. 2006
- [20] Norden E. Huang, “THE HILBERT-HUANG TRANSFORM AND ITS APPLICATIONS”, pp.1-15, Sep. 2005
- [21] Charles Proteus Steinmetz, “Complex Quantities and their use in Electrical Engineering”, Proceedings of the International Electrical Congress, Chicago, AIEE Proceedings, pp 33-74, 1893

- [22] Taylor, C. W. (2006), "Wide Area Measurement, Monitoring and Control in Power Systems", Presented at Workshop on Wide Area Measurement, Monitoring and Control in Power Systems, Imperial College, London, 16–17 Mar. 2006
- [23] "Macrodyne model 1690 PMU disturbance recorder", Macrodyne Inc. 4 Chelsea Plae, Clifton Park, NY, 12065
- [24] Hauer, J. F. & Taylor, C. W. (1998), "Information, Reliability, and Control in the New Power System", Proceedings of 1998 American Control Conference, Philadelphia, PA., June 24-26, 1998
- [25] "IEEE standard for synchrophasors for power systems", C37.118-2005, pp56-57, IEEE 1344-1995; Sponsored by the Power System Relaying Committee of the Power Engineering Society, pp 56-57
- [26] "IEEE standard for synchrophasors measurements for power systems", IEEE standard C37.118-2011
- [27] CIGRE WG C4.601 Report, "Wide Area Monitoring and Control for Transmission Capability Enhancement", 2007
- [28] A.G. Phadke, H. Volskis, R.M. de Moraes, Tianshu Bi, etc., "The wide world of wide-area measurement", IEEE Power and Energy Magazine, Vol.5, No.5, pp.52-65, 2008
- [29] Tianshu Bi, "WAMS Implementation in China Part I: Current status", available at http://www.naspi.org/meetings/workgroup/2010_june/presentations/session_03/bi_north_china_wams_20100608.pdf
- [30] Mitani Y, Saeki O, Hojo M, Ukai H. "Online monitoring system for Japan Western 60 Hz power system based on multiple synchronized phasor measurements", Papers of Technical Meeting on Power Engineering and Power System Engineering, IEE Japan, PE-02-60, PSE-02-70, 2002 (in Japanese)
- [31] R. Tsukui, P. Beaumont, T. Tanaka, and K. Sekiguchi, "Intranet-based protection and control", IEEE Computer Applications in Power, Vol.14, No.2, pp.14-17, Apr. 2001
- [32] Qing Liu, Dikpride Despa, Yasunori Mitani, "Application of Phasor and Node Voltage Measurements to Monitor Power Flow and Stability", International Journal on Electical Engineering and Informatics, Volume 4, Number 2, July, 2012

- [33] T. Hashiguchi, M. Yoshimoto, Y. Mitani, O. Saeki, and K. Tsuji, "Oscillation mode analysis in power systems based on data acquired by distributed phasor measurement units", Proceedings of the 2003 IEEE International Symposium On Circuits And systems, 2003
- [34] G. Liu, J. Quintero, and V. Venkatasubramanian, "Oscillation Monitoring System based on wide area synchrophasors in power systems" , Proc. IREP symposium 2007, Bulk Power System Dynamics and Control - VII, August 19-24, 2007, Charleston, South Carolina, USA
- [35] P. Kundur, Power System Stability and Control, (McGraw-Hill: New York, 1994)
- [36] B. Pal and B. Chaudhuri, Robust Control in Power Systems, Springer Inc. New York, 2005
- [37] Hasselblatt, Boris and Anatole Katok (2003), A First Course in Dynamics: With a Panorama of Recent Developments, Cambridge University Press. ISBN 0-521-58750-6
- [38] J. Guckenheimer and P. Holmes, "Nonlinear oscillations, dynamical systems, and bifurcations of vector fields" , Springer-Verlag, New York, 1997
- [39] R. Seydel, "Practical bifurcation and stability analysis," Springer-Verlag, New York, 1994
- [40] H. O. Wang, E. H. Abed, and A. M. A. Hamdan, "Bifurcations, chaos, and crises in voltage collapse of a model power system", IEEE Trans. Circuits and Systems-I: Fundamental Theory and Applications, vol. 41, pp. 294- 302, Mar. 1994.
- [41] R.Tsukui, P.Beaumont, T.Tanaka, and K.Sekiguchi, "Intranet-based protection and control", IEEE Comput Applications in Power, vol. 14, no. 2, pp.14-17, 2001
- [42] H.Bevrani, T.Hiyama,"On load-frequency regulation with time-delays: design and real-time implementation," IEEE Transactions on Energy Conversion, Vol.24, No.1, PP.292-300, 2009
- [43] SHI Chun xiang, LUO Qi feng, "Hilbert-Huang transform and wavelet analysis of time history signal", Acta Seismologica Sinica, vol. 16, No. 4, pp. 422-429, 2003
- [44] Huang, Norden E.(EDT)/Shen, SamuelS(EDT), "The Hilbert-Huang Transform and Its Applications" , pp.1-15, 2005
- [45] N. E. Huang, Z. Shen and S. R. Long et al, "The empirical mode decomposition and the Hilbert spectrum for nonlinear and non-stationary time series analysis", Proceedings of the Royal Society London, Series A, 454(1998) 903-995
- [46] Gomes, S. and Cortina, E., "Some Results on the Convergence of Sampling Series based on

- Convolution Integrals”, SIAM J. Math. Anal., 26,(5), 1386-1402, 1995
- [47] Jerri, A., “Error Analysis in Applications of Generalizations of the Sampling Theorem”, Advanced Topics in Shannon Sampling and Interpolation Theory, (R. J. Marks II, ed.), Springer-Verlag, New York, 1993
- [48] Jerri, A., “The Gibbs Phenomenon in Fourier Analysis” , Splines and Wavelet Approximations, Kluwer Academic Publishers, 1997
- [49] Karanikas, C., “Gibbs Phenomenon in Wavelet Analysis”, Result. Math., 34, 330-341, 1998
- [50] Shim H. T, Volkmer, “On the Gibbs Phenomenon on wavelet expansions”, J. Approx. Theory., 84, 1, 74-95, 1996
- [51] Helmberg, G., “The Gibbs Phenomenon for Fourier Interpolation”, J. Approx. Theory, 78, 41-63, 1994
- [52] Helmberg, G. and Wagner, P., “Manipulating Gibbs’ Phenomenon for Fourier Interpolation”, J. Approx. Theory, 89, 308-320, 1997
- [53] Walter, G. G., “Wavelets and other Orthogonal Systems with Applications”, CRC Press, 1994
- [54] Atreas N. D. and Karanikas C., “Gibbs phenomenon on sampling series based on Shannon’s and Meyer’s wavelet Analysis”, Fourier Analysis and Applications, 5,6, 575-588, 1999
- [55] Shim H. T, Volkmer, “On the Gibbs Phenomenon on wavelet expansions”, J. Approx. Theory., 84, 1, 74-95, 1996
- [56] Walter, G. G. and Shim, H. T., “Gibbs Phenomenon for sampling series and what to do about it”, Fourier Analysis and Applications 4,3, 357-375, 1998
- [57] Hazewinkel, Michiel, ed. (2001), "Spline interpolation", Encyclopedia of Mathematics, Springer, ISBN 978-1-55608-010-4
- [58] N.E. Huang, Z. Shen, S.R. Long, M.L. Wu, H.H. Shih, Q. Zheng, N.C. Yen, C.C. Tung and H.H. Liu, “The empirical mode decomposition and Hilbert spectrum for nonlinear and non-stationary time series analysis”, Proc. Roy. Soc. London A, Vol.454, 1998, pp. 903-995
- [59] Qing Liu, Dikpride Despa, Masayuki Watanabe, Yasunori Mitani, “Analysis of Oscillation Characteristic for Japan Eastern 50-Hz Power System Based on Campus WAMS”, Proceedings of the International Conference on Advanced Power System Automation and Protection (APAP2011),

Beijing, China. (4-pages CDROM),2011

[60] Qing Liu, Yasunori Mitani , “Application of HHT for Oscillation Mode Analysis in Power System Based on PMU”, Proceedings of the International Conference on Electric Power and Energy Conversion Systems (EPECS), No.96205.Sharjah, UAE,2011

[61] Qing Liu, Yasunori Mitani, Masayuki Watanabe, “Hilbert-Huang Transform and FFT Analysis of Oscillation Characteristics for Japan Power System Based on Campus WAMS”, Proceedings of the IASTED-International Conference on Power and Energy System (AsiaPES 2012), Phuket, Thailand (8-pages, CDROM),2012

[62] D. Despa, Y. Mitani, M. Watanabe, Yaser S. Q., T. Fujita, Q. Liu, M. Bernard, “PMU Based Monitoring and Estimation Power System Dynamic Stability Developed on 50-Hz Power System”, Proceedings of the IASTED-International Conference on Power and Energy System (AsiaPES 2012), Phuket, Thailand (8-pages, CDROM),2012

[63] Qing Liu, Taro Fujita, Masayuki Watanabe, Yasunori Mitani, “Hilbert-Huang Transform and Wavelet Analysis of Oscillation Characteristics for Japan 60[Hz] Power System Based on Campus WAMS”, Proceedings of the 8th Power Plant and Power System Control (PPPSC2012) Toulouse, France,2012

[64] Qing Liu, Yasunori Mitani, Masayuki Watanabe, Global “Oscillation Mode Analysis Using Phasor Measurement Units-based Real Data”, International Journal of Electrical Power and Energy Systems, accepted